

A Novel Energy-Saving Biomass Drying Process Based on Self-Heat Recuperation Technology

(自己熱再生技術を用いた省エネルギーバイオマス乾燥プロセスの開発)

劉 玉平

CONTENTS

CHAPTER 1 INTRODUCTION	1
1.1 Biomass	2
1.2 Water in biomass	4
1.3 Biomass dryers	7
1.3.1 Fixed and moving bed dryer	7
1.3.2 Rotary dryer	7
1.3.3 Conveyor dryer	8
1.3.4 Fluidized bed dryer	8
1.4 Energy-saving process	12
1.4.1 Hot air drying with conventional heat recovery	13
1.4.2 Multistage drying	14
1.4.3 Mechanical vapor recompression	15
1.4.4 Heat pump	16
1.4.5 Self-heat recuperation technology	17
1.5 Scope and structure of this research	20
References	23
CHAPTER 2 THEORETICAL INVESTIGATION FOR ENERGY SAVING IN BIOMASS DRYING PROCESSES	27
2.1. Exergy analysis of the heat transfer during drying process	28

2.2. Heat pairing	31
2.3. Existing energy-saving biomass drying systems	33
2.3.1. Conventional heat recovery drying process	33
2.3.2. Multistage drying process	34
2.3.3. Mechanical vapor recompression drying process	36
2.4. Initial evaluation of energy efficiency in a biomass fluidized bed dryer based on SHR technology	38
2.4.1. Concept of SHR technology based fluidized bed drying	38
2.4.2. Process Design and Calculations	41
2.4.3. Energy comparison of the drying processes	41
2.4.4. Exergy analyses of the proposed process	45
2.5. Conclusions	49
References	50

CHAPTER 3 SELF-HEAT RECUPERATION TECHNOLOGY FOR BIOMASS DRYING IN A FLUIDIZED BED DRYER

3.1 Process design of self-heat recuperative fluidized bed dryer for biomass drying	52
3.1.1. Introduction	52
3.1.2. Energy-saving drying process based on self-heat recuperation technology	52
3.1.3. Process calculations	57
3.1.4. Results and discussion	59

3.1.5. Conclusions	63
References	64
3.2. Biomass drying in the exergy recuperative fluidized bed dryer with air	65
3.2.1. Introduction	65
3.2.2. Experimental setup	65
3.2.3. Results and discussion	70
3.2.3.1 Thermal gravity analysis for rice straw	70
3.2.3.2. Drying kinetics in the semi-fluidized bed dryer	71
3.2.3.2.1. Effect of fluidization velocity and temperature	71
3.2.3.3. Heat transfer in the fluidized bed dryer	76
3.2.3.4. Stability of the fluidized bed dryer	80
3.2.4. Conclusions	85
References	86
CHAPTER 4 SELF-HEAT RECUPERATION TECHNOLOGY FOR BIOMASS DRYING IN OTHER DRYERS	87
4.1. Introduction	88
4.2. Process calculations	88
4.3. Results and discussion	94
4.4. Conclusions	101
References	103

CHAPTER 5 FURTHER ENERGY-SAVING BIOMASS DRYING BASED ON SELF-HEAT RECUPERATION TECHNOLOGY	105
5.1. A novel exergy recuperative drying module with superheated steam	106
5.1.1. Introduction	106
5.1.2. Basic concept of an exergy recuperative drying module	106
5.1.3. Design of an exergy recuperative drying system based on self-heat recuperation technology	107
5.1.3.1. Schematic layout of an exergy recuperative drying system	107
5.1.3.2. Energy balance in the exergy recuperative drying system	109
5.1.3.2.1. Zone of preheating period	109
5.1.3.2.2. Zone of constant drying period	109
5.1.3.2.3. Zone of falling rate drying period	110
5.1.4. Process simulation	111
5.1.4.1. Sorption isotherm of brown coal	112
5.1.4.2. Simulation conditions	113
5.1.4.3. Simulation results	115
5.1.4.3.1. Energy consumption in the exergy recuperative drying process	115
5.1.4.3.2. Effect of final water content on energy consumption of the exergy recuperative drying system	118
5.1.4.3.3. Effect of compressor adiabatic efficiency on the energy consumption of the exergy recuperative drying system	119
5.1.4.3.4. Exergy loss in the proposed drying process	121

5.1.4.3.5. Comparison with previous work	122
5.1.5. Conclusions	123
References	124
5.2. Fluidized bed drying of biomass with superheated steam based on self-heat recuperation technology	128
5.2.1. Introduction	128
5.2.2. Exergy recuperative biomass drying process	130
5.2.3. Simulation Conditions	134
5.2.4. Results and discussion	135
5.2.4.1. Energy consumption in the exergy recuperative drying process for free water removal	135
5.2.4.2. Free water and bound water removal	138
5.2.5. Conclusions	139
References	140
5.3. Biomass drying in the exergy recuperative fluidized bed dryer with superheated steam	142
5.3.1. Introduction	142
5.3.2. Experimental setup	142
5.3.3. Experimental procedure	145
5.3.4. Results and discussion	148
5.3.4.1. Mixing and fluidization performance of silica sand and sawdust	148
5.3.4.2. Batchwise experiment for biomass drying	151

5.3.4.3. Continuous experiment for biomass drying	155
5.3.4.4. Comparison of drying performance with air and superheated steam	157
5.3.5. Conclusions	160
References	161
5. 4. Novel fluidized bed dryer for biomass drying	162
5.4.1. Introduction	162
5.4.2. Materials and methods	163
5.4.2.1. Materials and experimental equipment	163
5.4.2.2. Experimental procedure	166
5.4.3. Results and discussion	167
5.4.3. 1. Fluidization behavior in the fluidized bed dryer	167
5.4.3. 2. Drying kinetics in the fluidized bed dryer	174
5.4.3. 3. Drying of binary mixture particles	178
5.4.4. Conclusions	181
References	182
CHAPTER 6 SUMMARY AND FUTURE WORK	185
6.1. Summary	186
6.2. Future work	190
6.2.1. Integration of biomass drying and torrefaction process	191
6.2.2 Brown coal drying	195
References	200

APPENDIX NOTATION AND ABBREVIATION	203
LIST OF PUBLICATIONS	208
CONFERENCES	210
ACKNOWLEDGEMENTS	216

CHAPTER 1
INTRODUCTION

1.1 Biomass

Biomass includes wood, vegetal waste (including wood waste and crops used for energy production) and animal materials/wastes. Biomass is one of the major renewable primary energy sources, due to its low net carbon dioxide emissions and potentially sustainable if the economical, environmental and social impacts are properly managed. At present, electricity power mainly depends on fossil fuel (petroleum, coal and natural gas) which caused the shortage of fossil fuel in the world. On the other side, carbon dioxide (CO₂) emission mainly comes from the combustion of fossil fuel and has thought to be the major cause of global warming as shown in Fig. 1-1 (Marland, G, 2007).

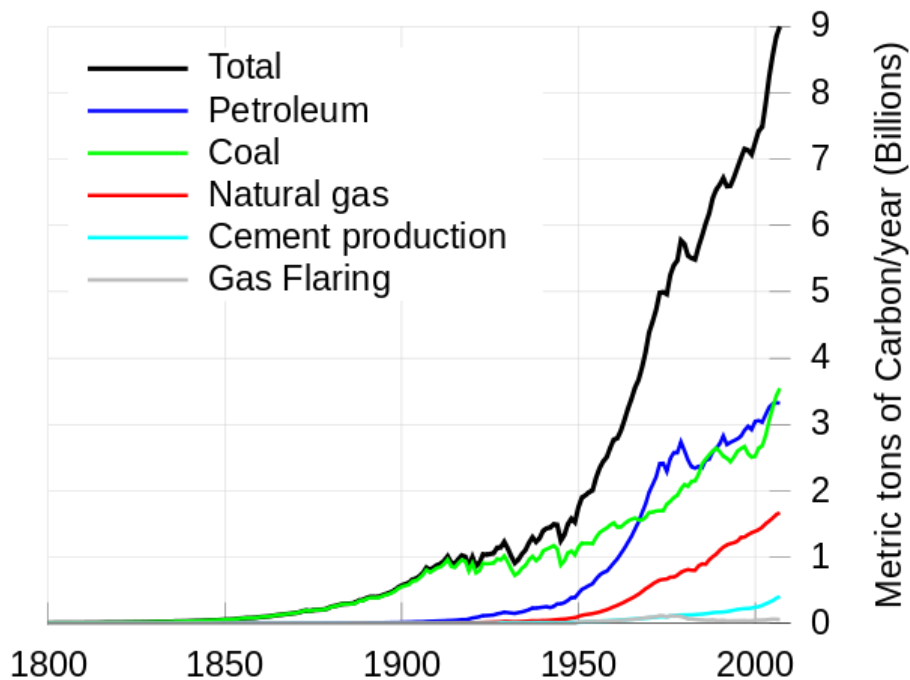


Fig. 1-1. Carbon dioxide (CO₂) emissions

To relieve the electricity insufficiency and carbon dioxide emission problems in the future, renewable energy has recently been promoted. There are many renewable energy systems, such as solar, wind, hydro and biomass. Among them, biomass is one of the renewable primary energy sources, touching all three major issues due to its competition with food on land use, low net CO₂ emissions and potentially sustainable. Biomass shows great potential as a sustainable energy and has been used as many kinds of energy sources: combustion and co-combustion with coal, and liquid production such as bioethanol (Maciejewska et al.; McKendry 2002; Wang et al. 2008). Biomass utilization also includes gas production by pyrolysis and gasification, solid formation by torrefaction based on the order of thermochemical stability of the biomass constituents as shown in Fig. 1-2.

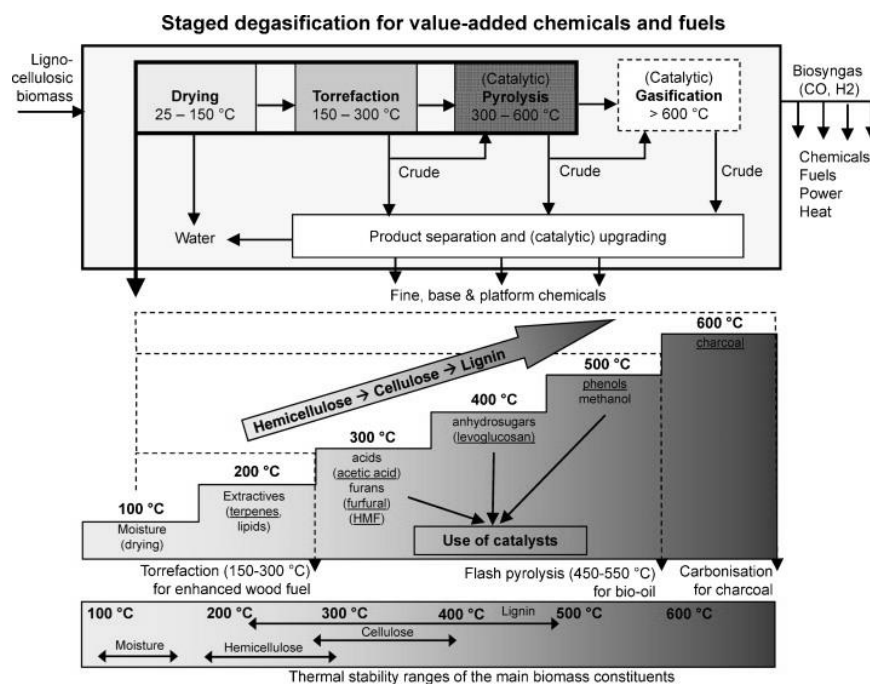


Fig. 1-2. Staged degasification concept within the thermochemical biorefinery (de Wild et al. 2009).

However, biomass suffers the problem of low energy density compared with traditional fossil fuels. This is mainly caused by the high moisture content that commonly exceeds 50 wt% (wet basis, wb), which also limits biomass applications as an alternate fuel due to the high transportation cost and storage difficulties reduced thermal efficiency during energy conversion.

1.2 Water in biomass

Water in biomass could be mainly divided as free water and bound water. Free water held by the capillary forces in the microcellular biomass and bound water absorbed by the porous cell wall of the biomass.

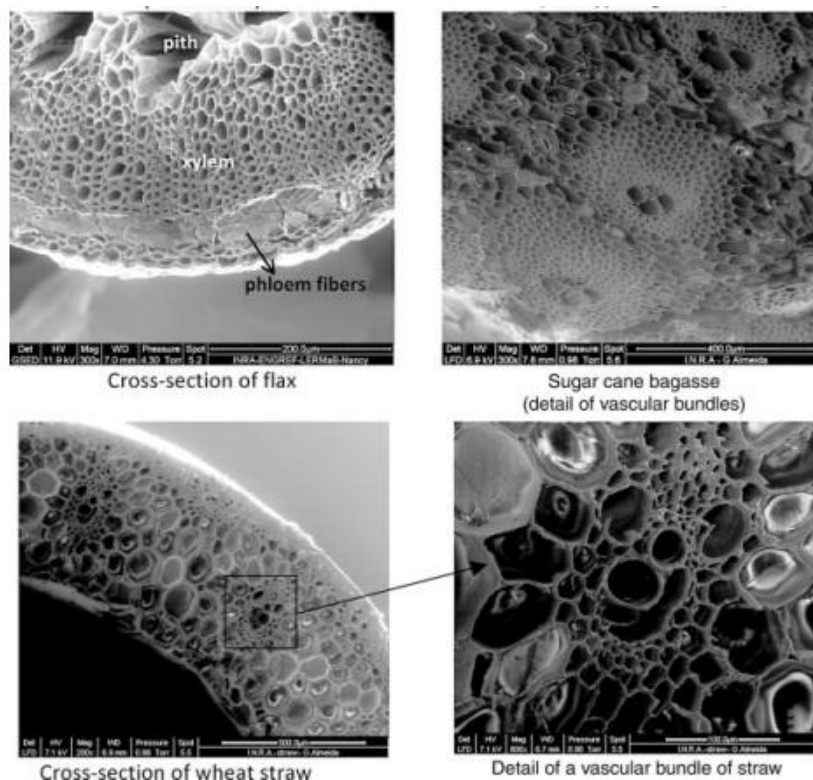


Fig. 1-3. Water in the biomass (Perre P., 2012)

The drying of biomass is complicated and requires an energy supply to overcome the many forces inside the biomass, such as capillary forces, forces relating to water diffusion, sorption forces and even chemical bonding forces. Free water evaporates as easily as water from a planar surface thus the enthalpy of free water is equal to liquid water; capillary water in the lumen of the fibers is more difficult to evaporate thus a higher temperature is required. Owing to interactions with the pore walls, concave menisci are formed, resulting in a decrease in vapour pressure, described by the Kelvin equation:

$$\ln\left(\frac{P_0}{P_c}\right) = \frac{2\gamma}{r} \frac{\bar{V}}{RT} \cos\theta \quad (1-1)$$

where P_c is the vapour pressure of capillary water, P_0 is the vapour pressure of ordinary water, γ is the surface tension of the air-water interface, r is the capillary radius, \bar{V} is the molar volume, θ is the contact angle and R is the gas constant. On the other side, bound water needs energy to desorb from the polymer chains within the cell wall. The bound water amount equals the amount of water existing below the fiber saturation point (FSP) (Berry and Roderick 2005). The FSP varies at a different temperature and can be commonly calculated by eq 1-2:

$$X_{\text{fsp}} = 0.30 - 0.001(T_{\text{dry}} - 20) \quad (1-2)$$

where T_{dry} is the biomass drying temperature in the fluidized bed (Siau 1984). The enthalpy of bound water could be written as (Stanish et al. 1986):

$$h_b = h_{\text{free}}(T) - 0.4\Delta H_{\text{vap}} \left[\frac{(X_{\text{fsp}} - X)}{X_{\text{fsp}}} \right]^2 \quad (1-3)$$

where H_{vap} is the heat of vaporization. For free water evaporation, 100 °C drying temperature is necessary, and for capillary and bound water evaporation drying temperature should increase over 100 °C to overcome the forces around the water molecular. To achieve lower final moisture content of biomass, the drying temperature would increase correspondingly (Fig. 1-4). The moisture content of biomass commonly should be decreased to 8–20 wt% (wb) prior to densification and energy conversion for economic use (Kaliyan and Morey 2009). Hence, biomass drying has been used effectively to increase the energy density and deliver bulk and widespread biomass to bioconversion plants.

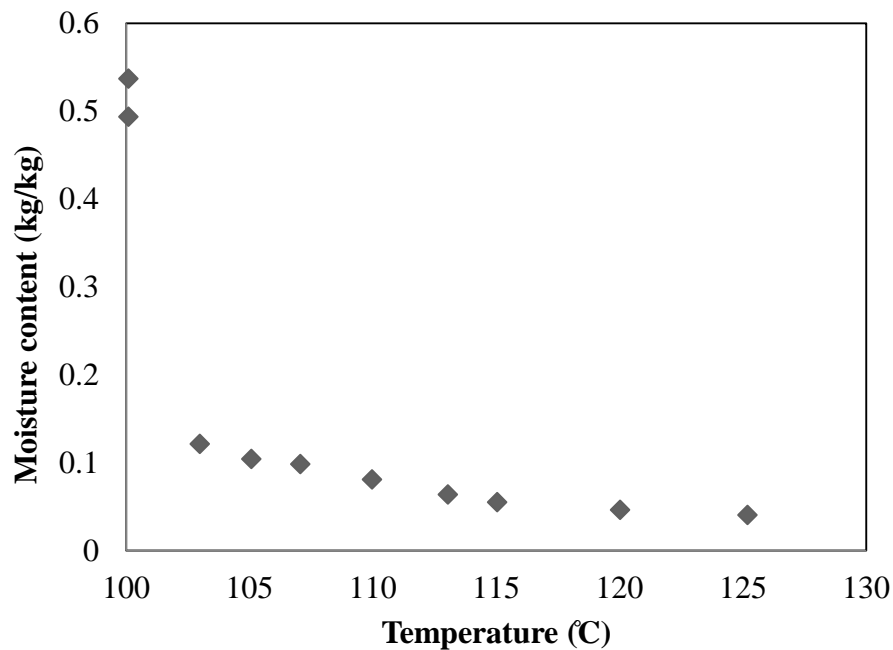


Fig. 1-4. Equilibrium moisture content of wood in three different temperatures of superheated steam (Pakowski, Z. 2007)

1.3. Biomass dryers

Many types of dryers or drying processes, such as the pneumatic conveying dryer, rotary dryer, fixed and moving bed dryer and pulsed fluidized bed dryer, have been explored for drying biomass through directly or indirectly heating method (Stahl et al. 2004). The common biomass drying systems are to be introduced in the following.

1.3.1 Fixed and moving bed dryer

Biomass temperature increases as the hot drying medium passes through the column and evaporated water could be carried out by the drying medium during this process. Gas velocity in the fixed and moving bed dryer was low which makes unnecessary to clean up the exhausted gas. The main drawback of the fixed and moving bed dryer was a large vertical gradient in temperature and moisture content of the dried bed in the relatively deep bed of biomass. Thus, dried materials should be mixed well before the energy conversion process. Moreover, heat transfer rate in this kind of dryer is very low, thus it usually takes a few hours for the biomass drying and is mainly suitable for small plant.

1.3.2 Rotary dryer

The rotary dryer is one of the most commonly used drying systems for biomass drying. In the rotary dryer, wet biomass is fed into a slowly rotating cylinder and then was lifted by longitudinal flights inside the cylinder to increase the contact surface with the drying medium. In a concurrent rotary dryer, wet biomass and hot drying medium, move at a same direction. In a countercurrent type, wet biomass and hot drying medium move at different directions. This could narrow the temperature

difference between the two streams for energy saving, however, increases the possibility of fire disaster due to overheating. In the case of indirectly rotary dryer for biomass drying, steam is passed through the shell of the rotary drum to heat the tubes through which wet biomass flows in a relatively inert atmosphere created by the evaporated water vapor.

1.3.3 Conveyor dryer

In a conveyor dryer, wet biomass is spread onto a moving perforated conveyor to dry the material in a continuous process. The drying medium pass through the conveyor and wet biomass to form heat exchange. The conveyor dryer is better to take advantage of waste heat for high energy efficiency for its lower temperatures than rotary dryers used in hot fuel drying. However, the footprint of single-pass conveyor dryer is commonly larger than that of a rotary dryer, thus multi-pass conveyor dryer are typically used on the industry for its small footprint and lower cost. It should be noticed that the conveyor dryer is not feasible for sticky materials drying and materials having a tendency to foul the heat transfer surface.

1.3.4 Fluidized bed dryer

In a fluidized bed dryer, biomass particles are fluidized by the high gas velocity from the distributor. Fluidized beds generally require less drying time for the large contact surface area between solids and gas, the uniform bed temperature, good degree of solid mixing, and the rapid transfer of heat and moisture between solids and gas, which shortens drying times (Daud, 2008). Wet materials in fluidized bed dryers could dry both in batchwise and continuous ways, in which bathwise

operation is mainly used for small scale production and continuous operation used for large scale production. In a continuous operation, there is a distribution of solid moisture content due to the residence times of solids compared with that in a batchwise operation. Thus multiple beds or a short-pass is required to prevent the distribution of moisture content. When particles are in the fluidized state, the hydrodynamic behavior varies significantly with the flow regimes containing particulate, bubbling, turbulent, fast fluidization and dilute transport. The key operating and design variables that affect the hydrodynamics of a fluidized bed include particle properties, fluid velocity, bed diameter, and distributor.

Table 1-1. Comparison of different types of dryers

Dryers	Heat transfer rate [W/(K m ²)] or Heat capacity rate ha [W/(m ³ K)]	Drying temperature T [°C]	Energy efficiency [%]	Final water content [%]	Shape of drying material	Note
Fluidized bed dryer (Hot air)	$ha=2000-7000$	100-600	50-65	1-10	Particle Slurry	<ul style="list-style-type: none"> • Processing capacity is large due to heat transfer is fast • Multi-chamber horizontal continuous is suitable if the product water content is not constant. • A stirring device, or a distributed input on top of the particle layer in fluidized drying process is used if wet material is easy to aggregation.
Rotary dryer (hot air)	$ha=110-230$	200-600	40-70	2-10	Particle Slurry Flake Fiber	<ul style="list-style-type: none"> • Used for a large continuous material drying at a relatively high temperature • A wide range of materials can be dried • The high construction costs • Need a large volume of the dryer and installation area large
Rotary Kiln dryer (Indirectly drying)	$U=20-50$	100-150	60-75	2-10	Particle Slurry Flake Fiber	<ul style="list-style-type: none"> • Used for material drying unsuitable for hot air contact.
Rotary dryer with steam drying	$U=40-120$	100-150	70-85	2-10	Particle Block Flake	<ul style="list-style-type: none"> • Capital cost is high • Maximum heat exchange surface area is 2000 m² • Low water content drying
Screw conveyor dryer (hot air)	$ha=350-950$	400-800	60-70	2-3	Particle Block Sludge	<ul style="list-style-type: none"> • Heat capacity is large • Large friction of stirring blades • High Mechanical power
Screw conveyor dryer (Indirectly drying)	$U=80-350$	100-150	70-85	2-3	Sludge Cake Flake	<ul style="list-style-type: none"> • High energy efficiency • Low exhausted gas • Small scattering material • Possible for high and low pressure operation

Data from Fluidization Handbook (Horio. M, 1999).

From Table 1-1, we could find that fluidized bed dryer has the highest heat transfer rated which is significantly higher than other types of dryers. To treat a large amount of high water content biomass, a higher heat transfer rate in the dryer could make the dryer more compacted and then decrease the capital costs. Hence, in this research, we mainly adapted fluidized bed dryer as the main dryer for the drying of wet biomass, the treatment amount of which is commonly over hundreds ton per day. Actually, fluidized bed dryer is currently widely used for the drying of over hundreds

ton per day of brown coal with water content over 60 wt% (wb), in the coal fire plant, using either hot gas or superheated steam as the drying medium for the same reason (Allardice DJ, 2007). The drying plant for the brown coal has been built and stability was investigated (Schmalfeld, 1996). However, different from brown coal, pure biomass particles could not be fluidized in the fluidized bed dryer due to its irregular shape and low density. To make biomass particles fluidization, biomass is usually fluidized by the following methods.

1.3.4.1 Co-fluidization with inert particles

Inert particles such as silica sands, glass beads and FCC (fuel cracking catalyst) particles could be fluidized well in the fluidized bed dryer. Through mixing biomass with the inert particles, biomass particles could also be fluidized. On the other side, inert particles addition could enhance the heat transfer rate in the fluidized bed dryer due to the increased heat exchange surface area.

1.3.4.2 Mechanical assisted fluidized dryer

Biomass particles could be fluidized without channeling or formation of large bubbles in the fluidized bed dryer with the assistance of vibration or agitation. Due to the assistance of vibration or agitation, lower gas velocity requires for a minimum fluidization velocity compared with a conventional fluidized bed dryer. For a vibrated fluidized bed dryer, a shallow bed is common for the effect of vibration imparted by the vibrating grid decays with distance from the grid. For an agitated fluidized bed dryer, a deeper bed is possible compared with a conventional fluidized bed dryer, due to the agitation which could increase fluidity of particles.

1.3.4.3 Spouted bed dryer

Spouted bed is able to handle granular products which are difficult to be fluidized. In a spouted bed dryer, gas with a very high velocity goes through the inlet with a small diameter at the bottom of the bed. Biomass particles then move with gas through the center of the bed from the bottom to the top. The particles fall back on the surface of spouted bed after losing the momentum which like a fountain action. Due to this action, biomass particles in the spouted bed could be mixed well. However, heat transfer rate was relatively decreased due to the inefficient gas-solid contact compared with general fluidized beds (Klassen and Gishler 1958).

1.4. Energy-saving process

The drying process consumes a large amount of energy for latent heat of the phase change. Theoretically, assuming an ambient temperature of 15 °C, the energy required for water evaporation ranges from 2.48 to 2.57 MJ per kilogram of evaporated water depending on the wet-bulb temperature (Brammer and Bridgwater 1999). In most industrialized countries, 10–25% of national industrial energy is used in drying processes (Strumillo, 2006). It is very necessary to develop an energy-efficient drying technology system with lower environmental impacts.

Since the 1970s, energy saving has contributed to various elements of societies around the world for economic reasons. Recently, energy saving technology has attracted increased interest in many countries as a means to suppress global warming and to reduce the use of fossil fuels. The combustion of fossil fuels for heating

produces a large amount of carbon dioxide, which is the main contributor to global greenhouse gas effects (Eastop & Croft 1990, Kemp 2007). Thus, the reduction of energy consumption for heating is a very important issue. Strumillo et al. (2006) summarized the important points regarding the reduction of energy consumption during drying: 1) the intensification of heat and mass transfer and, 2) heat recovery and efficient energy utilization. Regarding the latter, several methods have been developed to improve energy saving during drying, including pinch technology (Kemp 2005), mechanical vapor recompression (Fitzpatrick and D. Lynch 1995), heat-pump drying (Colak and Hepbasli 2009), solar combined drying (Yumrutas et al. 2003), multistage drying (Djaeni et al. 2007) and heat recovery by recycling exhausted air and integrating the drying system with other exothermic processes (Kemp 2005; Svoboda et al. 2009). However, for many of the drying systems employing conventional heat recovery, only about 20–30% of heat energy can be recycled because a minimum temperature difference is needed for heat exchange between the hot and cold streams according to the second law of thermodynamics (Linnhoff and Hindmarsh 1983).

1.4.1 Hot air drying with conventional heat recovery

In direct drying process, the heat required for water evaporation is provided mainly by the sensible heat of the air as the drying medium, and the major energy loss in the conventional drying process is from the exhausted steam. Thus, heat recovery from the exhausted air is a key to increase the energy efficiency of the dryer. The exhausted air–steam mixture could be utilized to preheat both drying medium

and wet material. However, due to the minimum temperature difference existing in the heat exchanger, 20–30 % of energy in the exhausted steam could be recovered.

1.4.2 Multistage drying

To fully utilize the input energy and to enhance the overall energy efficiency, multistage drying was developed. This technology shows a great energy-saving potential which could enable the use of lower temperature inlet steam. In superheated steam drying, Potter et al. (1981; 1990) developed a multistage drying process for brown coal drying to utilize steam condensation heat with heat recovery between successive fluidized beds (Fig. 1-5). Firstly, superheated steam with high temperature and pressure is generated from the steam generator by receiving the combustion energy from the heater. The generated superheated steam flows into the immersed tubes of the first stage to provide the drying heat for wet solid and then condenses into water, which is used to preheat the inlet wet solid. Latent heat of the evaporated water from the first stage is then used for the next stage drying. To utilize the latent heat of vaporization from the previous stage, the pressure decreases with increasing stage number. The multistage dryer efficiently use the heat of input superheated steam, however, a large amount of energy input still occurs due to the fuel combustion for the steam generation. The device cost will also increase as the stage number increasing.

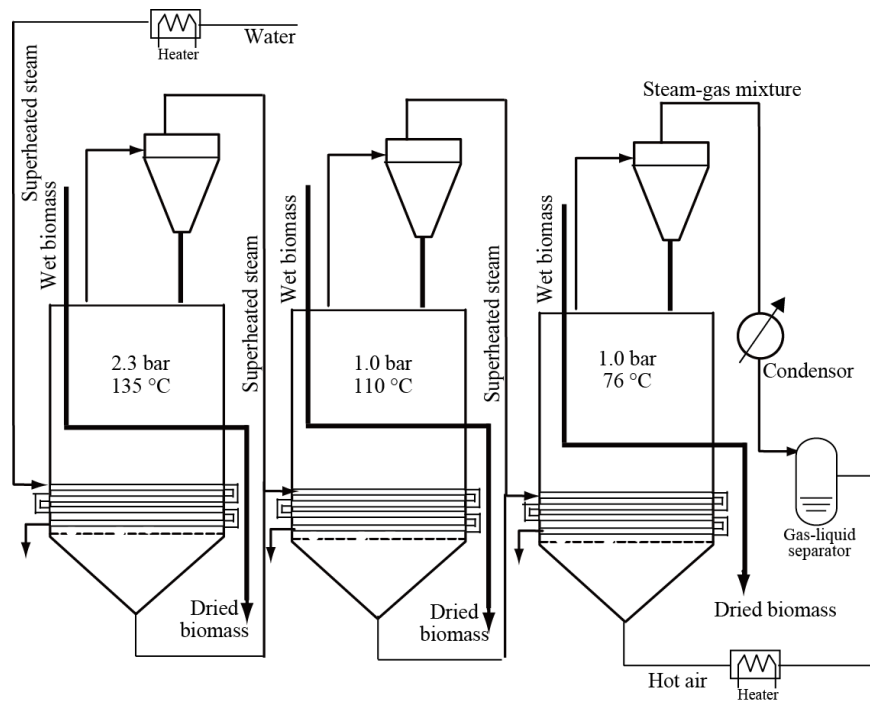


Fig. 1-5. Schematic process of multistage drying system

1.4.3 Mechanical vapor recompression

Fig. 1-6 shows the schematic process diagram of mechanical vapor recompression system with superheated steam as fluidizing/drying medium as it has been suggested by Fitzpatrick and Lynch (1995) which also referred to work done by Potter et al. (1984). The exhausted steam from the dryer is split into re-circulated and purged superheated steam which is equivalent to the water evaporated from the wet brown coal. The purged superheated steam is compressed by compressor and hence its temperature is elevated. Then, it flows to the fluidized bed for latent heat exchange (condensation of compressed steam mixture and evaporation of water possessed by biomass) and finally to heat exchanger for sensible heat exchange.

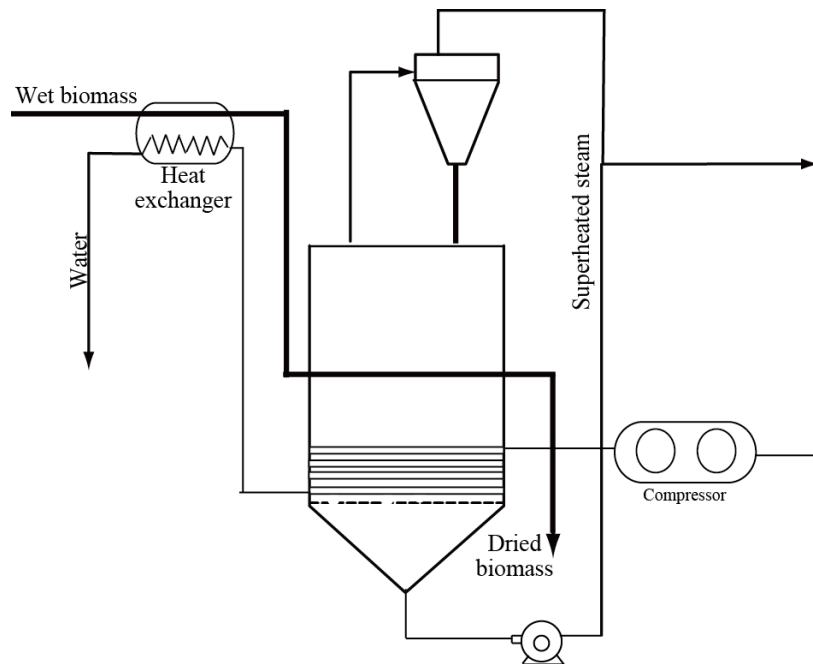


Fig. 1-6. Schematic process of mechanical vapor recompression system

There is no heat recuperation utilizing the sensible heat of the dried product, because the temperature, as well as the exergy rate, of the vapor is higher than that of the dried product. Therefore, the addition of heat equal to the sensible heat of the dried product is required to be input to the system.

1.4.4 Heat pump drying process

The heat pump dryer was explored since the 1970s and demonstrated as a promising energy saving process. The principle of heat pump dryer is to dehumidify and heat the exhausted gas through recovering the latent heat in the exhausted gas by heat exchange between the exhausted gas and the refrigerants. It is now commonly used for low temperature drying under 50 °C such as agricultures and fruits which need a low temperature list from the environment temperature (Lee et al. 2010).

However, it is not suitable for high temperature drying in case of an over 100 °C temperature lift, because more compressor work is required to provide to large amount of energy for a high temperature lift, which causes a low coefficient of performance (COP) (Kemp 2005).

1.4.5 Self-heat recuperation technology (SHR)

To further save consume energy in a process, Kansan et al. developed a theory of self-heat recuperation technology (SHR), in which both the latent heat and the sensible heat of the process stream can be circulated without any heat addition (Kansha et al. 2009). In this technology, i) a process unit is divided on the basis of functions to balance the heating and cooling loads by performing enthalpy and exergy analysis and ii) the cooling load is recuperated by compressors and exchanged with the heating load. As a result, the heat of the process stream is perfectly circulated without heat addition, and thus the energy consumption for the process can be greatly reduced. By means of the compression of the effluent stream, the effluent stream is heated to provide the minimum temperature difference for heat exchange with the feed stream, and all of the self-heat of the process stream is recycled based on exergy recuperation to reduce the energy consumption (Fig. 1-7). The input energy (compressor work) in SHR was dramatically reduced to 1/5-1/22 of that of heat pinch technology (Kansha et al. 2009).

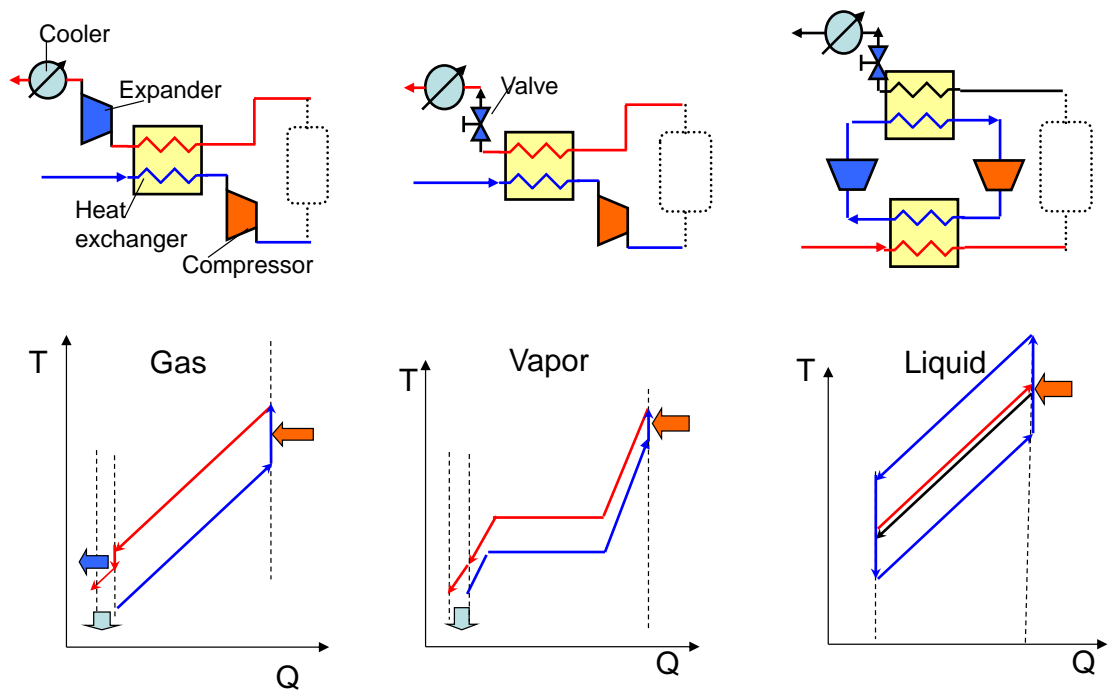


Fig. 1-7. Self-heat recuperation technology.

There are similarities between a heat pump dryer and an SHR dryer that both systems elevate low-exergy exhausted heat to high-exergy heat and recycle the heat for subsequent drying. The principle of a common heat pump dryer is to dehumidify and heat the exhausted gas through recovering latent heat in the exhausted gas by heat exchange between the exhausted gas and refrigerants for energy saving (Kiang and Jon 2009). Heat pump dryer is now commonly used for low-temperature drying below 50 °C such as that in agriculture and fruit production, which require a small increase in temperature from the environment temperature (Lee et al. 2010). However, the heat pump dryer is not suitable for high-temperature drying where the temperature needs to be raised more than 100 °C, because more compressor work is required to provide a large amount of energy for a large temperature rise, which

results in a low coefficient of performance (Kemp 2005). Additionally, much exergy is lost in the heat transfer owing to the large temperature difference between the hot and cold streams. By contrast, an SHR dryer can use the self-heat of the effluent, and therefore, only a small amount of work is required to provide a minimum temperature difference between the hot and cold streams for heat exchange. An SHR dryer thus has wider application and achieves greater energy savings than a heat pump dryer (Fig. 1-8). Coefficient of performance (COP) is usually used to check the performance of a heat pump. The COP of SHR is calculated as high as 30. This value is much higher than that of heat pump which commonly under 10. Thus, SHR is hopeful to be applied for heat and cooling process, separation process and reaction process which mainly exist in chemical plant.

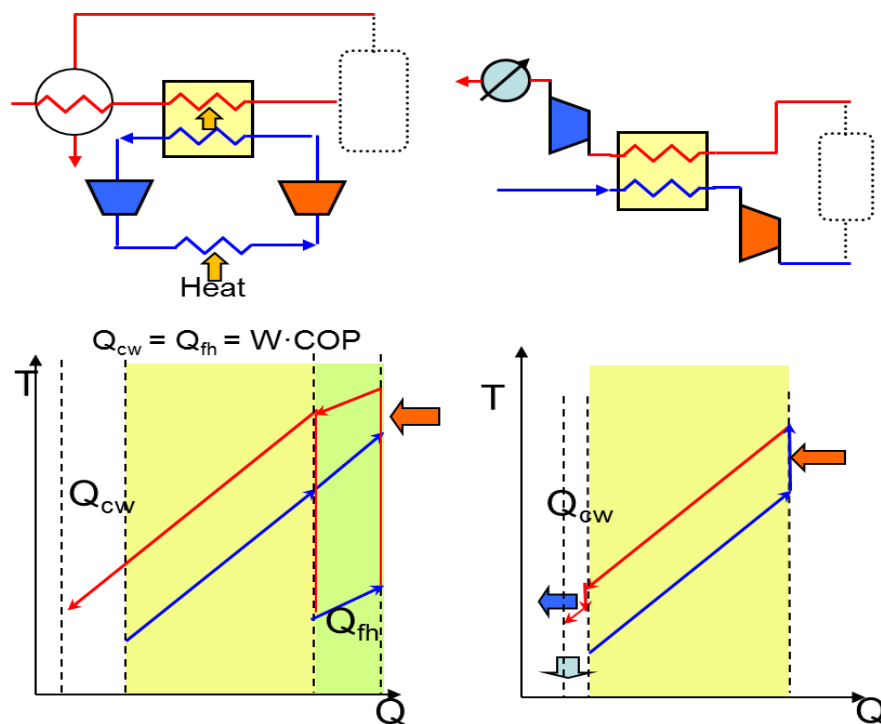


Fig. 1-8. Comparison of SHR with Heat pump dryer.

1.5. Scope and structure of this research

Wet biomass has low energy density which limited by economic feasibility compared with fossil fuels causing less biomass is used currently. In this research, a self-heat recuperative biomass dryer was developed, with the objective of reducing the energy consumption required for biomass drying and to develop a more compact and efficient dryer.

In Chapter 2, exergy losses were investigated in the drying process and heat pairing concept was brought out to apply SHR technology for the drying process. Energy analysis was performed for the investigations of in the existing energy-saving drying processes.

In Chapter 3, SHR technology was succeeded to be applied for biomass drying in a fluidized bed dryer for reducing energy consumption. Biomass drying experiments were conducted in the exergy recuperative fluidized bed dryer to investigate hydrodynamic behavior and stability in the fluidized bed dryer based on the simulation conditions.

In Chapter 4, SHR technology was applied to other biomass drying systems (Rotary dryer and screw conveyor dryer) with gas as the drying medium and exergy analysis was conducted in the proposed drying process.

In Chapter 5, a further energy-saving drying module using superheated steam as the drying medium based on SHR technology was brought out and applied for biomass drying processes. Biomass drying experiments with steam as the drying medium were conducted in the fluidized bed dryer based on the simulation

conditions. Moreover, a novel fluidized bed dryer was proposed was designed and used for biomass drying, which was more compact and economical without inert particles or mechanical assistant.

In Chapter 6, summary and future work of this research was discussed. SHR technology is to be applied to a combined drying and torrefaction process for the production of torrefied wood pellets. The success will enable the development markets for forest and agricultural biomass residues, contributing to the sustainable development of natural resources. SHR technology also shows a good front view by applying for brown coal drying.

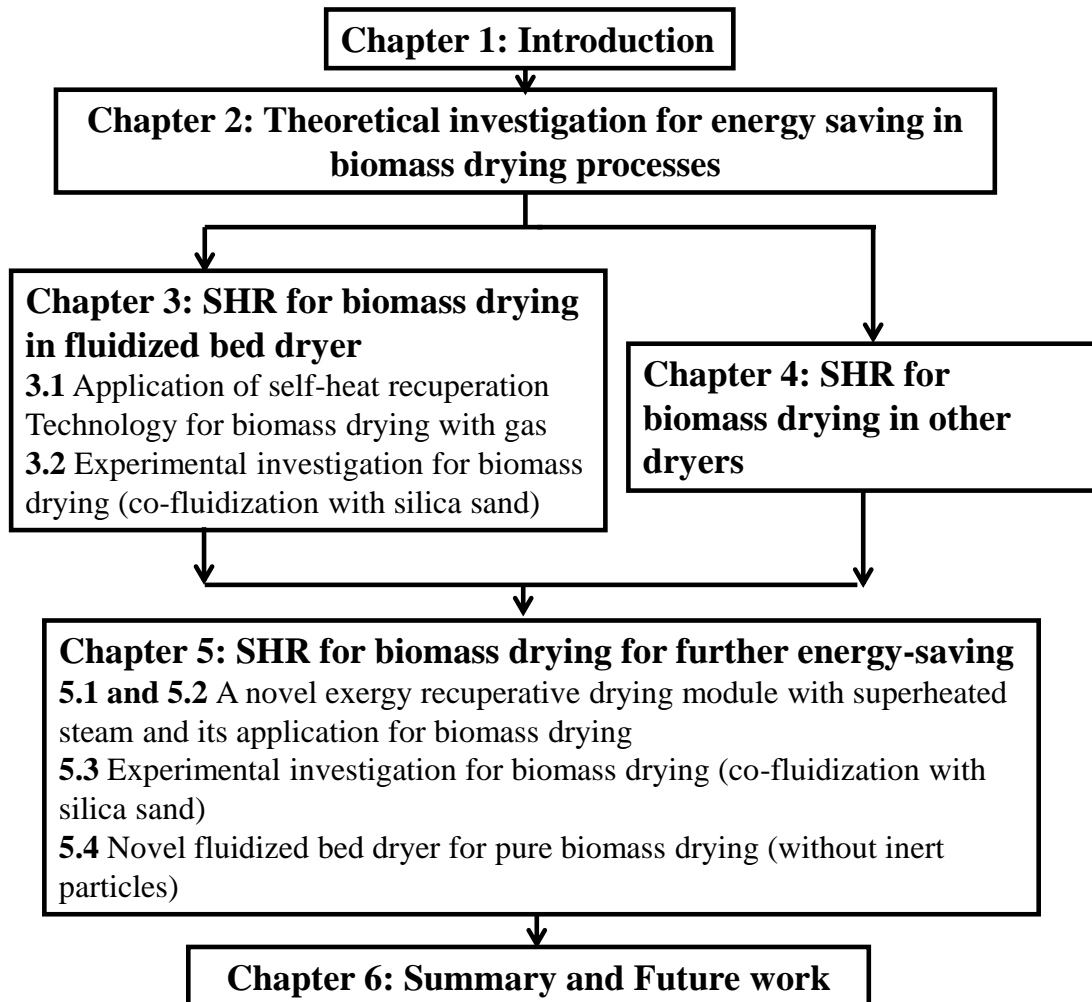


Fig. 1-9. Scope and structure of this research.

References

- Allardice DJ, Chaffee AL, Jackson WR, Marshall M (2004) Water in brown coal and its removal. In: Li CZ (ed) *Advances in the science of Victorian brown coal*. Elsevier, Oxford, pp. 85-133.
- Berry, S. L. and M. L. Roderick. 2005. Plant-water relations and the fibre saturation point. *New Phytologist*, 168(1), 25-37.
- Brammer, J. G. and A. V. Bridgwater. 1999. Drying technologies for an integrated gasification bio-energy plant. *Renewable & Sustainable Energy Reviews*, 3(4), 243-289.
- Colak, N. and A. Hepbasli. 2009. A review of heat-pump drying (HPD): Part 2-Applications and performance assessments. *Energy Conversion and Management*, 50(9), 2187-2199.
- Daud, W. R. W. 2008. Fluidized Bed Dryers - Recent Advances. *Advanced Powder Technology*, 19(5), 403-418.
- De Wild, P. J., H. den Uil, et al. 2009. Biomass valorisation by staged degasification A new pyrolysis-based thermochemical conversion option to produce value-added chemicals from lignocellulosic biomass. *Journal of Analytical and Applied Pyrolysis*, 85(1-2), 124-133.
- Djaeni, M., P. Bartels, et al. 2007. Multistage zeolite drying for energy-efficient drying. *Drying Technology*, 25(4-6), 1053-1067.
- Eastop, T.D. & Croft, D.R. (1990). *Energy Efficiency for Engineers and Technologists*,

Longman Scientific & Technical, ISBN 0-582-03184-2, London, UK

Fitzpatrick, J. and D. Lynch. 1995. Thermodynamic analysis of the energy saving potential of superheated steam drying. *Trans. IChemE*, 73 (C), 3-8.

Fitzpatrick, J. J. and D. Lynch. 1995. Thermodynamic analysis of the energy saving potential of superheated steam drying. *Food and bioproducts processing : transactions of the Institution of Chemical Engineers, Part C.*, 73, 3-8.

Horio, M. and Mori, S. 1999. *Fluidization Handbook*. Japan, Association of Powder Process Industry & Engineering.

Kaliyan, N. and R. V. Morey. 2009. Factors affecting strength and durability of densified biomass products. *Biomass & Bioenergy*, 33(3), 337-359.

Kansha, Y., N. Tsuru, et al. 2009. Self-Heat Recuperation Technology for Energy Saving in Chemical Processes. *Industrial & Engineering Chemistry Research*, 48(16), 7682-7686.

Kemp, I. C. 2005. Reducing dryer energy use by process integration and pinch analysis. *Drying Technology*, 23(9-11), 2089-2104.

Kemp, I.C. 2007. *Pinch Analysis and Process Integration A User Guide on Process Integration for the Efficient Use of Energy* 2nd Ed., Elsevier, ISBN 13 978-0-75068-260-2, Oxford, UK

Kiang, C. S. and C. K. Jon 2009. Heat Pump Drying Systems. Handbook of Industrial Drying. A. S. Mujumdar. New York, Taylor & Francis Group: 1103-1131.

Lee, K. H., O. J. Kim, et al. 2010. Performance Simulation of a Two-Cycle Heat

- Pump Dryer for High-Temperature Drying. *Drying Technology*, 28(5), 683-689.
- Linnhoff, B. and E. Hindmarsh. 1983. The Pinch Design Method for Heat-Exchanger Networks. *Chemical Engineering Science*, 38(5), 745-763.
- Maciejewska, A., H. Veringa, et al. Co-firing of biomass with coal: constraints and role of biomass pre-treatment. http://ie.jrc.ec.europa.eu/publications/scientific_publications/2006/EUR22461EN.pdf
- Marland, G., T.A. Boden, and R. J. Andres. 2007. Global, Regional, and National CO₂ Emissions. In *Trends: A Compendium of Data on Global Change*. [Carbon Dioxide Information Analysis Center](#), Oak Ridge National Laboratory, [United States Department of Energy](#), Oak Ridge, Tenn., U.S.A.
- McKendry, P. 2002. Energy production from biomass (part 2): conversion technologies. *Bioresource Technology*, 83(1), 47-54.
- Pakowski, Z., B. Krupinska, et al. (2007). "Prediction of sorption equilibrium both in air and superheated steam drying of energetic variety of willow *Salix viminalis* in a wide temperature range." *Fuel* **86**(12-13): 1749-1757.
- Perre P., Almeida G., and Colin J., Energy issues of drying and heat treatment for solid wood and other biomass sources. In *Modern Drying Technology, Energy Savings*, Tsotsas, E.; Mujumdar, A. S., Eds. Wiley-VCH: 2012; pp 245-289.
- Potter, O. E., C. J. Beeby, et al. 1984. Drying Brown Coal in Steam-Heated,

- Steam-Fluidized Beds. *Drying Technology*, 2(2), 219-234.
- Schmalfeld, Frankfurt, et al. 1996. Experience with the operation of the steam-fluidized-drying (SFBD plant Ioy yang, Australia, VDI conference on energy and power technology in Siegen.
- Siau, J. F. (1984). Transport Processes in Wood. New York, Springer-verlag.
- Stahl, M., K. Granstrom, et al. 2004. Industrial processes for biomass drying and their effects on the quality properties of wood pellets. *Biomass & Bioenergy*, 27(6), 621-628.
- Stanish, M. A., G. S. Schajer, et al. 1986. A Mathematical-Model of Drying for Hygroscopic Porous-Media. *AIChE Journal*, 32(8), 1301-1311.
- Strumillo, C., Jones, P. L., Zylla, R., *Handbook of Industrial Drying*, Ch.46, 2006, New York.
- Svoboda, K., J. Martinec, et al. 2009. Integration of biomass drying with combustion/gasification technologies and minimization of emissions of organic compounds. *Chemical Papers*, 63(1), 15-25.
- Wang, L., C. L. Weller, et al. 2008. Contemporary issues in thermal gasification of biomass and its application to electricity and fuel production. *Biomass & Bioenergy*, 32(7), 573-581.
- Yumrutas, R., M. Kunduz, et al. 2003. Investigation of thermal performance of a ground coupled heat pump system with a cylindrical energy storage tank. *International Journal of Energy Research*, 27(11), 1051-1066.

CHAPTER 2

THEORETICAL INVESTIGATION FOR

ENERGY SAVING IN BIOMASS DRYING

PROCESSES

2.1. Exergy analysis of the heat transfer during the drying process

Exergy changes of both streams by heat transfer can be calculated by the following equations with the law of energy conservation.

$$dEX_{\text{loss}} = dh - T_0 ds \quad (2-1)$$

dh is the enthalpy change and ds is the entropy change of both streams. Exergy loss in the hot and cold streams can be calculated as following:

$$dEX_{\text{loss,hot}} = dh_{\text{hot}} - T_0 ds_{\text{hot}} = -dQ - T_0 ds_{\text{hot}} \quad (2-2)$$

$$dEX_{\text{loss,cold}} = dh_{\text{cold}} - T_0 ds_{\text{cold}} = dQ - T_0 ds_{\text{cold}} \quad (2-3)$$

Thus, exergy loss (dEX_{loss}) associated with this differential heat (dQ) can be derived as:

$$dEX_{\text{loss}} = -(dEX_{\text{loss,hot}} + dEX_{\text{loss,cold}}) = T_0 (ds_{\text{hot}} + ds_{\text{cold}}) \quad (2-4).$$

Here, ds_{hot} has a negative value. It is known that

$$dQ = T ds_{\text{cold}} = -(T + \Delta T) ds_{\text{hot}} \quad (2-5).$$

Thus, Eq. 2-4 can be rewritten with the temperature difference (ΔT) between the hot and cold streams, the temperature of cold streams (T), as shown in eq. 2-6 (Kansha et al, 2013):

$$dEX_{\text{loss}} = -\frac{T_0}{T} \Delta T ds_{\text{hot}} = \frac{T_0}{T + \Delta T} \Delta T ds_{\text{cold}} \quad (2-6)$$

This means that exergy loss of heat transfer is a function of temperature difference between hot and cold streams (ΔT) and that the exergy loss increases with increasing of ΔT . If heat exchange temperature ΔT is much smaller than T_0 and T , and the

temperature of the cold stream (T) is close to the standard temperature (T_0). The exergy loss in heat transfer can be simply expressed by the following equation:

$$\Delta EX_{\text{loss}} \approx \Delta T \Delta s \quad (2-7)$$

Eq. 2-7 means that ΔEX_{loss} becomes close to $\Delta T ds_{\text{cold}}$ when T is close to T_0 . Thus, the total exergy loss (EX_{loss}) during heat transfer becomes $\Delta T \Delta s$ due to the summation of this exergy loss.

For biomass drying, water in the biomass is divided into two forms—free water held by the capillary forces in the microcellular biomass and bound water absorbed by the porous cell wall of the biomass. The drying of biomass is complicated and requires an energy supply to overcome the many forces inside the biomass, such as capillary forces, forces relating to water diffusion, sorption forces and even chemical bonding forces. Here, we consider the two main factors, i.e., capillary forces and sorption forces. Thus, the input exergy for biomass drying (E) should include both the exergy required for irreversibility during heat exchange (E_{HX}) and bound-water desorption (E_{sorp}):

$$E = E_{\text{HX}} + E_{\text{sorp}} \quad (2-8)$$

To separate water from the biomass by thermal drying, both free water and bound water need to be heated. The exergy required owing to irreversibility during heat exchange is calculated in eq 2-9:

$$E_{\text{HX}} = (m_p \Delta S_p + m_l \Delta S_l) \Delta T + (m_{\text{free}} + m_{\text{sorp}}) \frac{\Delta H_{\text{trs}}}{T_{\text{trs}}} \Delta T \quad (2-9)$$

The first and second terms on the right side of eq 2-9 represent the exergy required

for preheating of wet biomass and evaporation of water in the biomass, respectively. Here, m_p , m_l , m_{free} and m_{sorp} are the mass of (dry) biomass, water in the wet biomass, free water and evaporated bound water, respectively. ΔH_{trs} and T_{trs} are the evaporation enthalpy following phase transition and the phase transition temperature. ΔS_p and ΔS_l are the entropy change of biomass and water during the heating process, and ΔS_p can be calculated:

$$\Delta S_p = \int_i^f \frac{C_p}{T} dT \quad (2-10)$$

where C_p is the heat capacity of the biomass and calculated from eq 2-11 (Simpson and TenWolde 1999).

$$C_p = 0.1031 + 0.003867T \quad (2-11)$$

In addition, bound water needs energy to desorb from the polymer chains within the cell wall. The bound water amount equals the amount of water existing below the fiber saturation point (FSP) (Berry and Roderick 2005). The FSP varies at a different temperature and can be commonly calculated by eq 2-12 (Siau 1984):

$$X_{fsp} = 0.30 - 0.001(T_{dry} - 20) \quad (2-12)$$

where T_{dry} is the biomass drying temperature in the fluidized bed and is 90 °C in this work. X_{fsp} is calculated as 0.23 which means 1 kg dry biomass contains 0.23 kg bound water. Then, evaporated bound water, m_{sorp} can be calculated as

$$m_{sorp} = m_1 \left(\frac{X_{fsp}}{1 + X_{fsp}} - X_{final} \right) \quad (2-13)$$

where X_{final} is the final water content of the dried biomass which is 10 wt% (wb) in this work. The water sorption heat in biomass, ΔH_{sorp} , can be calculated from the

sorption isotherm using the Clausius–Clapeyron equation given as eq 2-14 (Skaar 1988). R is the universal gas constant ($8.314 \text{ kJ (kmol K)}^{-1}$), M_v is the molar mass of water, P_v/P_{vs} is the ratio of equilibrium vapor pressure to saturated vapor pressure and T_{sorp} is the adsorption temperature. ΔH_{sorp} is expected to be consistent as the sorption heat for the oven-dry biomass which is 1000 kJ kg^{-1} (Skaar 1988).

$$\Delta H_{\text{sorp}} = -\frac{R}{M_v} \frac{d(\ln \frac{P_v}{P_{vs}})}{d(T_{\text{sorp}}^{-1})} \quad (2-14)$$

The exergy required for bound water desorption is given:

$$E_{\text{sorp}} = \sum_{n=1}^n (m_{n-1w} - m_{nw}) \Delta H_{\text{sorp}} \quad (2-15)$$

Based on the above equations, we could find that temperature difference should be near to the minimum temperature difference (ΔT_{min}) of the heat exchanger for exergy loss minimization drying the heat exchange process.

2.2. Heat pairing

To make the heat exchange temperature difference is the ΔT_{min} at each point in the heat exchanger. We brought a new concept named heat pairing. Heat pairing which means that the sensible and latent heats are paired with the corresponding sensible and latent heats, is feasible to form the heat circulation for exergy loss minimization. If the heat capacity is independent from the pressure, hot and cold streams are always in parallel and separated by the ΔT_{min} . Thus, exergy loss becomes the minimum and all of the heat including latent and sensible heats in the system can be recirculated

effectively by the least compression work input. Heat pairing concept for biomass drying is shown in Fig. 2-1. The dryer can be separated into three parts, in which the sensible heat of water is exchanged for preheating to boiling point (dryer 1), the latent heat of water is exchanged for evaporation (dryer 2), and the sensible heat of steam is exchanged for superheating (dryer 3). The final status of the cold stream is compressed to create a temperature difference and recycled for heat exchange with cold stream for self-heat recuperation.

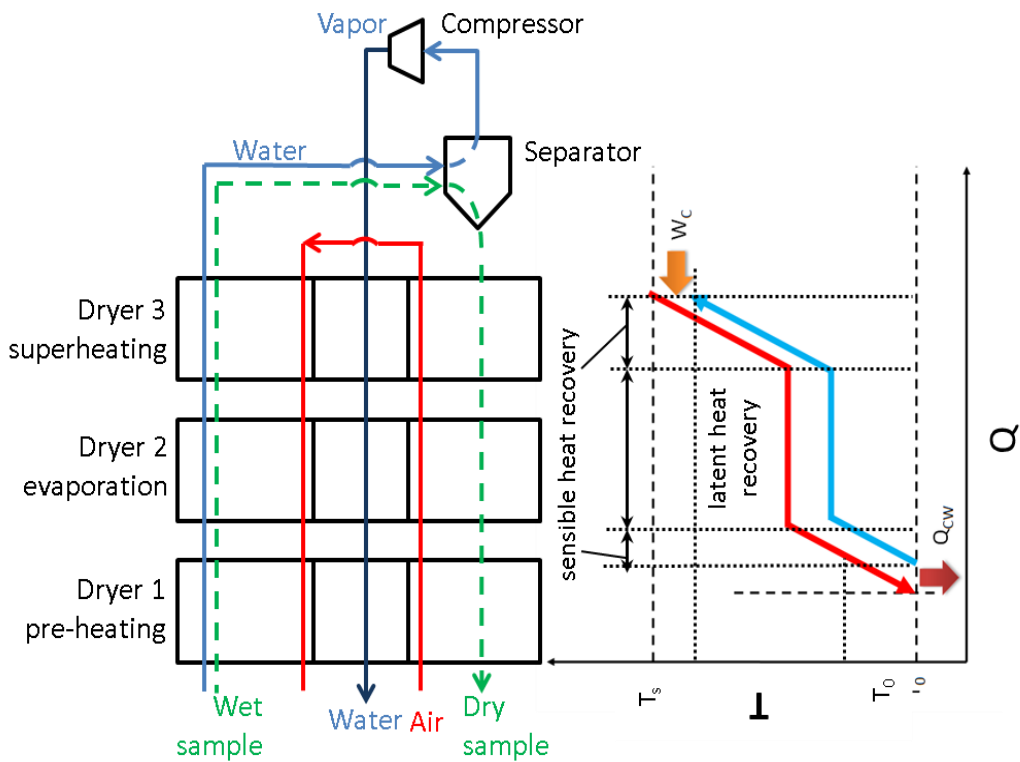


Fig. 2-1. Basic concept of heat pairing: left) flows of sample, water and gas and right) temperature diagram of water.

Actually we found the mismatched heat pairing is the main reason that the existing energy-saving biomass drying processes are still consuming a large amount of energy. We will explain it in detail in the following.

2.3. Existing energy-saving biomass drying systems

Thermodynamic analysis is conducted on the existing energy-saving drying systems. These systems can be divided into the conventional heat recovery drying process (CHR), multistage drying process (MSD) and mechanical vapor recompression drying process (MVR).

2.3.1. Conventional heat recovery drying process

Fig. 2-2 shows the configuration of a conventional heat recovery dryer. The boxes represent units, and the lines represent the flow of materials or energy. The material flow in the diagrams comprises the flow of air, (dry) biomass and water, and wet biomass is considered as combined (dry) biomass and water. We assumed that a heat exchanger (HX) can be divided into a self-heat transmitter (HT) and a self-heat receiver (HR). The concept of the CHR arises from the heat cascade utilization. The exhausted steam is utilized to preheat the wet solid. In the CHR, a large amount of latent heat and sensible heat of water below 373 K cannot be recovered as a minimum temperature approach between the hot and cold streams required for heat exchange. In general, a perfect heat matching is impossible because of the existence of pinch point, resulting in a large amount of exergy loss.

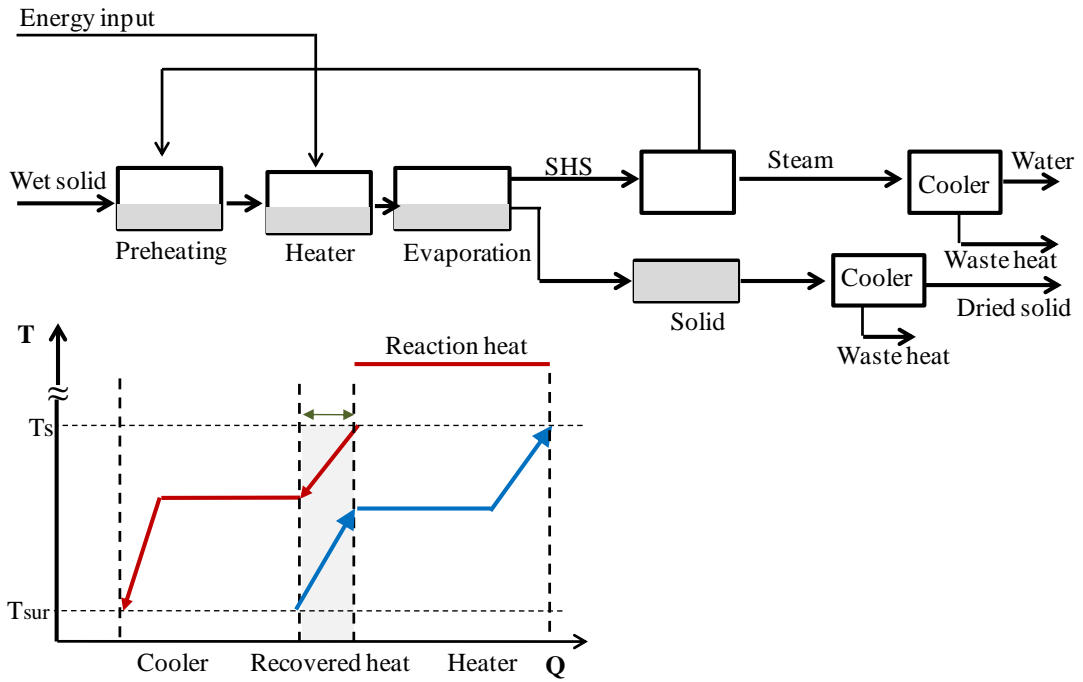


Fig. 2-2. Conventional heat recovery drying. SHS stands for superheated steam.

2.3.2. Multistage drying process

Energy balances for the steam generator and each stage of the MSD can be conducted as follows:

- 1) Energy input for the generation of high-temperature and high-pressure superheated steam

$$H_{\text{MSD}} = m_{\text{SHS}} [L_{0e} + C_{\text{pw}} (T_{\text{super}} - T_{\text{sur}})] \quad (2-16)$$

- 2) First stage

$$m_{\text{SHS}} [L_{0e} + C_{\text{pw}} (T_{\text{super}} - T'_{\text{super}})] = \frac{w_1 - w_2}{1 - w_1} m_1 L_{1e} + \Delta H_1 + m_1 w_1 C_{\text{pw}} (T_1 - T_{\text{sur}}) + m_1 (1 - w_1) C_{\text{ps}} (T_1 - T_{\text{sur}}) \quad (2-17)$$

- 3) "i" stage

$$\frac{w_1 - w_2}{1 - w_1} m_{i-1} \left[L_{i-1e} + C_{pw} (T_{i-1} - T'_{i-1}) \right] = \frac{w_1 - w_2}{1 - w_1} m_i L_{ie} + \Delta H_i + m_i w_1 C_{pw} (T_i - T_{sur}) + m_i (1 - w_1) C_{ps} (T_i - T_{sur}) \quad (2-18)$$

where w_2 is the final water content of the dried solid. T_{super} , T'_{super} and T_1 are the inlet superheated steam temperature, condensed water temperature and drying temperature, respectively, at Stage 1. T_{i-1} , T'_{i-1} and T_i are the inlet superheated steam temperature, condensed water temperature and drying temperature, respectively, at Stage i . L_{0e} , L_{1e} and L_{ie} are latent heats of water evaporation at different pressures; m_1 , m_{i-1} and m_i are the wet solid input amounts at the corresponding stage. The total amount of treated wet solid in the MSD is:

$$m_{tot} = \sum m_i = m_1 + m_2 + m_3 + \dots + m_i \quad (2-19)$$

Compared with the CHR, the MSD could utilize the energy of the inlet steam in the drying process efficiently. However, a large amount of exergy loss still occurs due to the fuel combustion for the steam generation as shown in Fig. 2-3, in which the solid and dash-dot lines represent the heating and cooling streams. Condensed water is cooled to purge the additional exergy which is the gray colored area in Fig. 2-3, and the total amount is equal to the exergy loss during the combustion based on the energy balance. Thus, the larger the gray area is, the more exergy loss occurs in the drying process.

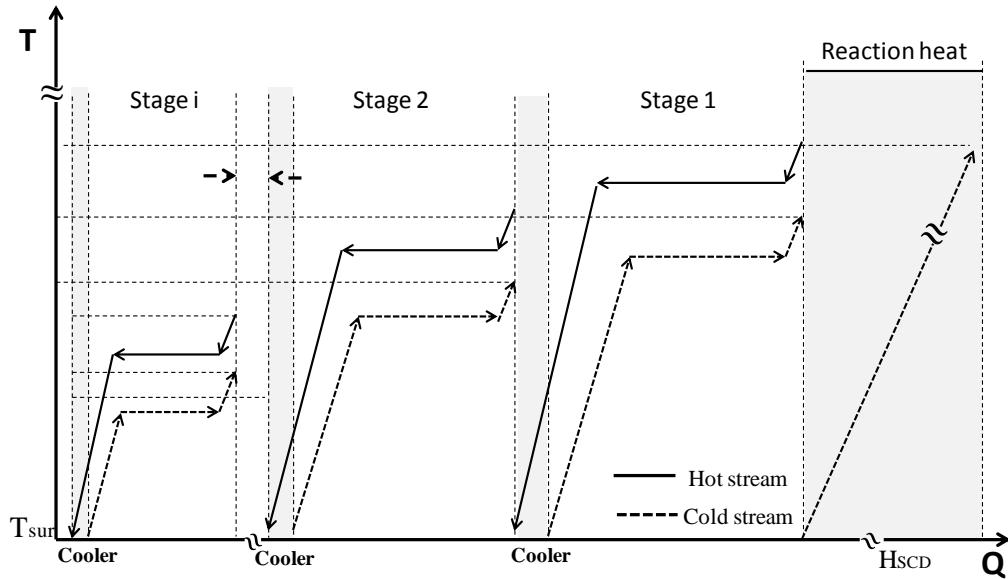


Fig. 2-3. Temperature and heat diagram of the MSD.

2.3.3. Mechanical vapor recompression drying process

The MVR technology could recycle the latent heat of evaporated solvent for decreasing the input energy and has already been applied to the desalination (Darwish and ElDessouky, 1996), distillation (Brousse et al., 1985; Lynd and Grethlein, 1986) and drying processes (Ewers et al., 2003; Kakaras et al., 2002). The exhausted steam is compressed for a higher exergy rate and recirculated to be utilized as a heat source for successive wet solid drying. Energy consumption of the MVR is equal to the enthalpy increase of the inlet streams based on the energy balance:

$$W_{cp,MVR} = \left[(1-w_1)m_{wet}C_{ps} + w_1m_{wet}C_{pw} \right] (T_2 - T_{sur}) + \frac{w_1 - w_2}{1-w_1} m_{wet}C_{pw} (T_2' - T_{sur}) \quad (2-20)$$

T_2 and T_2' are the drying temperature and temperature of the outlet condensed water,

respectively, and m_{wet} is the input wet solid amount.

The MVR reduces energy consumption by the compression of the exhausted steam and this eliminates the exergy loss occurring in the steam generator. Unfortunately, this system cannot recover the sensible heat of the condensed water effectively, as shown in Fig. 2-4. The condensed water with a high temperature is wasted in a cooler shown as the gray colored area. This occurs because of unmatched heat pairing in the MVR. Thus, additional energy equal to the unrecovered heat energy in the hot stream, is required to be input into the system through the compressor.

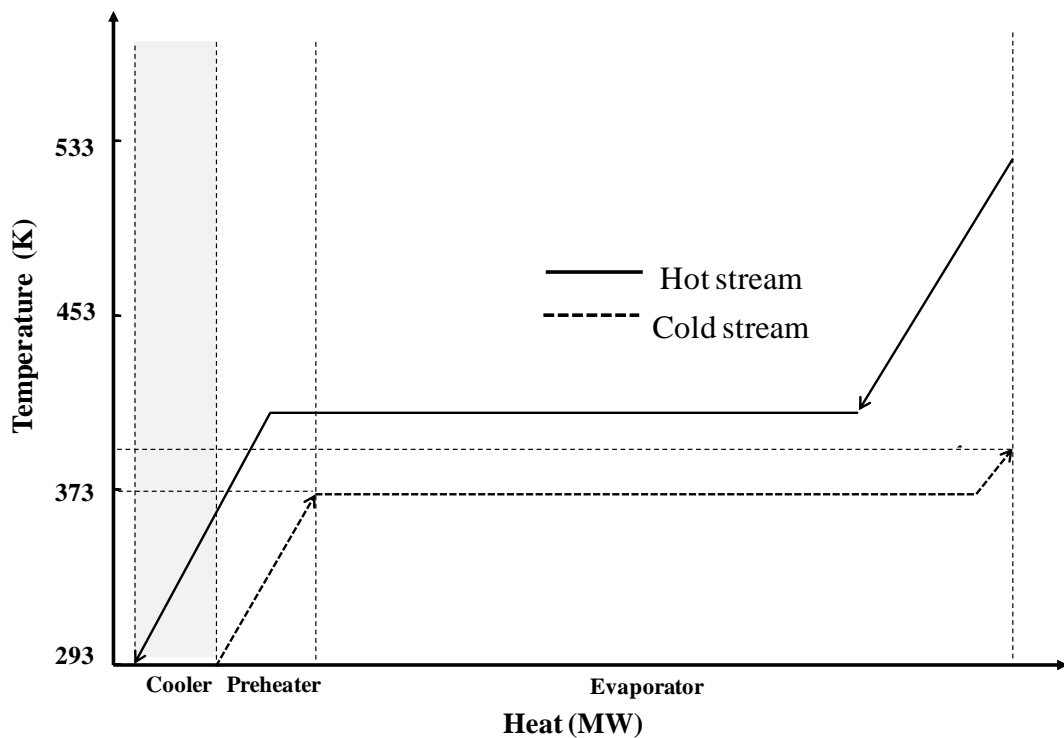


Fig. 2-4. Temperature and heat diagram of the MVR.

2.4. Initial evaluation of energy efficiency in a biomass fluidized bed dryer based on SHR technology

2.4.1. Concept of SHR technology based fluidized bed drying

Principally, state-of-the-art SHR technology is developed based on the idea of SHR technology, by which both latent and sensible heat from the process stream can be circulated without heat addition. The hot stream is heated by compression, to provide the minimum temperature difference required for heat pairing and exchange with the cold stream, and all of the self-heat of the process stream is recirculated based on exergy recuperation. As a result, all of the heat involved in drying can be recuperated and reused as a heat source for the subsequent drying process. This includes recuperation of sensible heat from the gas serving as the drying medium, both sensible and latent heat of the evaporated water and the sensible heat of the dried products. In addition, SHR also recovers the energy utilized to increase the exergy rate of the evaporated water and drying medium exhausted from the dryer.

A schematic of the SHR-FBD designed for the biomass drying system, using air as the drying/fluidizing medium, is shown in Fig. 2-5. Wet biomass is fed and heated through a pre-heater (dryer 1a) to a certain temperature. Subsequently, the main drying stage (water evaporation) is performed inside the FBD (dryer 2). The internal heat exchangers, which are filled by a compressed mixture of air and steam, are immersed inside the FBD, providing the heat required for water removal. The exhausted mixture of air and steam is then superheated (dryer 3) and continuously flows to a compressor for pressure increase. The compressed vapor (air-steam

mixture), with higher exergy rate, is circulated back and utilized as the heat source for superheating (dryer 3), evaporation (dryer 2) and pre-heating (dryer 1a), in that order. In addition, the sensible heat of the hot, dried biomass is recovered by the drying medium, to further reduce drying energy consumption (dryer 1b).

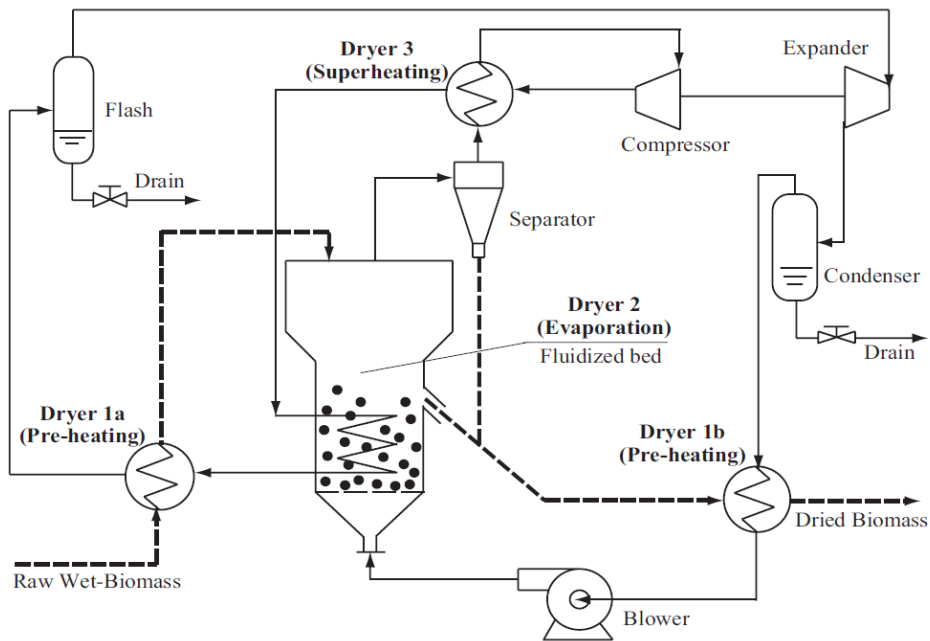


Fig. 2-5. Schematic layout of the SHR-FBD using air as the fluidizing/drying medium.

In general, as the pressure increases, the saturation temperature of the exhausted mixture of air and steam rises accordingly. Pressure increase is conducted so that the heat pairing and exchange between each sensible and latent heat matches optimally. Here, the determination of the optimal pressure increase becomes one of the key factors for successfully achieving the maximum energy reduction in the proposed

drying process. In addition, a superheating stage (dryer 3) can be introduced, with the objective of preserving a complete vapor phase (vapor quality, x , equal to 1.0) to avoid water condensation during compression. This superheating stage is optional, and its existence/extent depends strongly on the relative humidity of the exhausted mixture of air and steam and also the system performance (heat loss, etc).

The compressor increases the saturation temperature of the exhausted air-steam mixture. An expander is utilized to recover the compression work from the compressed air-steam mixture. In addition, a blower is installed to provide the pressure difference required for fluidization. A flash is installed before the expander, which drains the condensed water to ensure the high quality of the vapor entering the expander. Finally, a condenser cools the air-steam mixture and subsequently drains the condensed water. Hence, the moisture carrying capacity of the air increases. Here, it should be noted that although air is used as a drying medium in both the SHR drying system and in conventional hot air drying, the systems are significantly different in terms of the heat source required for water removal. In hot air drying, the latent heat required for water evaporation is provided only by the sensible heat of the air drying medium, using an external heat source such as a furnace or electric heater. Thus, the temperature of the air is usually high, resulting in a high risk of fire, difficulty during drying operations, and high drying energy consumption. On the other hand, in the proposed SHR drying system, the evaporation heat is provided by the condensation heat of the compressed vapor (air-steam mixture). Hence, the temperature of the inlet air is significantly lower than that used for hot air drying.

2.4.2. Process Design and Calculations

To evaluate the energy efficiency of the SHR-FBD, the mass and energy balance was calculated using Pro/II ver. 9.0 software (Invensys Corp.). The energy consumption of the SHR-FBD is compared with that of the CHR and that of the SHR-FBD assuming (1) the FBD with internal heat exchanger can be as a mixer, a heat exchanger and a separator, (2) complete mixing inside the FBD, (3) the heat exchange is cocurrent in the FBD and countercurrent in other heat exchangers, (4) the minimum temperatures (ΔT_{\min}) in the FBD and other heat exchangers approach are 10 and 30 K respectively, (5) in order to compare the energy consumption in the different drying processes, we assume that the biomass inlet flow rate is the same as 5000 kg h^{-1} with the initial moisture content of 75 wt% (wb), (6) drying is conducted until a moisture content of 10 wt% (wb) is reached in all the drying processes, (7) the air velocity is set to be three times minimum fluidization velocity for the biomass drying in the FBD based on the experimental result from section 4.2, (8) the adiabatic efficiencies of the compressor, blower and expander are 80%, 80% and 90%, respectively, (9) drying is performed under atmospheric conditions, (10) thermodynamic calculations employ the Soave–Redlich–Kwong (SRK) method, (11) there is no heat loss from the system and no mass transport resistance in any phase.

2.4.3. Energy comparison of the drying processes

The energy balance is calculated for the entire drying system according to the energy conservation law:

$$\sum_{i \text{ n}} m_{i \text{ n}} h_{i \text{ n}} = \sum_{o \text{ u t}} m_{o \text{ u t}} h_{o \text{ u t}} + H \quad (2-21)$$

where m_{in} and m_{out} are the input and output mass flows of material, h_{in} and h_{out} are the input and output specific enthalpy and H_{loss} is zero, assuming no heat loss from the system to the surroundings.

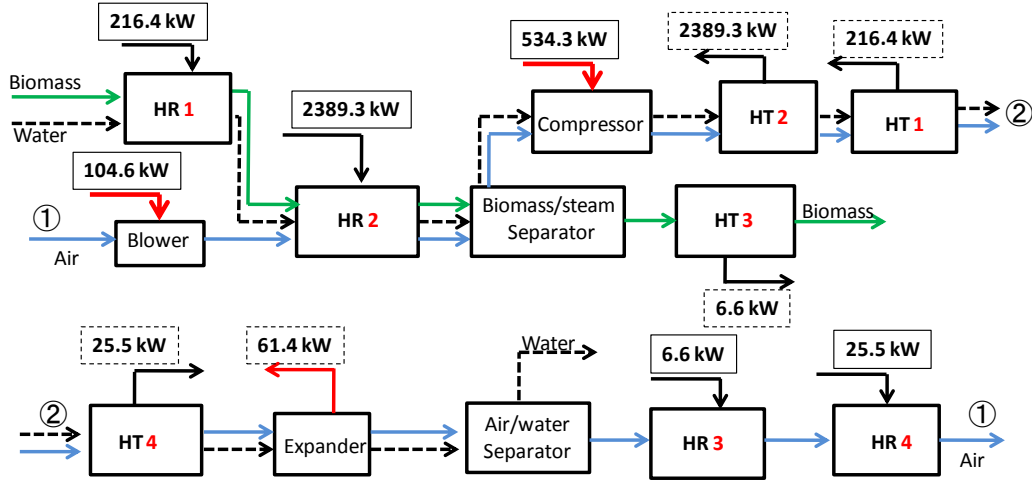


Fig. 2-6. Energy and materials flow diagrams of SHR-FBD drying process

Fig. 2-6 is a schematic diagram of the SHR-FBD process. Wet biomass was preheated and evaporated in HR1 (216.4 kW) and HR2 (2389.3 kW), which were paired with HT1 and HT2 and supplied with sensible and latent heat of the compressed air–steam mixture, respectively. During the heat exchange, vapor in the air–steam mixture turned into liquid water and was separated from air. Moreover, the sensible heat of the dried biomass was recuperated by air in HX3 (6.6 kW). The total energy input in the SHR-FBD, $W_{tot,SHR}$, is:

$$W_{tot,SHR} = W_{cp} + W_{bl} - W_{ex} \quad (2-22)$$

where W_{bl} is the power of the blower; and W_{cp} is the compression work of the

compressor, which can be partly recovered by the expander as expander work W_{ex} .

No external heater is required in the SHR dryers. Once the necessary heat for drying is injected, all the heat in the process can be circulated with the compression and expansion of the air–steam mixture. Thus, energy consumption of the SHR-FBD can be reduced dramatically to 1/4 of that for the CHR, respectively. Energy consumption in each unit of the four drying processes is presented in Table 2-2. It is very important to note that in the MVR system, the sensible heat of the dried biomass is abandoned without recovery, because its temperature and exergy rate are same or lower than those of the fluidizing/drying medium. On the other hand, in the proposed SHR-FBD system, all of the heat, including the sensible heat of the dried biomass, is recovered. This results in a more significant energy saving.

Table 2-2. Energy consumption and CO₂ emissions in the biomass drying processes

Case	CHR (Basic)	MSD	MVR	SHR-FBD	Efficiency
<i>Energy input (kW)</i>					
Heater	2313.1	1015.8	-	-	
Blower	104.6	135.6	174.1	104.6	80%
Compressor	-	-	665.6	534.3	80%
Expander	-	-	-	-66.5	90%
Total	2417.7 (100%)	1151.4 (50%)	839.7 (35%)	572.4 (24%)	

Fig. 2-7 shows the temperature and enthalpy diagram of each heat exchanger in the proposed drying system, with the heat exchangers and temperatures corresponding to those in Fig. 2-5. The solid and dotted lines express the hot and cold streams in each heat exchanger, respectively. Compared with other heat exchangers, the amount of heat exchange in HX2 (in the FBD) was the largest due to the latent heat exchange between the compressed steam and the water of the biomass. The heat curves of the hot stream (compressed air-steam mixture) and cold stream (wet biomass and air) were almost parallel. Thus, the exergy loss in the heat exchanger could be minimized. The remaining heat of the compressed air-steam mixture was utilized for pre-heating of wet biomass (HX1) and air (HX4) before a part of the compression work was recovered as electrical work by the expander. The sensible heat of the dried biomass was also used for air pre-heating (HX3). It can be seen that heat could be recuperated effectively by the proposed SHR technology in heat exchangers HX1, HX2, HX3 and HX4.

The minimum exergy required for the process is seldom described previously although it is critical for an energy-saving process design. By comparing with the theoretical minimum input exergy, it could clearly show the reduce potential for the energy input of the process. Thus, we calculated the theoretical minimum input exergy required for the biomass drying. The theoretical minimum input exergy for the drying of wet biomass stream (5000 kg h^{-1}) from the water content of 75 wt% (wb) to 10 wt% (wb) described in this paper is calculated as 98.0 kW. As can be seen in Table 2-2, the energy consumed by the SHR-FBD can be reduced to about 30% of

that consumed by the CHR, however, is still much higher than the theoretical minimum input exergy. The difference is due to the irreversibilities in the SHR-FBD. In the following, to clarify the reason for the additional energy input in the drying system and to develop a more energy-saving system based on the SHR technology, we conducted exergy analysis.

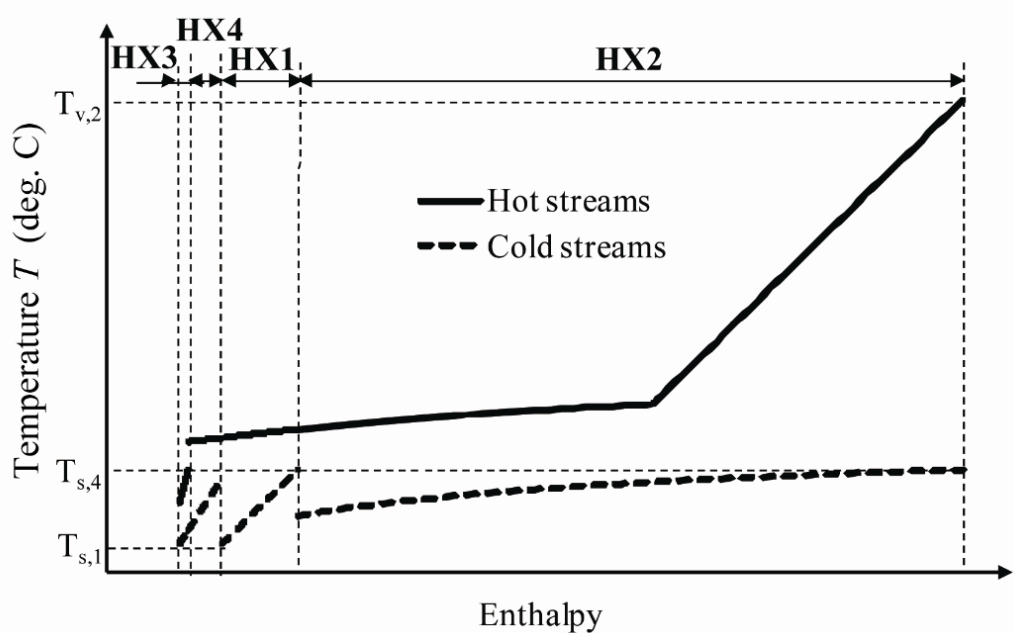


Fig. 2-7. Temperature-enthalpy diagram for the SHR-FBD

2.4.4. Exergy analyses of the proposed process

Exergy analysis has been proven to be useful for understanding and optimizing the design of thermal systems that are more efficient (Dincer and Cengel 2001) and has been applied successfully to various engineering applications (Dincer and Sahin 2004; Zhang et al. 2009). The exergy balance in each unit or in the whole SHR-FBD is expressed as

$$\sum_{\text{out}} E_i - \sum_{\text{in}} E_i = \sum_{\text{tot}} E_{\text{wk}} - \sum_{\text{tot}} E_{\text{loss}} - E_{\text{sur}} \quad (2-23)$$

where $\sum_{\text{out}} E_i$ and $\sum_{\text{in}} E_i$ are the exergy accompanying outgoing mass flows and incoming mass flows, respectively; $\sum_{\text{tot}} E_{\text{wk}}$ is the exergy of input work; $\sum_{\text{tot}} E_{\text{loss}}$ is the exergy loss in the drying process and E_{sur} is the exergy loss to the surroundings which is zero assuming no heat loss from system to the surroundings. Properties of the streams from the simulation results in the SHR-FBD are illustrated in Table 2-3.

Table 2-3. Properties of the steams in the SHR-FBD

Stream no.	phase	mass flow m_i (kg h ⁻¹)	temp. (°C)	pressure (kPa)	enthalpy h_i (kJ kg ⁻¹)	entropy s_i (J kg ⁻¹ K ⁻¹)
sample	mixed	5000	20.0	101	35.0	3810
2	mixed	5000	54.4	101	127.5	4108
3	mixed	11066	90.0	101	947.9	7877
4	mixed	9677	322.3	500	1392.6	8938
5	mixed	10677	145.9	470	1299.5	8788
6	mixed	10677	99.3	455	457.3	6647
7	mixed	10677	95.6	430	428.9	6582
8	vapor	6937	95.1	420	446.1	6956
9	mixed	6937	64.4	145	344.2	6989
10	vapor	6066	20.0	135	49.0	6267
11	vapor	6066	69.3	130	99.0	6436
12	vapor	6066	111.7	181	141.9	6458
13	liquid	3739	95.2	420	397.1	5902
14	liquid	2739	95.2	420	397.1	5902
15	liquid	2739	50.0	420	228.2	5413
16	liquid	1000	95.2	420	397.7	5903

The exergy of each stream can be calculated by eq 2-24.

$$E_i = (m_i h_i - m_i h_0) - T_0 (m_i s_i - m_i s_0) \quad (2-24)$$

where E_i is the exergy of a stream, m_i is the mass flow, h_i and s_i are the specific

enthalpy and specific entropy of the stream, respectively, h_0 and s_0 are the specific enthalpy and specific entropy, respectively, of the stream at a standard state (20 °C and 1 atm). T_0 is the temperature of the surroundings, which is assumed to be 20 °C in this paper. Then, the exergy change between the outgoing and incoming streams is:

$$\sum_{\text{out}} E_i - \sum_{\text{in}} E_i = (m_{\text{out}} h_{\text{out}} - m_{\text{in}} h_{\text{in}}) - T_0 (m_{\text{out}} s_{\text{out}} - m_{\text{in}} s_{\text{in}}) \quad (2-25)$$

Moreover, according to eq 2-25, the exergy of compression/expansion work (E_w) equals to the exergy increase/decrease between the outgoing and incoming streams of the compressor, the blower or the expander and can be calculated by eq 2-26:

$$E_{\text{wk}} = \sum_{\text{out}} E_i - \sum_{\text{in}} E_i \quad (2-26)$$

The exergy of input work in the SHR-FBD is

$$\sum_{\text{tot}} E_{\text{wk}} = E_{\text{cp}} + E_{\text{bl}} - E_{\text{ex}} \quad (2-27)$$

where E_{cp} and E_{bl} are the input exergy through the compressor and the blower, respectively, and E_{ex} is the output exergy through the expander. The exergy of input work is calculated as 610.0 kW ($E_{\text{cp}} = 764.7$ kW, $E_{\text{bl}} = 60.9$ kW and $E_{\text{ex}} = 215.6$ kW) according to eq 2-26 and eq 2-27. Furthermore, system exergy efficiency η_{system} is defined as the ratio of the theoretical minimum input exergy to the exergy of input work:

$$\eta_{\text{system}} = \frac{W_{\text{min}}}{\sum_{\text{tot}} E_{\text{wk}}} \quad (2-28)$$

The system exergy efficiency of the SHR-FBD is calculated as 0.16 according to eq 2-28. Assuming exergy loss of the whole system tends to approach a minimum

value equal to W_{\min} , exergy efficiency will be approximately 1.0, which means all the exergy of input work is used for separation water from biomass. However, in an actual case, a large amount exergy of work is used to compensate for the exergy loss due to irreversible heat transfer and pressure losses resulting from friction or phase change and owing to the heat capacity of air and water/steam changing with compression and heating. Hence, it is critical to decrease the exergy loss in the process, and then it increases the exergy efficiency. From Table 2-4, we can find that there are still significant exergy losses in the overall system, and the largest exergy loss (479.7 kW) occurs in the FBD. The reason is that the temperature difference between the hot and cold streams in the FBD is much larger than the ΔT_{\min} (10 K) in the FBD. Further energy saving can be predicted if the temperature difference between the hot and cold streams is decreased near to the ΔT_{\min} in the fluidized bed dryer, thus diminish the irreversibility. Based on the energy and exergy analyses, the proposed design showed a good energy saving potential and further energy-saving solutions were conceived raised. The largest amount of heat exchange in the drying process was found to occur in the FBD which was selected as an evaporator in this study.

Table 2-4. Exergy loss in each heat exchanger and mixer in the SHR-FBD.

Unit	Biomass preheater	Fluidized bed dryer	Air preheater
E_{loss} (kW)	40.0	479.7	18.6

T_0 is the temperature of the surroundings (20 °C).

2.5. Conclusions

Exergy loss was investigated in the drying process and heat pairing concept was brought out for applying SHR technology to the drying process. Energy analysis was performed for the investigations of in the existing energy-saving drying processes. We also conducted exergy analysis for the SHR-FBD and calculated the theoretical minimum input exergy and exergy loss in each unit. Results show that the exergy loss is greater in the FBD than in other units in the SHR-FBD and solutions for the further energy saving for the SHR-FBD are suggested.

References

- Berry, S. L. and M. L. Roderick. 2005. Plant-water relations and the fibre saturation point. *New Phytologist*, 168(1), 25-37.
- Dincer, I. and Y. A. Cengel. 2001. Energy, entropy and exergy concepts and their roles in thermal engineering. *Entropy* 3(3), 116-149.
- Dincer, I. and A. Z. Sahin. 2004. A new model for thermodynamic analysis of a drying process. *International Journal of Heat and Mass Transfer*, 47(4), 645-652.
- Kansha, K., Kotani, Y., Aziz, M., Kishimoto, A., Tsutsumi, A. (2013) Evaluation of a self-heat recuperative thermal process based on thermodynamic irreversibility and exergy. *Journal of Chemical Engineering of Japan*, 46(1) 87-91,
- Siau, J. F. (1984). Transport Processes in Wood. New York, Springer-verlag.
- Simpson, W. and A. TenWolde (1999). Wood Handbook-Wood as an Engineering Material, Forest Product Laboratory, USDA, Forest Service, Madison, WI.
- Skaar, C. (1988). Wood-Water Relations. Berlin, Germany, Springer Verlag.
- Zhang, X. P., C. Solli, et al. 2009. Exergy analysis of the process for dimethyl ether production through biomass steam gasification. *Industrial & Engineering Chemistry Research*, 48(24), 10976-10985.

CHAPTER 3

SELF-HEAT RECUPERATION

TECHNOLOGY FOR BIOMASS DRYING IN

A FLUIDIZED BED DRYER

3.1. Process design of self-heat recuperative fluidized bed dryer for biomass drying

3.1.1. Introduction

In Chapter 2, SHR technology was applied to a fluidized bed dryer for biomass drying. The process showed that up to 75 % energy-saving potential could be achieved compared with a conventional heat recovery dryer. However, energy consumption was still much higher which could be found from the temperature-heat diagram Fig. 2-7. Exergy analysis study illustrated that exergy loss occurred due to the mismatched heat pairing in the drying process. Thus, it is necessary to overcome this problem for a further energy-saving.

3.1.2. Energy-saving drying process based on self-heat recuperation technology

Fig. 3-1-1 shows the schematic layout of a self-heat recuperative drying process for biomass drying. Compared to the previous drying process, the advanced drying process focuses on performing heat pairing for sensible heat and latent heat. Good heat pairing which means that the sensible and latent heats are paired with the corresponding sensible and latent heats, is feasible to form the heat circulation for the energy saving. Heat capacities of hot and cold streams are slightly affected by the pressure rather than the temperature. Thus, a good heat pairing makes lines of hot and cold streams at different pressures in the temperature-heat diagram in almost parallel which are separated by the minimum temperature difference. Initially, wet biomass is fed into heat exchangers (HX1–HX4) for preheating to a certain temperature. HX1, HX2 and HX3 are heat exchangers to recuperate the sensible heat

of condensed water, dried biomass and hot air, respectively. The sensible heat of the air–steam mixture is used for preheating the wet biomass (HX4). Thus, the latent heat of steam condensation could be paired with the latent heat of water evaporation in HX5 where the liquid water in the biomass is converted into vapor. HX5 is a concurrent heat exchanger in the case of fluidized bed dryer. The air–steam mixture from the evaporator is compressed by a compressor, and recirculated for subsequent biomass drying. Air humidity decreases due to temperature drop of the air–steam mixture following the heat exchange and expansion in the expander to recuperate a part of compression work. During this process, water vapor can be separated from air. Then, the dry air is recycled for the subsequent drying process. As a result, all the heat involved in drying can be recuperated and reused. This includes recuperation of the sensible heat from the gas serving as the drying medium, the dried products, and both the sensible and latent heats of the evaporated water.

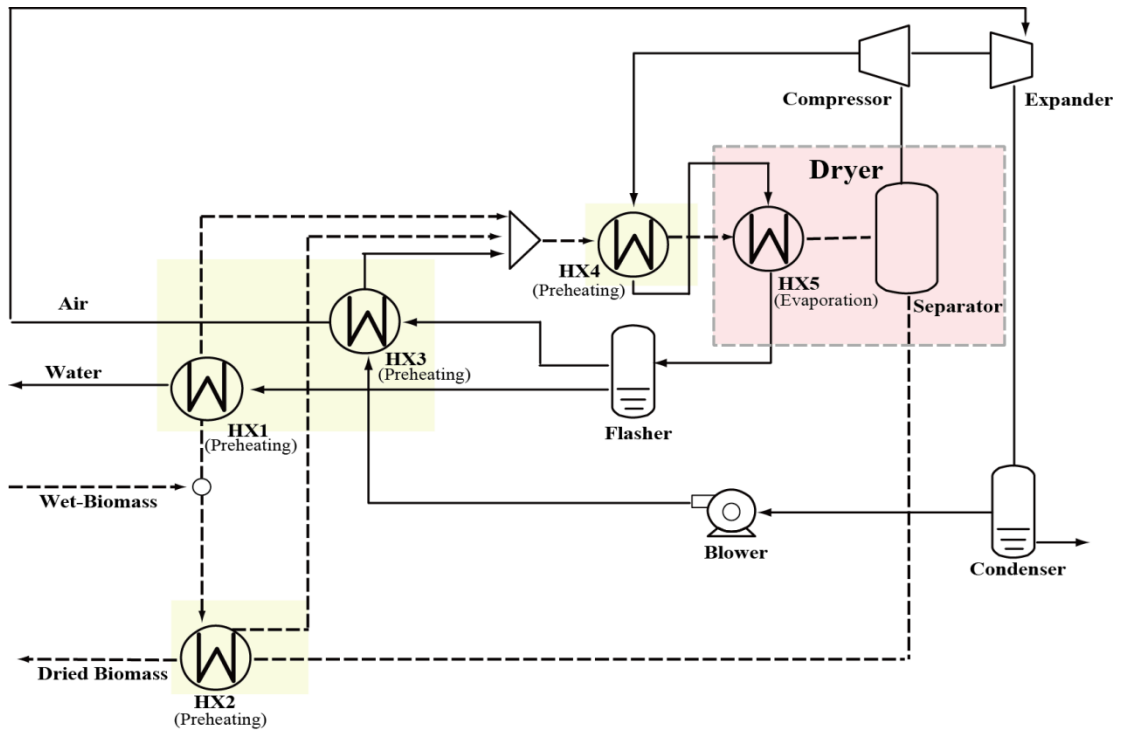


Fig. 3-1-1. Schematic layout of the advanced drying process

The energy and material flow diagrams shown in Fig. 3-1-2, present the method for improvements in the system energy efficiency by distinguishing the heating and cooling loads of the process. The boxes represent the units, and the lines represent the flow of materials or energy. The material flow in the diagrams comprises the flow of air, (dry) biomass and water. A better heat pairing has been performed in the advance drying process as shown in Fig. 3-1-2a, compared with the previously designed self-heat recuperative drying process as shown in Fig. 3-1-2b. Hot dried biomass and hot air are exchanged with cold biomass and cold air, correspondently. The compressed air–steam mixture provides heat for the water evaporation. The total heating energy is provided by self-heat exchange because of the increase in the

effluent temperature due to adiabatic compression. Thus, energy input in the advanced drying process can be calculated as:

$$W_{\text{tot,SHR}} = W_{\text{cp}} + W_{\text{mc}} - W_{\text{ex}}, \quad (3-1-1)$$

where W_{mc} is mechanical energy consumptions of blower and motor, and W_{cp} is the compression work, which can be partly recovered by the expander as the expander work W_{ex} . As a basic case, a conventional heat recovery dryer based on pinch technology is investigated as shown in Fig. 3-1-2c. The exhaust heat from the dryer including the heat of drying medium, evaporated water and dried biomass is recovered for preheating of drying medium and wet biomass. In general, efficient heat matching between sensible heat with sensible heat, and latent heat with latent heat, is impossible because of the existence of the pinch point, resulting in a large amount of energy input. Thus, additional energy in the form of heat is required to evaporate the water. Energy consumption of the conventional heat recovery dryer is given by:

$$W_{\text{tot,CHR}} = W_{\text{ht}} + W_{\text{mc}}. \quad (3-1-2)$$

3.1.3. Process calculations

The simulation was conducted using PRO/II Ver. 9.0 (Invensys, Corp.) to examine the energy consumption required for the drying processes of biomass. Three different kinds of dryers: fluidized bed, rotary and screw conveyor dryers were evaluated for biomass drying. Properties of biomass and each dryer investigated in this work are shown in Table 3-1-1. In simulations, Soave-Redlich-Kwong equation was selected for the state equation. The adiabatic efficiencies of the compressor, blower and expander were assumed to be 80 %, 80 % and 90 %, respectively. In addition, the minimum temperature differences for the heat exchangers were assumed to be 10 K for the fluidized bed dryer and 30 K for the other heat exchangers. Heat exchange is concurrent in the fluidized bed dryer and countercurrent in the other heat exchangers. The biomass has the same flow direction as the air in the drying system. No heat loss is assumed from the drying system to the surroundings. The equilibrium moisture content of biomass depends on the water activity which is the relative humidity of gas for gas drying (Bjork and Rasmuson 1995). To dry the biomass to a water content of 20 wt% (wb) with air, the relative air humidity should be kept below 0.9 based on the research results of Pakowski et al. (2007).

Mechanical energy consumptions, W_{mc} , for the blower and motor were calculated in each dryer. In the fluidized bed dryer, energy consumption comes from the blower to compensate for the pressure loss in the fluidized bed. The fluidization gas volume can be calculated according to the velocity of fluidization. The blower work to provide a pressure increase Δp_f that is required for fluidization can be calculated according to

the equation proposed by Kunii and Levenspiel (1991) as follows:

$$\Delta p_f = \Delta p_b + \Delta p_d, \quad (3-1-3)$$

$$\Delta p_b = (1 - \varepsilon_{mf})(\rho_p - \rho_g)h_b \frac{g}{c}, \quad (3-1-4)$$

$$\Delta p_d = 0.4\Delta p_b, \quad (3-1-5)$$

where Δp_b and Δp_d are pressure drops across the bed and distributor, respectively.

Table 3-1-1. Properties of biomass particle and drying devices

Properties	Values
<i>Biomass</i>	
Flow rate (10^3 kg h^{-1})	10
Fed temperature(°C)	20
Initial water content (wt% wb)	50
Final water content (wt% wb)	20
Bulk density (kg m^{-3})	180
Particle density(kg m^{-3})	400
Min. fluid. velocity (m s^{-1})	0.88
Size	Side length 10 mm, Thickness 3 mm
Sphericity (-)	0.6
<i>Fluidized bed dryer</i>	
Shape	Square
Side length (m)	4
Bed aspect ratio (-)	1.0

3.1.4. Results and discussion

Fig. 3-1-3 shows that an increase of air amount which results in an increase in its partial pressure in the air–steam mixture, would decrease the drying temperature for biomass. On the other side, in the self-heat recuperative drying system, an increase of air amount also required less compression ratio for a smaller temperature increase due to the reduced drying temperature.

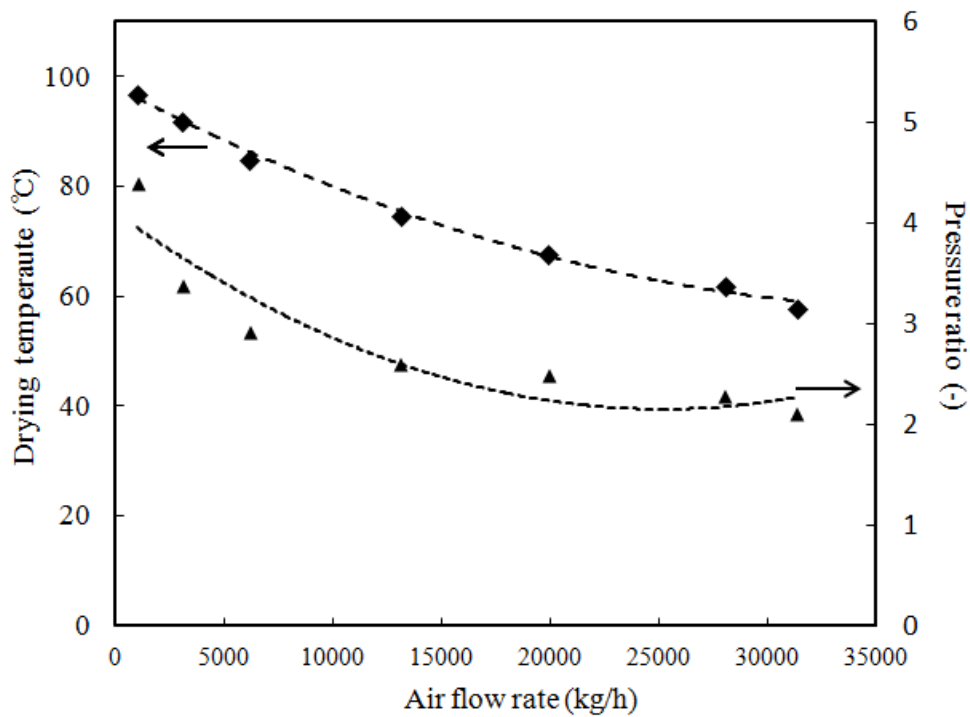


Fig. 3-1-3. Drying temperature for different amounts of drying medium air

Energy consumptions required for drying in the fluidized bed drying systems including the conventional heat recovery drying process, the previous drying process developed by Aziz et al. (2011), and the proposed drying process were investigated.

Fig. 3-1-4 shows the total energy input required for drying in the above fluidized bed drying systems. Compared to the conventional heat recovery drying system, both self-heat recuperative drying systems reduced the total energy input of the drying process and the proposed process consumed 1/4–1/6 of that required in drying using conventional heat recovery. The variation in energy consumption in each drying system is the result of the difference of blower work due to the change of fluidization velocity. The fluidization velocity increases accordingly to the increase of volumetric amount of the drying medium. Moreover, an increase amount of drying medium increases the duty of compressor for the additional gas compression.

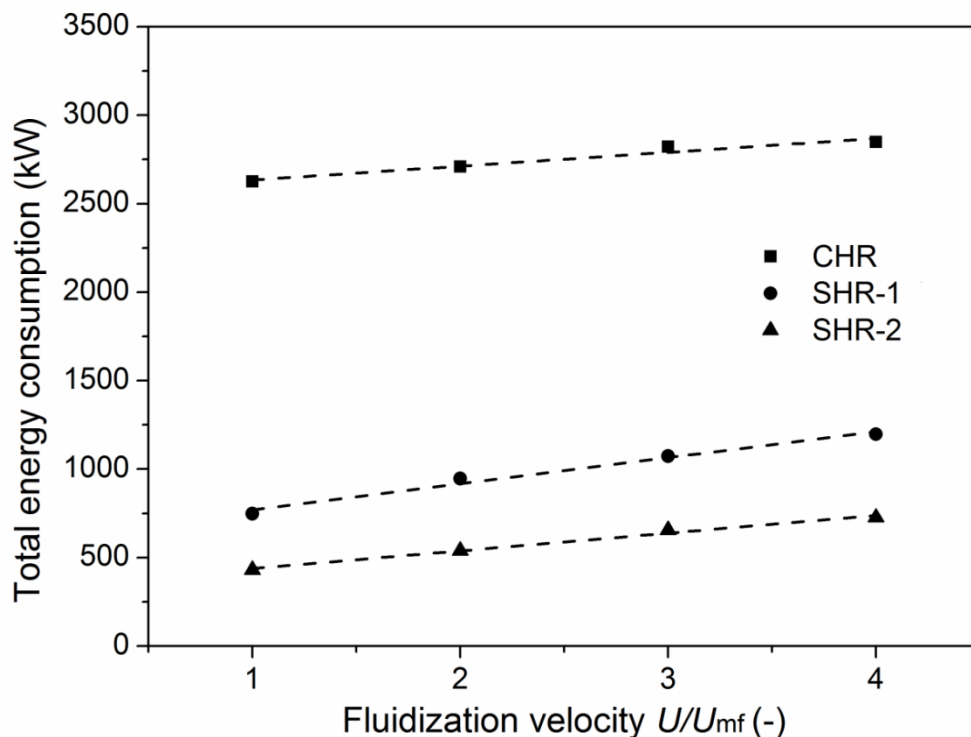


Fig. 3-1-4. Energy consumption in the drying processes

Figs. 3-1-5 and 3-1-6 show the temperature-heat diagrams for the biomass drying system developed by Aziz et al. (2011) and the advanced drying system, respectively. The solid line represents the hot stream and the dashed line represents the cold stream. The heating duty is expressed as the sum of internal self-heat exchange load. That the exergy loss due to the heat transfer becomes the minimum can be reflected from the area between the hot and cold streams lines; a small area means a small exergy loss. Exergy loss amount was calculated as shown in Table 3-1-3. In the previous drying process, the largest amount of exergy loss 479.7 kW, occurred in the evaporation period which was represented as the space area between the hot stream (compressed air–steam mixture, 10→11) and cold stream (wet biomass and air, 5→6) in Fig. 3-1-5. This is due to unmatched heat pairing in the overall drying system. A large amount of sensible heat in the air is generated during the compression of the air–steam mixture causing unmatched heat pairing. Some part of the sensible heat of the compressed air–steam mixture is paired with the latent heat of water evaporation, resulting in part of the latent heat of steam being paired with the sensible heat of the biomass and the water. The unmatched heat pairing increases the temperature difference because of the different heat capacities of the paired streams, which causing different temperature changes. The air–steam mixture after heat exchange in

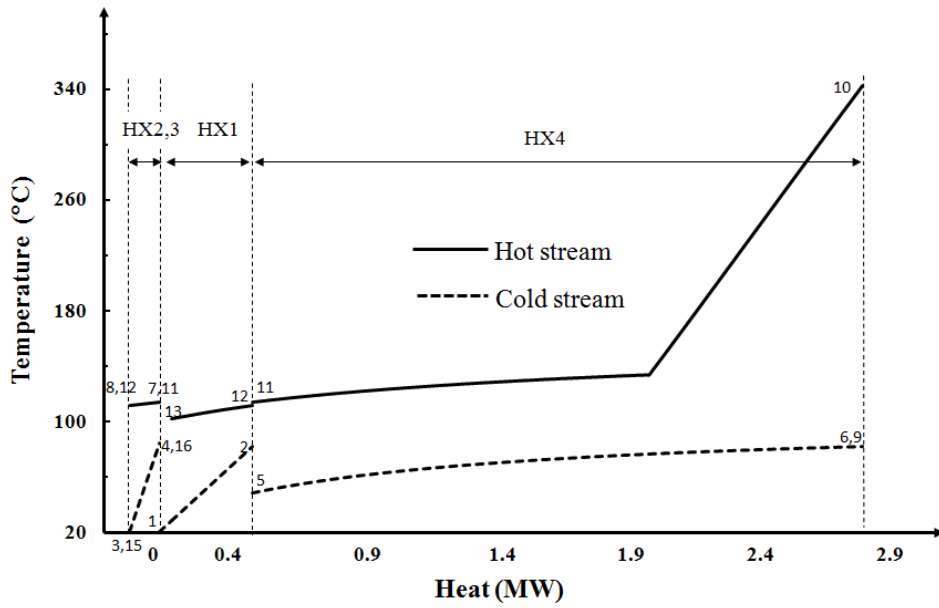


Fig. 3-1-5. Temperature-heat diagram for the biomass drying system developed in Section 2.1.1

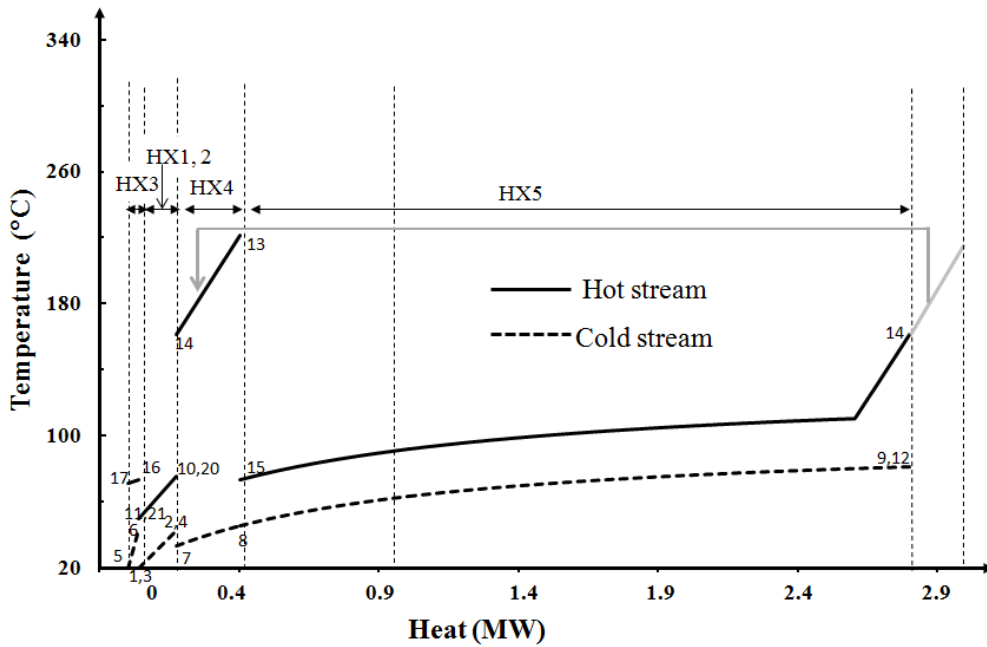


Fig. 3-1-6. Temperature-heat diagram for the advanced biomass drying system

Compared with Fig. 3-1-5, Fig. 3-1-6 shows better heat pairing by removing the sensible heat of compressed air (13→14) through the sensible heat exchange with the wet biomass and air (7→8). Thereafter, the latent heat of steam condensation (14→15) can be exchanged with the latent heat of water evaporation (8→9), and then the effluent stream (10, 20→11, 21) (16→17) is cooled through heat exchange with the biomass (1, 3→2, 4) and air (5→6), respectively, for self-heat exchange to recuperate its sensible heat. Heat exchange temperature difference could be further reduced by increasing the number of fluidized bed stages (Holmberg and Ahtila 2005). However, the pressure loss in the fluidized bed increases due to the increasing number of stages. Thus, we chose a two-stage fluidized bed as the evaporator by balancing the energy consumption due to the pressure loss and temperature difference by increasing the fluidized bed stages. Due to the improved heat pairing, exergy loss in the water evaporation was reduced to from 479.7 kW to 189.0 kW. As a result, energy consumption can be saved by 40 % of the energy consumed by the previous drying process as shown in Fig.2-5.

3.1.4. Conclusions

The SHR technology was succeeded to be applied for biomass drying in a fluidized bed dryer for reducing energy consumption. Energy consumption was reduced to 1/6 of the conventional heat recovery dryer due to the heat pairing formed in the proposed drying process.

References

- Aziz, M., C. Fushimi, et al. (2011). "Innovative Energy-Efficient Biomass Drying Based on Self-Heat Recuperation Technology." Chemical Engineering & Technology **34**(7): 1095-1103.
- Bjork, H. and A. Rasmuson (1995). "Moisture Equilibrium of Wood and Bark Chips in Superheated Steam." Fuel **74**(12): 1887-1890.
- Holmberg, H. and P. Ahtila (2005). "Evaluation of energy efficiency in biofuel drying by means of energy and exergy analyses." Applied Thermal Engineering **25**(17-18): 3115-3128.
- Kunii, D. and O. Levenspiel (1991). Fluidization Engineering. Washington, Butterworth-Heinemann.
- Pakowski, Z., B. Krupinska, et al. (2007). "Prediction of sorption equilibrium both in air and superheated steam drying of energetic variety of willow *Salix viminalis* in a wide temperature range." Fuel **86**(12-13): 1749-1757.

3.2. Experimental Investigation on biomass drying in the exergy recuperative fluidized bed dryer with air

3.2.1. Introduction

With the process simulator PRO/II ver. 9.0, we could investigate the energy consumption in the designed drying processes. However, for the complex heat and mass transfer phenomena in the fluidized bed dryer (FBD), especially the lack study on effect of the heating element immersion to the drying performance (Groenewold and Tsotsas 2007), it is difficult to obtain concrete information such as the hydrodynamic behavior and drying performance in the FBD through the simulator Pro/II ver. 9.0. Besides, it is necessary to investigate the system stability of the drying system based on conditions of the SHR technology in the simulation part. Thus, we conducted experimental investigations in the following. The objective of this study is to observe the drying characteristics of the biomass particles in the FBD in relation to the fluidization velocity, drying temperature and mass ratio of the fluidizing particle (sand) to the biomass particle (rice straw). Rice straw, as well as other type of straws (wheat and barley), is selected as sample considering its high potential as material for bioethanol production because it is secondary products and does not affect the supply food unlike corn etc.

3.2.2. Experimental setup

The water in the rice straw was initially investigated through a thermal gravity analyzer shown in Fig. 3-2-1. The system mainly consists of a quartz thermobalance reactor of 25 mm in inner diameter, an inner quartz tube of 13 mm in inner diameter,

an infrared gold image furnace, and a balance sensor. The inner quartz tube was installed to avoid influence of buoyancy change due to gas convection during heating. A ceramic basket of 8 mm in diameter and 10 mm in length was suspended in the thermal balance. The ceramic basket was covered with a platinum sheet to absorb radiative heat from the furnace for rapid heating. Temperature was kept at around 100 °C. Two platinum mesh sheets (150 meshes) were put at the bottom of the ceramic basket. Temperature was measured by an R-type thermocouple with diameter of 0.1 mm put near the sample during the drying process. Biomass sample (10 mg) was placed in the ceramic basket. The weight loss of the sample during drying process was recorded by the computer at time intervals of 0.2 s. The weight loss per unit time reflects the drying rate. The experiments were conducted at atmospheric pressure.

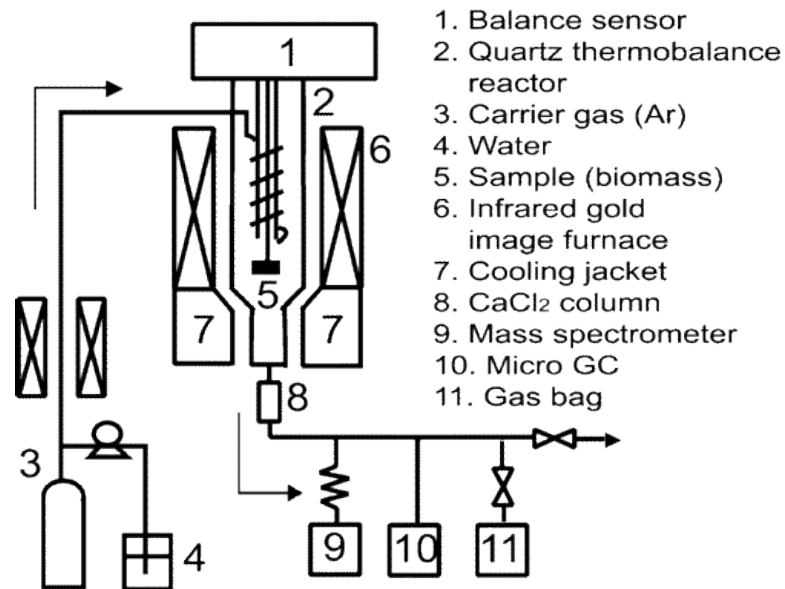


Fig. 3-2-1. Device of thermal gravity analyzer (Fushimi, Wada et al. 2011).

After that, a laboratory-scale fluidized bed dryer for the biomass drying in which wet rice straw was fed and discharged intermittently was set up. Moreover, since the peculiar shape of biomass inhibits fluidization, silica sand ($d_p = 0.3$ mm) was added to the bed and fluidized together with the biomass to enhance the fluidity. A mixture of sand and wet rice straw were fed at intervals of 10 min. Meanwhile, the dried rice straw was discharged together with sand from the outlet in every 25 min. The discharged sand-straw mixture was separated by sieving and then weighed. The separated sand was circulated with the wet rice straw for the next drying process. A schematic diagram of the FBD and the detailed properties are presented in Fig. 3-2-2 and Table 3-2-1, respectively. The size of the fluidized bed and holes for sensor were described in Fig. 3-2-3a and b. Air was preheated to the bed temperature before entering the FBD. As the drying progressed, the water in the sample evaporated into the air. To measure the temperature distribution across the bed, two K-type thermocouples T_{b1} (bed bottom) and T_{b2} (bed top) with diameter of 1.6 mm (Hayashi Denko, Japan), were installed at bed heights of 25 and 150 mm from the distributor, respectively. The humidity of the air-steam mixture is measured by a hygrometer probe (Rotronic, UK) fixed at the height of 275 mm above the distributor. In the experiment on the temperature and fluidization velocity effect, three sheathed heaters were installed inside the FBD horizontally at a height of 25 mm above the distributor to act as a compressed air-steam mixture that was used as a heat source for drying. Phenolic foam insulation was fixed around the surface of the fluidized bed to prevent heat loss from the bed to the environment. In this study, we focused on the drying of

rice straw, but the drying principle and drying technology can be applied to the drying of other kinds of biomass.

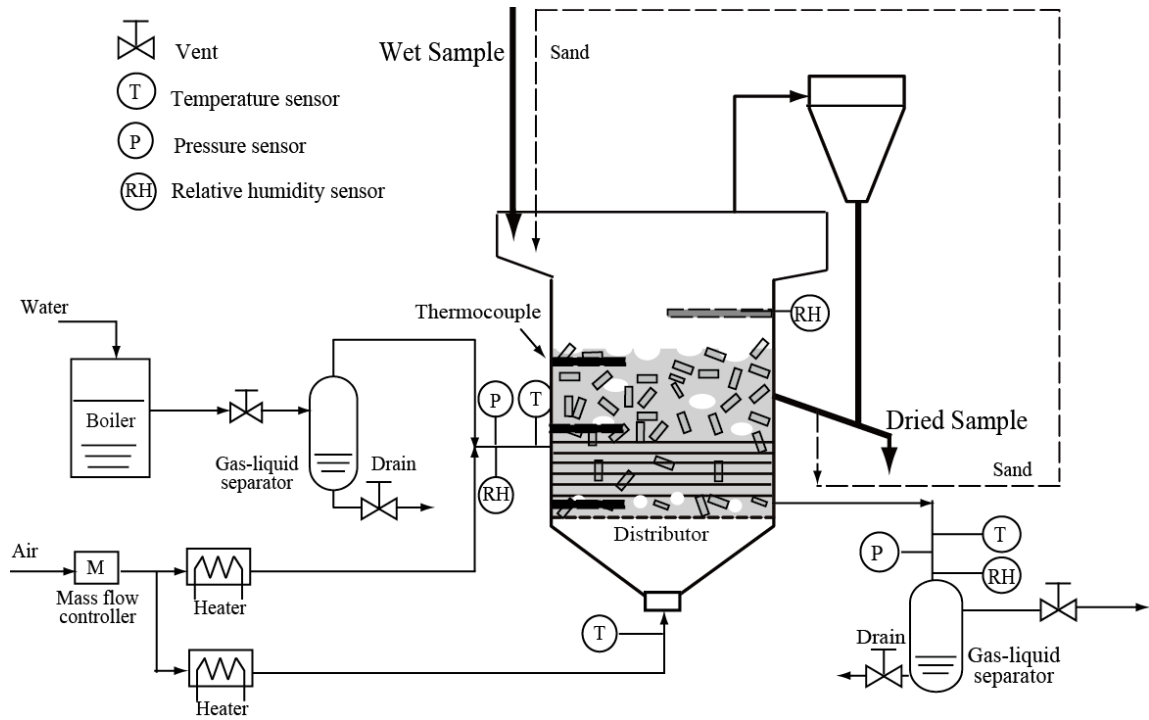


Fig. 3-2-2. Schematic diagram of an experimental fluidized bed dryer

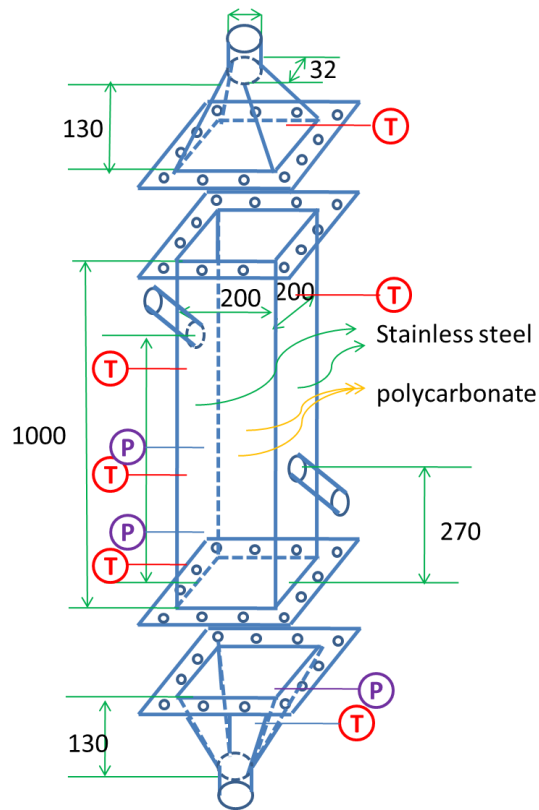


Fig. 3-2-3a. The detail about the fluidized bed dryer

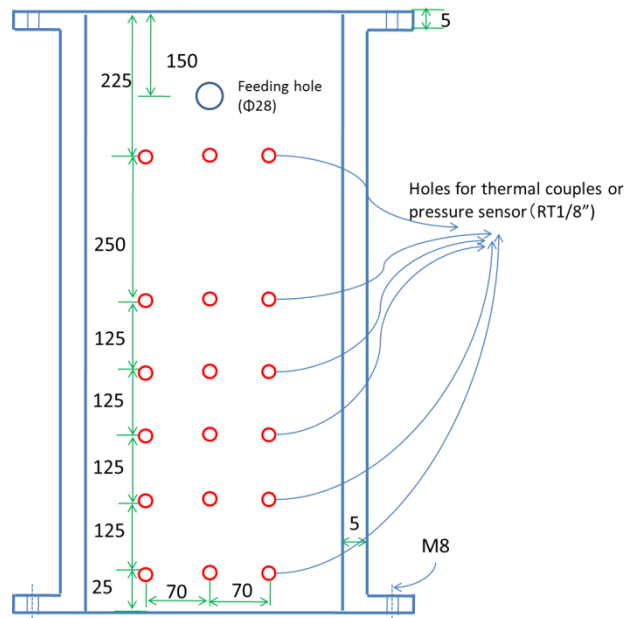


Fig. 3-2-3b. The size and arrangement of sensors in the fluidized bed dryer

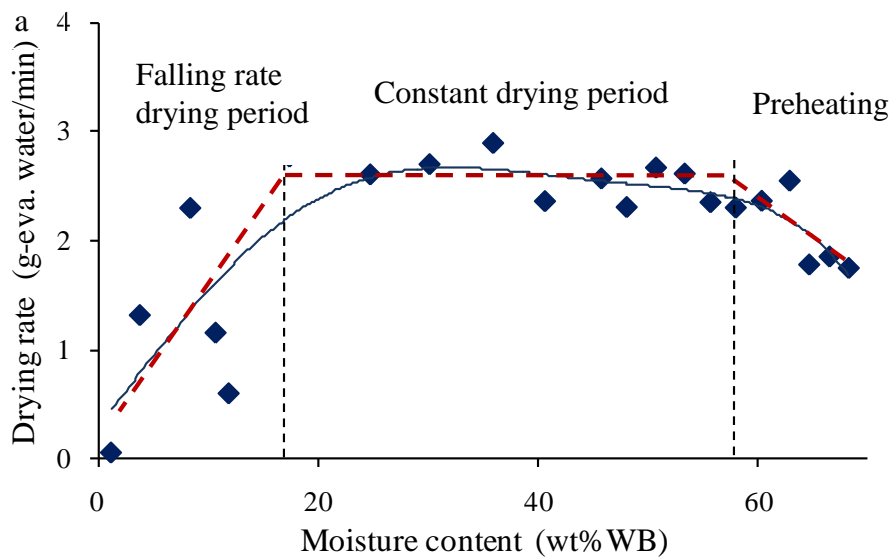
Table 3-2-1. Properties of fluidizing particle, biomass particle, bed and immersed heating element

Properties	Values
<i>Fluidizing inert particle</i>	
Type	Silica sand
Average diameter (mm)	0.3
Heat capacity ($\text{kJ kg}^{-1}\text{K}^{-1}$)	1.1
Particle density (kg m^{-3})	2600
Min. fluid. velocity (m s^{-1})	0.041 Basic experiment
<i>Biomass</i>	
Type, shape	Rice straw, hollow cylinder
Average length (mm)	20
Average diameter (mm)	6
As-received MC (wt% wb)	75
Bulk density (kg m^{-3})	180
Particle density (kg m^{-3})	400
Min. fluid. velocity (m s^{-1})	0.88
<i>Bed</i>	
Shape	Square
Side length (m)	0.2
Bed height (m)	0.2
Aspect ratio (-)	1
<i>Heating element</i>	
Type	Sheathed heater (Sakaguchi corp, Japan)
Dimension	Diameter 6 mm, length 120 mm
Resistance R (Ohm)	60.5
Number	3

3.2.3. Results and discussion

3.2.3. 1 Thermal gravity analysis for rice straw

From Fig. 3-2-4a, it is known that the constant rate drying period continued until the moisture content of paddy straw was dried to less than 18 wt% (wb). Thus, bound water in the rice straw was less than 18 wt% (wb). Moisture content decreased with the particle temperature increasing during the drying process to remove the capillary water and bound water from the rice straw as shown in Fig. 3-2-4b.



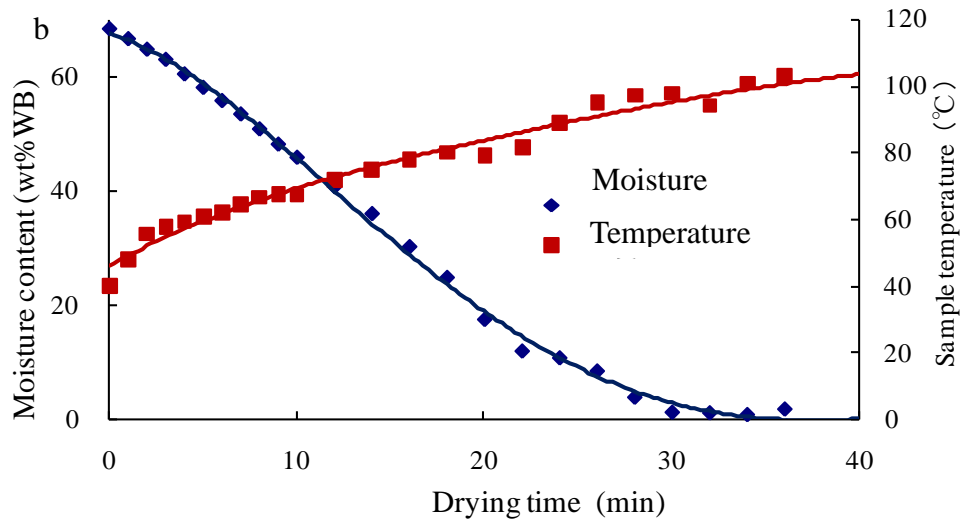


Fig. 3-2-4. a) Drying rate of rice straw with moisture content and b) Moisture content and temperature change during the drying process

3.2.3.2. Drying Kinetics in the semi-fluidized Bed Dryer

3.2.3.2.1 Effect of fluidization velocity and temperature

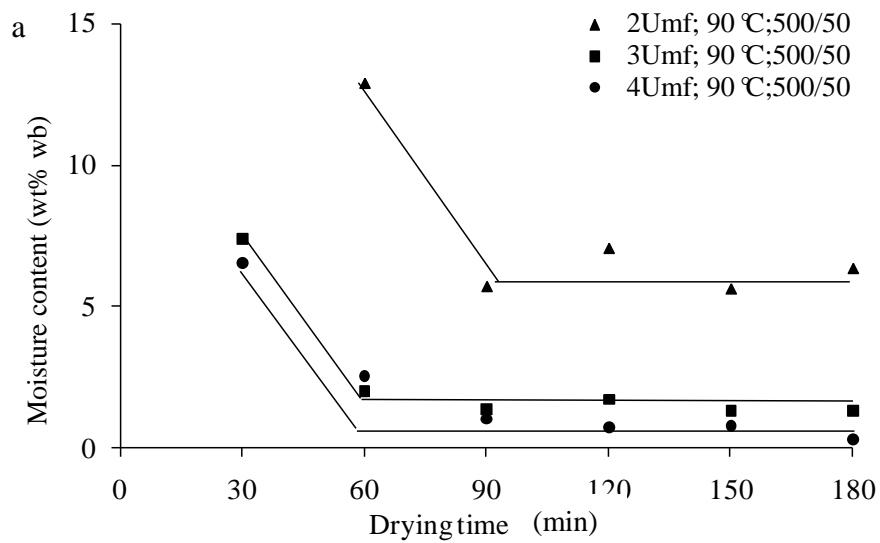
In the next step, effect of the fluidization velocities on the drying performances of rice straw was evaluated. The moisture contents of the rice straw dried at different fluidization velocities were measured according to the ASTM D4442-07 standard; the dried biomass was weighted by the balance (M_1) and then moved to the oven at 103 °C, and 101 kPa for 24 hours (M_2). The water content could be calculated as

$$W_{\text{wet}} = \frac{M_1 - M_2}{M_1} \times 100\% \quad (3-2-1)$$

where, M_1 is the weight of the sampled dried rice straw and M_2 is the weight of the dried rice straw after kept in the oven for 24 h. The effects of the fluidization velocity on the moisture content of the dried straw are shown in Fig. 3-2-5. It illustrates that

the water content in the dried rice straw decreased with an increase in the fluidization velocity from $2U_{mf}$ to $3U_{mf}$, suggesting that the fluidization velocity greatly affects the water content. The reason for the relationship is that an increase of the fluidization velocity can reduce the partial pressure of steam in the air-steam mixture, leading to a lower relative humidity of the air-steam mixture. As a result, the driving force for water movement in the biomass and evaporation increased, resulting in lower moisture content. Another important reason why the high fluidization velocity dramatically decreases the final water content of dried rice straw is that high fluidization velocity results in a good mixing status in the fluidized bed which increases the heat transfer rate between the hot air and wet biomass. However, when the fluidization velocity increased from $3U_{mf}$ to $4U_{mf}$, the moisture content of the dried straw changed slightly due to the internal diffusion control (Chandran, Rao et al. 1990). It is assumed that velocities below $2U_{mf}$ provides insufficient particle mixing resulting in partial fluidization and, thus non-uniform heat transfer and temperature across the bed. Beyond a velocity of $3U_{mf}$, a homogeneous bed formed. This demonstrates that the mixing quality mainly depends on fluidization velocity in that a low fluidization velocity causes segregation while a high fluidization velocity increases the mixing quality. These results show the same tendency with the results reported by Rowe et al., (1965) and Hemati et al., (1990) in which strong segregation occurred when the gas velocity was under 2 times the minimum fluidization velocity of jetsam particles and 2.5 times the minimum fluidization velocity of sand, separately. Results show that the fluidization velocity, which was $3U_{mf}$, is feasible for

the actual biomass drying, and a good drying performance of rice straw could be also confirmed in this condition. Fig. 3-2-6 illustrates the effect of the bed temperature to the moisture content of the dried rice straw in the case of fluidization velocity $U_o = 3U_{mf}$. The final water content of dried straw decreases as the bed temperature increases. The increase of bed temperature and mass ratio at a constant fluidization velocity U_o causes the decrease of relative humidity (relative vapor pressure) and finally, increasing the driving force of water movement inside the particle and its evaporation into the air.



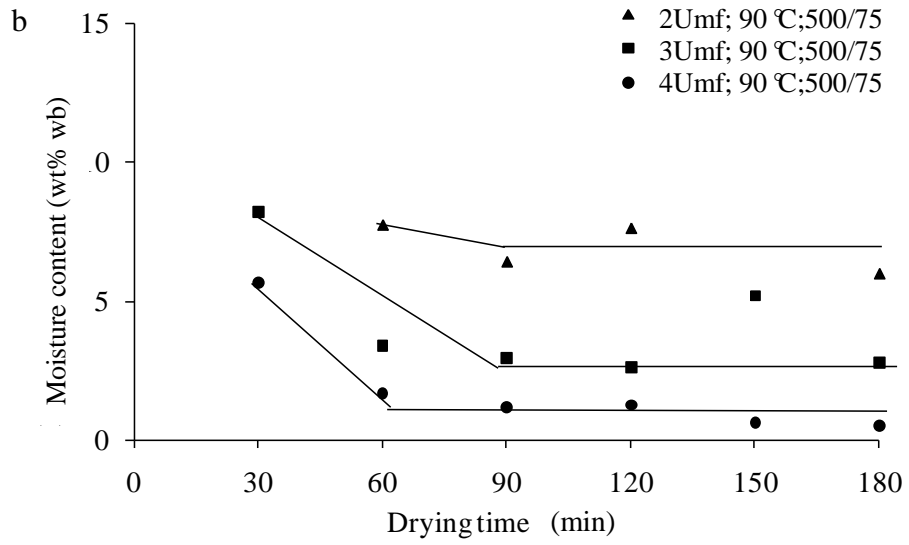
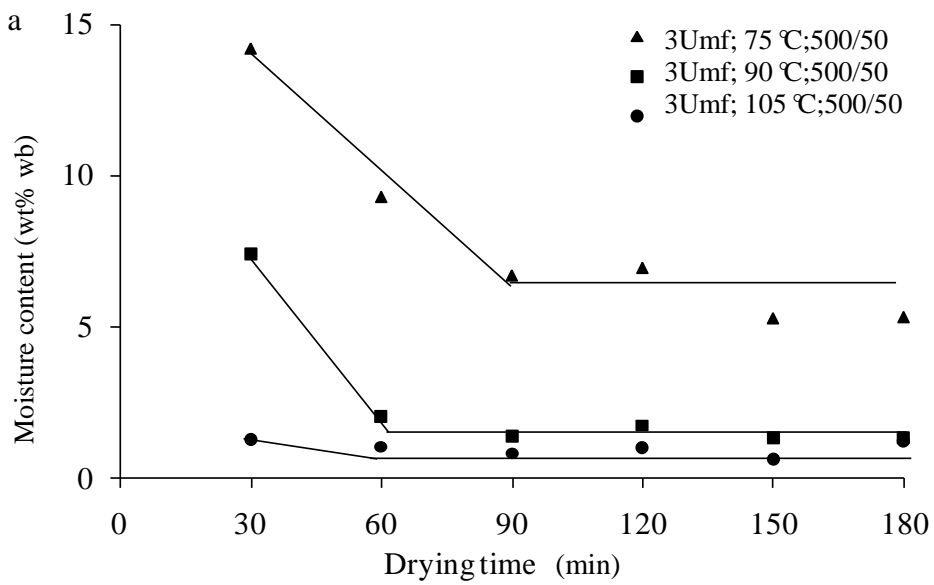


Fig. 3-2-5. Effect of fluidization velocity U_o to moisture content of dried straw (a) Mass ratio m_r of 500/50 and (b) Mass ratio m_r of 500/75



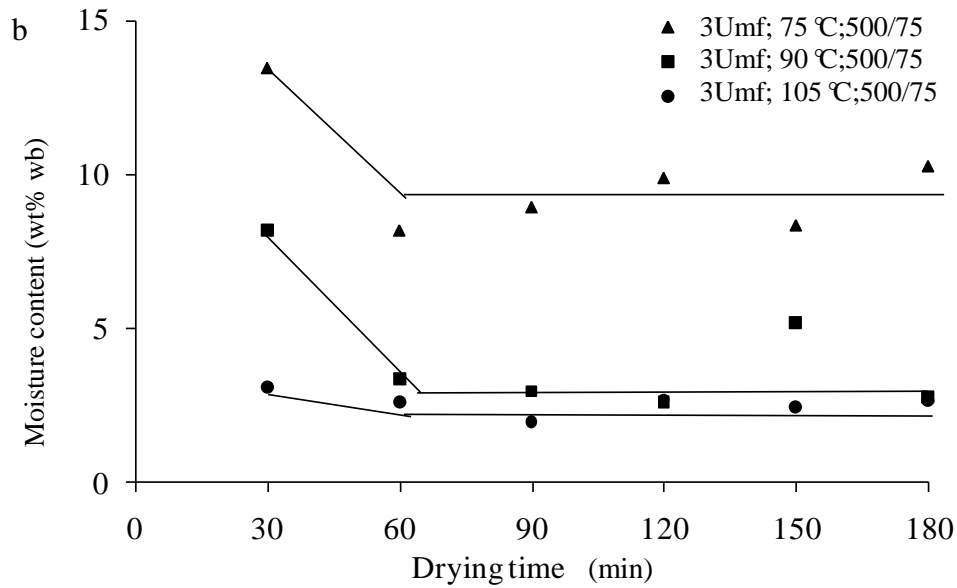


Fig. 3-2-6. Effect of bed temperature T_b to moisture content of dried straw, (a) Mass ratio m_r of 500/50 and (b) Mass ratio m_r of 500/75

3.2.3. 2. Heat transfer in the fluidized bed dryer

Heat transfer study in the fluidized bed dryer was very important for predicting the feasibility of heat exchange in the proposed drying system. The approximate thermodynamic model used for heat exchange inside the SHR-FBD involving inert particles is shown in Fig. 3-2-7. The compressed mixture of air and steam flows inside the heat transfer tube. Thus, in-tube condensation occurs and heat is transferred to the bed via the tube wall and is finally transferred from the bed to the biomass sample through the inert particles. The in-bed immersed tube behaves as a heat exchanger filled with the compressed air-steam mixture and as the main heat source for drying. The condensation heat from the compressed vapor is exchanged with the evaporation heat of the water in the wet biomass. The required length of the

heat transfer tube immersed inside the FBD is shown in Fig. 3-2-9 based on the simulation conditions as shown in Section 2.1. Length of tube increased as the amount of air flowing in the system and the mixing ratio of biomass to the silica sand increased. Effects of the mixing ratio and pressure of the air-steam on the heat transfer rate were also investigated through the experiments. With mixing ratio of the air-steam increasing, UA increased which was considered to be due to the more moisture condensation in the high mixing ratio of the air-steam (Fig. 3-2-10a). Fig. 3-2-10b showed the impact of the total pressure of the air-water vapor on the heat transfer rate. When the pressure of the air-steam increased, there was no significant difference between UA , but with a little increase. This seems total pressure of the air-steam. This was because as the pressure increased, the temperature of the air-steam also increased correspondingly. Temperature difference between the tube inside and outside would increase causing a high heat transfer rate eventually.

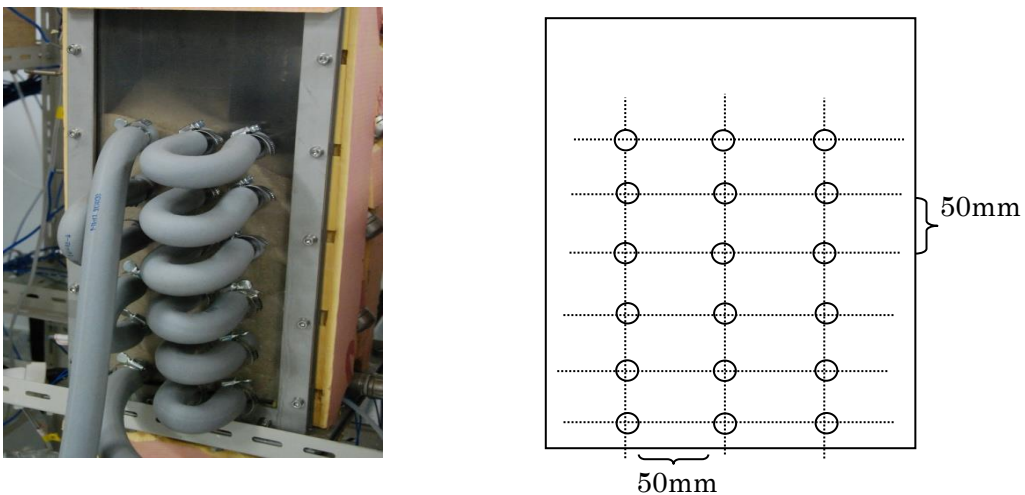


Fig. 3-2-7. Internal heat exchanger in the fluidized bed dryer

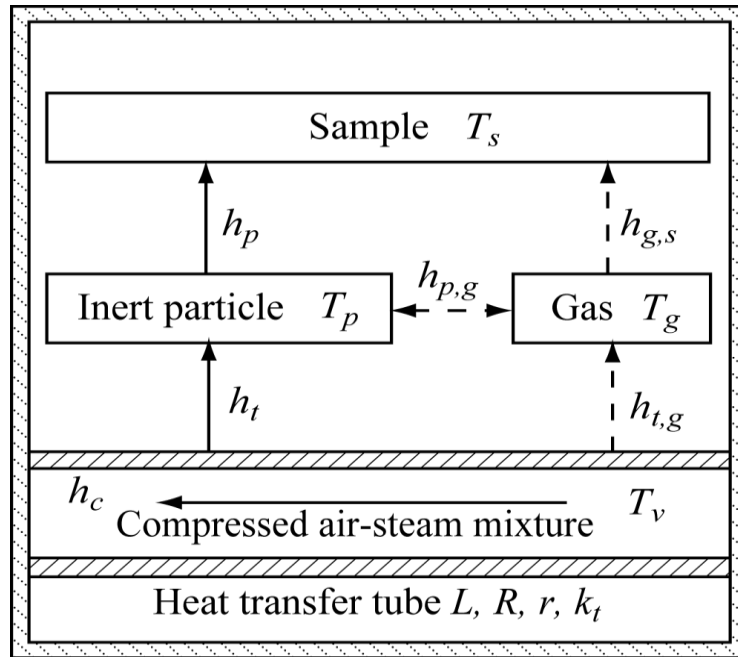


Fig. 3-2-8. Thermodynamic model of the fluidized bed dryer with internal heat exchanger

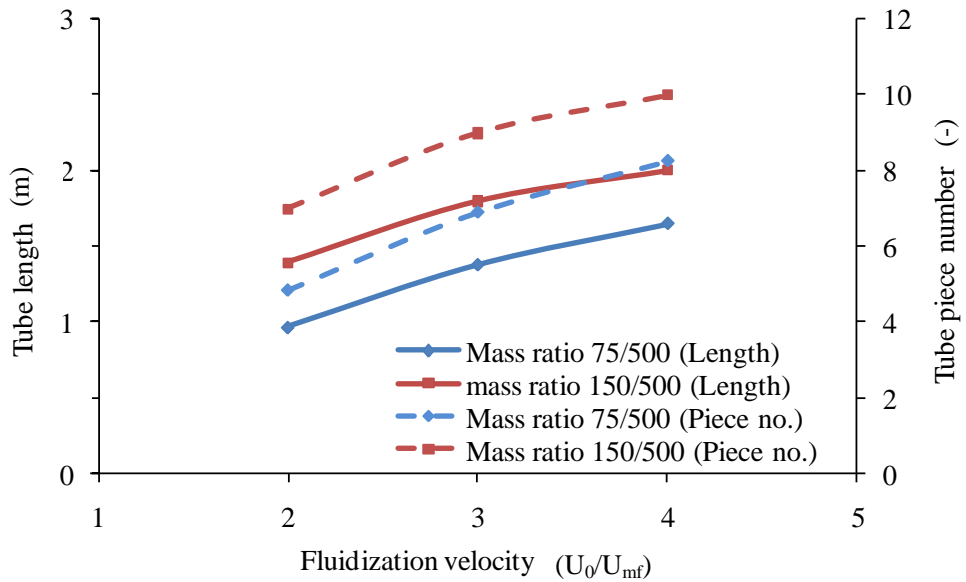


Fig. 3-2-9. Required tube length in the fluidized bed dryer

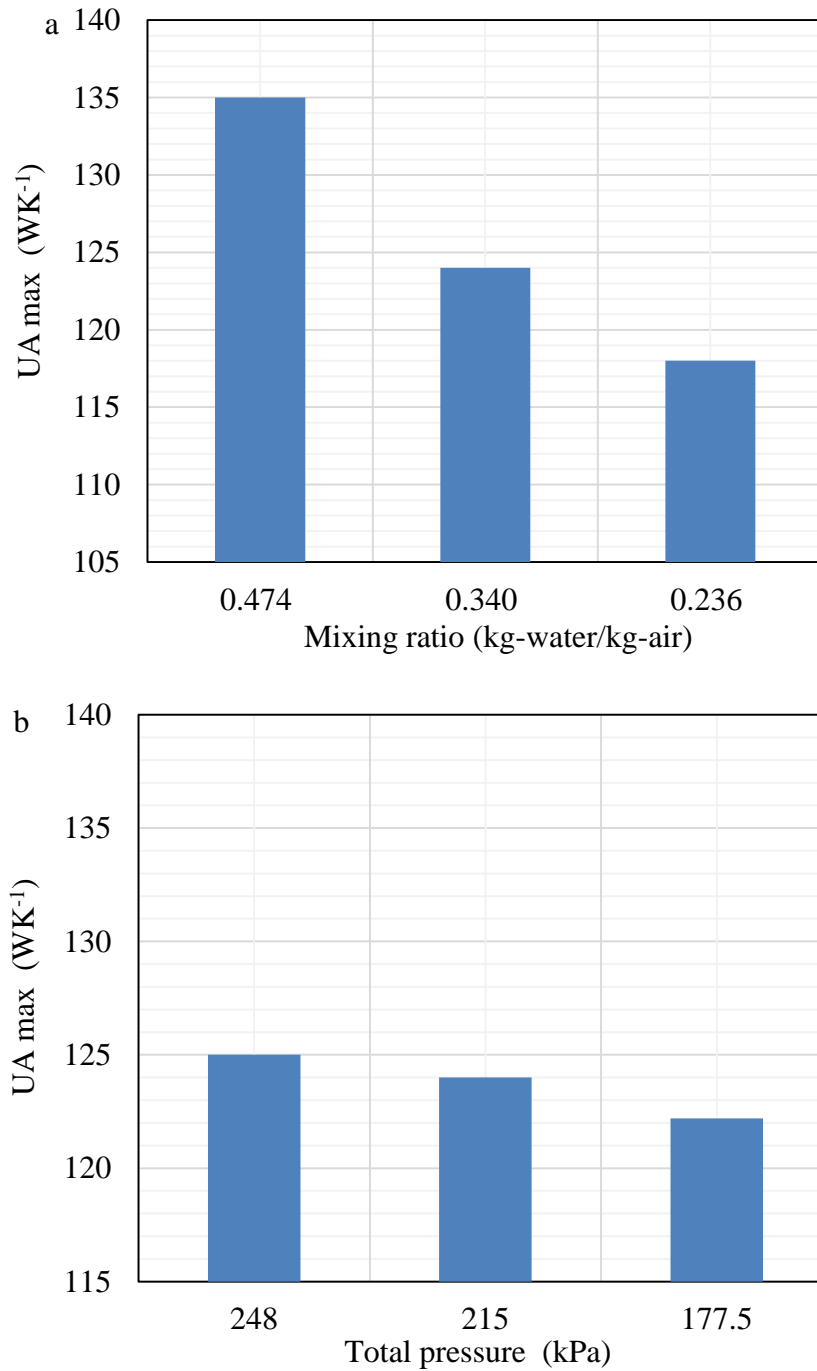


Fig. 3-2-10. a) Effect of air-steam ratio on the overall heat transfer rate, and b) effect of air-steam pressure on the overall heat transfer rate

3.2.3. 3. Stability of the fluidized bed dryer

In the stability investigation experiment, a high-temperature compressed air–steam mixture flowed through the immersed tubes inside the FBD and was used as the heat source for water evaporation. Properties of tubes and the air–steam mixture are presented in Table 3-2-2, and the fluidization velocity was $3U_{mf}$ and the bed temperature was maintained at 90 °C, to act as the same conditions with inlet air–steam mixture in the simulation part. Samples were taken and the water content of the sampled rice straw was measured using the ASTM D4442-07 standard.

Table 3-2-2. Properties of heat transfer tubes immersed inside FBD and mixture of air and steam in the drying experiment

Properties	Values
<i>Tube</i>	
Tube Material	SUS316 (18% Cr, Ni 12%, Mo 2.5%, 67.5% Fe)
Thermal conductivity (W mK ⁻¹)	16.7
Inner diameter (mm)	8
Outer diameter (mm)	10
Arrangement	Horizontal
Pitch distance (mm)	50
<i>Mixture of air and steam</i>	
Mixing ratio (kg-steam/kg-air)	0.52
Flow rate (NL min ⁻¹)	100
Relative humidity (-)	0.45
Inlet temperature (°C)	114.3
Inlet pressure (kPa)	215

The mixture of sand and dried rice straw was added in every 10 min from the inlet; meanwhile, a sample was taken from the outlet of the FBD. Fig. 3-2-11 shows that the temperatures in the bed, especially the bed top temperature, dropped at the time of wet biomass feeding under the influence of the cold wet biomass feeding from the top of the bed. Afterward, the temperature soon returned to the mean temperature owing to the good mixing in the fluidized bed. The temperature difference among the top, middle and bottom levels was very small, indicating a homogenous state in the fluidized bed.

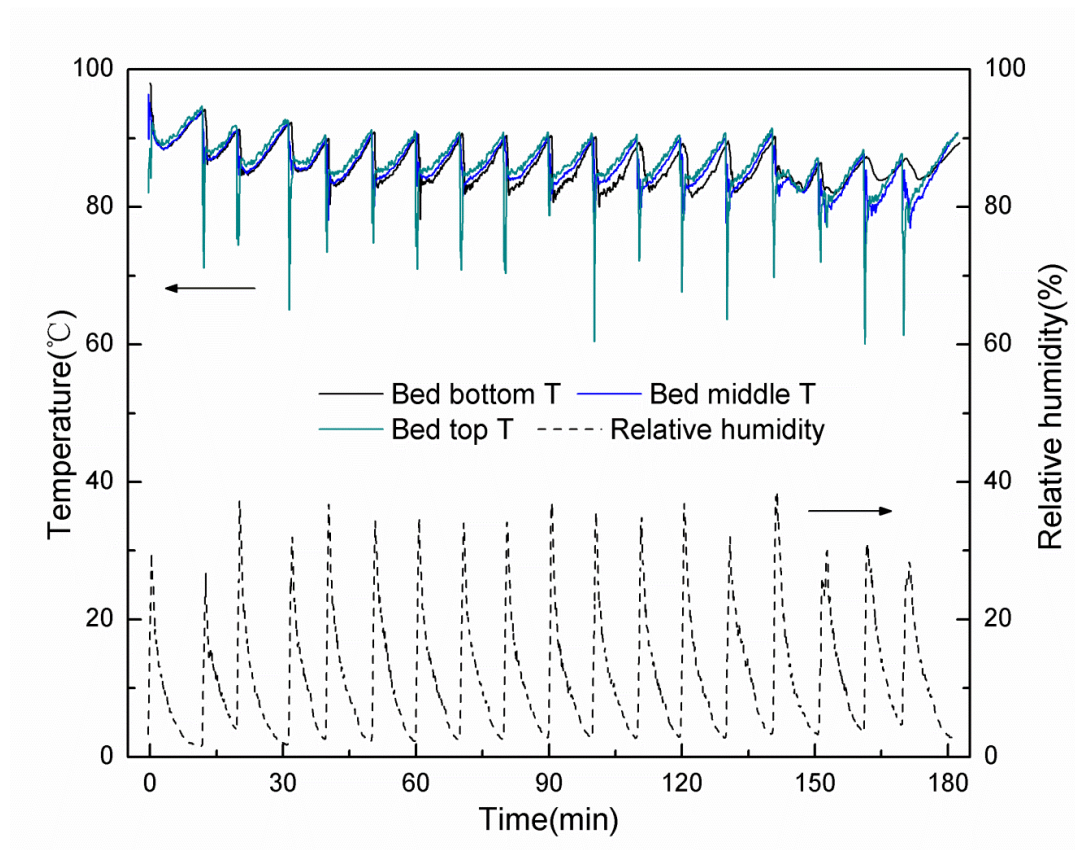


Fig. 3-2-11. The bed temperature distribution and relative humidity of outlet moist air in the FBD

Moreover, no segregation tendencies were observed visually between the rice straw and silica sand in the fluidized bed. The relative humidity of the outlet air was highest for a large amount of evaporated free water, when the rice straw was added to the bed, and decreased as time passed owing to the removal of the surface water and the internal water ratio increased. Consistent temperature and pressure of the air–steam mixture at the outlet of heat-exchange tubes are confirmed and shown in Fig. 3-2-12. The mean values of the outlet absolute pressure and temperature of the air–steam mixture were about 185 kPa and 95 °C, respectively, indicating a stable heat exchange between the immersed tubes and the fluidized bed. The drops in pressure and temperature through the 18 immersed tubes during the heat exchange were about 30 kPa and 20 K, respectively, owing to the consistent heat exchange with the wet biomass and the condensation of vapor in the compressed mixture.

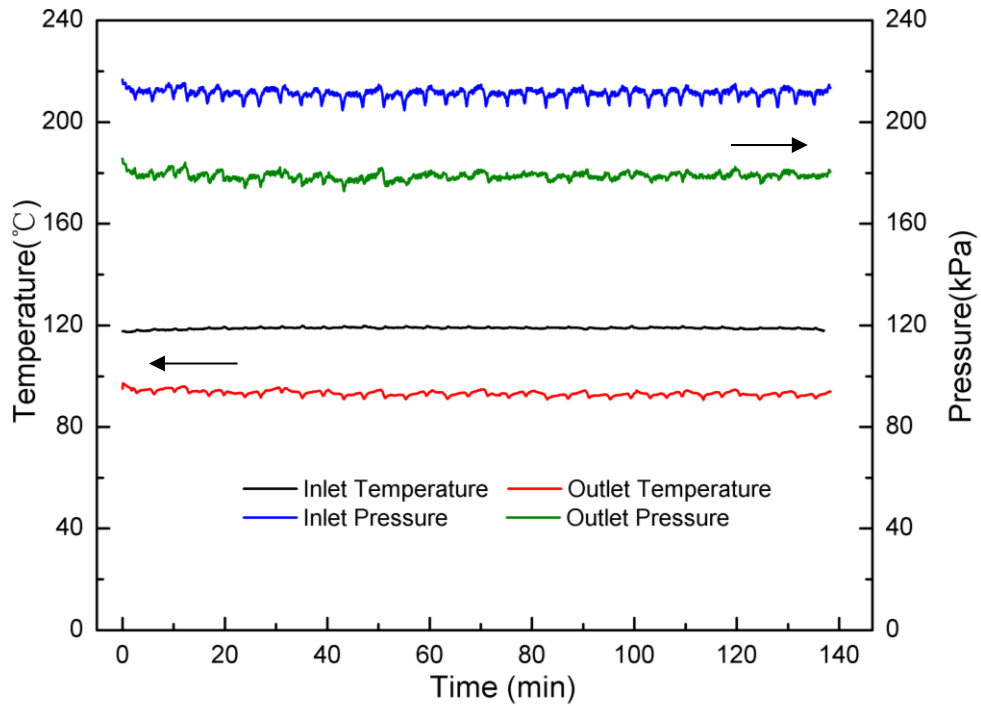


Fig. 3-2-12. Temperature and pressure of the air–steam mixture at the inlet and outlet of the FBD

Mixture of sand and biomass was sampled from bed in every 15 min. Average water content of the dried biomass was detected using the formal method. The weight ratio of biomass to sand is also constant (Fig. 3-2-13a). The value shows stable and 14.6 ± 1.6 wt% (Fig. 3-2-13b).

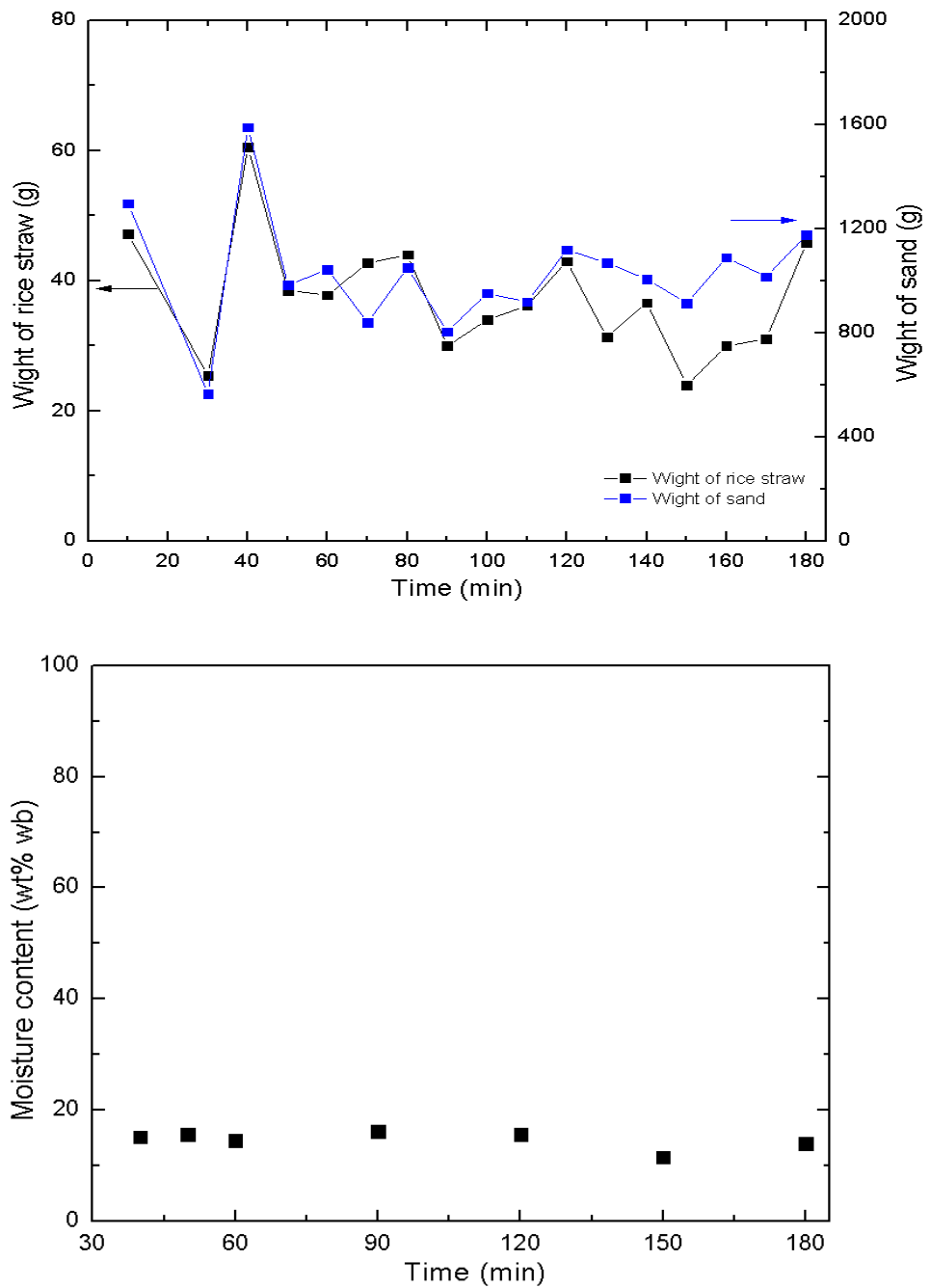


Fig. 3-2-13. a) the weight ratio of dried biomass to sand at the outlet of fluidized bed dryer, b) moisture content of the dried rice straw at the outlet of fluidized bed dryer.

3.2.4. Conclusions

In the experiment, we investigated the hydrodynamic behavior inside the FBD with silica sand as the fluidizing particles and immersed heating elements as a heat source. The results show that good solid mixing, as well as a uniform temperature across the bed, can be achieved under the condition that the fluidization velocity is at least three times the minimum fluidization velocity of sand and a good drying performance can be also achieved in this situation. Heat transfer in the fluidized bed has also been studied between the compressed air-steam mixture in the heat transfer tubes with biomass particles in the fluidized bed and showed the possibility of using compressed air-steam mixture as the heating source. Furthermore, a stability investigation of the FBD was conducted in which a good stability has been found in the experiments.

References

- ASTM Standard D4442-07, 2003. *Standard Test Methods for Direct Moisture Content Measurement of Wood and Wood-Base Materials*. ASTM International, West Conshohocken, PA, 2003.
- Chandran, A. N., S. S. Rao, et al. (1990). "Fluidized-Bed Drying of Solids." *AICHE Journal* **36**(1): 29-38.
- Fushimi, C., T. Wada, et al. (2011). "Inhibition of steam gasification of biomass char by hydrogen and tar." *Biomass & Bioenergy* **35**(1): 179-185.
- Groenewold, H. and E. Tsotsas (2007). "Drying in fluidized beds with immersed heating elements." *Chemical Engineering Science* **62**(1-2): 481-502.
- Hemati, M., K. Spieker, et al. (1990). "Experimental-study of sawdust and coal particle mixing in sand or catalyst fluidized-beds." *Canadian Journal of Chemical Engineering* **68**(5): 768-772.
- Rowe, P., B. Partridge, et al. (1965). "The mechanics of solids mixing in fluidised beds." *Trans. Inst. Chem. Eng.* **43**: 271-286.

CHAPTER 4

SELF-HEAT RECUPERATION

TECHNOLOGY FOR BIOMASS DRYING IN

OTHER DRYERS

4.1. Introduction

SHR technology has so far only been applied to fluidized bed dryers. It is known that there are many other drying systems for biomass drying, such as the rotary dryer (Zabaniotou 2000), conveyor dryer (Waje, Thorat et al. 2006; Waje, Thorat et al. 2007) and fixed and moving bed dryers (Zanoelo, di Celso et al. 2007). No investigation into the application of SHR technology to these drying systems has been conducted. This chapter aims to evaluate the energy-saving potential by applying SHR technology to biomass drying systems including both concurrent and countercurrent dryers. Energy consumption of each drying system was calculated and compared with that of a conventional heat recovery drying process. Reasons for energy saving in biomass drying system were discussed and factors such as the heat exchange type, ratio of air to product, minimum temperature difference in the heat exchanger, and drying medium were evaluated when applying SHR technology to a biomass drying system. The basic concept of the drying process is the same with that in Chapter 3, however, the dryer for biomass water evaporation was change from the fluidized bed dryer to the rotary dryer and screw conveyor dryer.

4.2. Process calculations

The simulation was conducted using PRO/II Ver. 9.0 (Invensys, Corp.) to examine the energy consumption required for the drying processes of biomass. Three different kinds of dryers: fluidized bed, rotary and screw conveyor dryers were evaluated for biomass drying. Properties of biomass and each dryer investigated in this work are shown in Table 3-1-1. In simulations, Soave-Redlich-Kwong equation was selected

for the stage equation. The adiabatic efficiencies of the compressor, blower and expander were assumed to be 80 %, 80 % and 90 %, respectively. In addition, the minimum temperature differences for the heat exchangers were assumed to be 10 K for the fluidized bed dryer and 30 K for the other heat exchangers. Heat exchange is concurrent in the fluidized bed dryer and countercurrent in the other heat exchangers. The biomass has the same flow direction as the air in the drying system. No heat loss is assumed from the drying system to the surroundings. The equilibrium moisture content of biomass depends on the water activity which is the relative humidity of gas for gas drying (Bjork and Rasmuson 1995). To dry the biomass to a water content of 20 wt% (wb) with air, the relative air humidity should be kept below 0.9 based on the research results of Pakowski et al. (2007). Water is transferred from the wet biomass to the air during the drying process and could be illustrated as (Pang and Mujumdar 2010):

$$m_g \frac{\partial Y}{\partial z} = -m_s \frac{\partial X}{\partial t} , \quad (4-1)$$

Table 4-1. Properties of biomass particle and drying devices

Properties	Values
<i>Biomass</i>	
Flow rate (10^3 kg h^{-1})	10
Fed temperature(°C)	20
Initial water content (wt% wb)	50
Final water content (wt% wb)	20
Bulk density (kg m^{-3})	180
Particle density(kg m^{-3})	400
Min. fluid. velocity (m s^{-1})	0.88
Size	Side length 10 mm, Thickness 3 mm
Sphericity (-)	0.6
<i>Fluidized bed dryer</i>	
Shape	Square
Side length (m)	4
Bed aspect ratio (-)	1.0
<i>Rotary dryer</i>	
Diameter (m)	4.5
Length (m)	36
Rotary speed (rpm)	7.7
<i>Screw conveyor dryer</i>	
Diameter (m)	0.5
Length (m)	60

where Y is the air humidity, X is the moisture content of biomass (dry basis), and z is the length of the dryer. Drying process in the self-heat recuperative drying process can be separated into preheating and evaporation periods. In the evaporation period,

drying usually takes place in two stages: constant drying rate period and falling rate drying period. During the constant drying rate period, free water is evaporated from the surface of the material. Furthermore, during the falling rate drying period, water evaporation rate is controlled by diffusion mechanism. The inner moisture is first transported to the particle surface by diffusion and then evaporated. In this paper, biomass drying is conducted to the water content of 20 wt% (wb) which is higher than the fiber saturation point. Thus, mainly free water is evaporated. The drying rate, R_w , could be calculated based on Eq. 4-2:

$$R_w = -m_s \frac{\partial X}{\partial t} = \frac{q_s}{\Delta H_{\text{vap}}} \quad (4-2)$$

The drying rate is constant as 3,750 kg-water h⁻¹ for drying 10,000 kg h⁻¹ biomass from 50 to 20 wt% (wb). For water evaporation, evaporation heat, q_s , is transferred from the compressed air–steam mixture inside the heat transfer tubes to the wet biomass, and can be approximate as

$$q_s = UA(T_{\text{vap}} - T_s); \quad (4-3)$$

the corresponding heat balance was calculated as

$$UA(T_{\text{vap}} - T_s) = m_s \Delta H_{\text{vap}} \frac{\partial X}{\partial t} + (m_s C_{ps} + m_l C_{pl} + m_g C_{pg}) \frac{\partial T_s}{\partial t} \quad (4-4)$$

Kinetics of heat transfer in the recuperative dryer and required heat exchange surface were also evaluated. The overall heat transfer coefficient, U , and surface area, A , is approximated by the following equation:

$$\frac{1}{UA} = \frac{1}{A_c \alpha_c} + \frac{\ln(R/r)}{2\pi L \lambda_t} + \frac{1}{\alpha_t A_t} . \quad (4-5)$$

Heat transfer coefficient due to the horizontal heat element immersed inside the fluidized bed can be represented as (Borodulya, Teplitsky et al. 1989; Borodulya, Teplitsky et al. 1991; Yang, W.C., 1999)

$$Nu_t = 0.74 Ar^{0.1} \left(\frac{\rho_p}{\rho_g} \right)^{0.14} \left(\frac{C_p}{C_g} \right)^{0.24} \nu_p^{2/3} + 0.46 Re Pr \frac{\nu_p^{2/3}}{\nu_g} , \quad (4-6)$$

$$\text{where, } Nu_t = \frac{a_t d_p}{\lambda_g} . \quad (4-7)$$

Convection heat transfer coefficient for flow in tube bundles in the rotary dryer is depending on the dryer rotational speed, and flow rate of air which is used to carry away evaporated vapor. Heat transfer coefficient between samples and jacket is calculated from the correlation of Schlünder (1984) for immersed heating surface to the drying samples. Heat transfer from the hot surface to materials in the screw conveyor dryer is 6 to 70 W m⁻² K⁻¹, depending on the screw speed and water content of the material (Nonhebel 1971). Heat transfer coefficient of film condensation in the horizontal tubes is approximated using a general correlation proposed by Shah (1979) based on the Dittus-Boelter equation as follows:

$$\alpha_c = \frac{0.023 Re_1^{0.8} Pr_1^{0.4} \lambda_1}{2r} \left[(1-x)^{0.8} + \frac{3.8x^{0.76} (1-x)^{0.04}}{\left(\frac{p}{p_{crit}} \right)^{0.38}} \right] . \quad (4-8)$$

In the rotary dryer, energy is consumed because of the power of blower which

compensates for the pressure loss in the rotary dryer and motor power to drive the rotary dryer. The former can be calculated as follows :

$$\Delta p_s = \left[\frac{4f(N_b + 1)D_s G_s^2}{2D_e \rho_{\text{vap}}} \right] \times 0.5, \quad (4-9)$$

$$f = 1.87 \left(\frac{G_s D_e}{\mu_{\text{vap}}} \right)^{-0.2}, \quad (4-10)$$

where Δp_s is the pressure drop across the rotary dryer. The motor power, *bhp*, given in the break horsepower (1 *bhp* is equal to 0.75 kW), can be calculated by the following equations (Krokida, Marinos-Kouris et al. 2009):

$$bhp = \frac{N \left[4.75 D W_{\text{mat}} + 0.1925 (D + 2) W_{\text{tot}} + 0.33 W_{\text{tot}} \right]}{100,000} \quad (4-11)$$

In the screw conveyor dryer, energy is consumed in turning the screw and moving the drying materials. Equations for the calculation of energy consumption in the screw conveyor dryer are available in the research of Waje et al. (2006; 2007).

Exergy analysis was conducted in the drying systems to investigate and quantify the exergy loss, and could be divided to inevitable and avoidable exergy losses.

$$Ex_{\text{loss}} = Ex_{\text{inv}} + Ex_{\text{avi}} \quad (4-12)$$

Inevitable exergy loss is the minimum exergy loss for the drying process and avoidable exergy loss occurs from the heat transfer due to the heat exchange temperature difference larger than the minimum temperature difference. Inevitable exergy loss owing to irreversibility during heat exchange during preheating and evaporation can be calculated by Eqs 4-13 and 4-14, respectively:

$$Ex_{inv,pre} = (m_p \Delta S_p + m_1 \Delta S_1) \Delta T_{min}, \quad (4-13)$$

$$Ex_{inv,evp} = m_1 \frac{\Delta H_{vap}}{T_{trs}} \Delta T_{min}. \quad (4-14)$$

Exergy balance in the heat exchanger could be expressed as:

$$Ex_{loss} = \sum_{in} Ex_i - \sum_{out} Ex_i. \quad (4-15)$$

Exergy of each stream can be calculated by Eq. 4-16,

$$Ex_i = (m_i h_i - m_i h_0) - T_0 (m_i s_i - m_i s_0). \quad (4-16)$$

Then, the exergy change between the outgoing and incoming streams is:

$$\sum_{in} Ex_i - \sum_{out} Ex_i = (m_{in} h_{in} - m_{out} h_{out}) - T_0 (m_{in} s_{in} - m_{out} s_{out}). \quad (4-17)$$

For the compressor, exergy balance could be presented as:

$$\sum_{in} Ex_i + W_{elect} = \sum_{out} Ex_i + Ex_{loss}. \quad (4-18)$$

4.3. Results and discussion

SHR technology has also been applied to other biomass drying systems. Table 4-2 illustrates that energy consumptions in both rotary and screw conveyor dryers could be reduced to 1/5–1/7 of that of a conventional heat recovery dryer. It was also found that the rotary and screw conveyor dryers consumed less energy compared to the fluidized bed dryer to dry the same amount of biomass. The reason was that compression works for rotary and screw conveyor dryers were much less than that for

the fluidized bed dryer which were shown in Table 4-2. Energy consumption in the self-heat recuperative dryers mainly comes from the compressor as shown in Eq. 4-19. The compression work for the heat circulation in a self-heat recuperative drying system is given by

$$W_{cp} = m_{stm} C_{vs} \Delta T + m_g C_{vg} \Delta T , \quad (4-19)$$

where ΔT is the temperature difference between the outlet and inlet of the compressor. The steam amount, m_{stm} , in the dryer is fixed for drying the same amount of wet biomass to the same water content. Thus, a large amount of input air would increase the energy input for the compressor and generate a large amount of sensible heat of air causing the unmatched heat pairing. In the fluidized bed dryer, a large amount of air with high velocity is required to form the fluidization of particles in the fluidized bed. In the rotary dryer, biomass particles are moved down throughout the dryer due to gravity following the slop of the drum and drag force of the gas, and in the screw conveyor dryer, particles are moved by a screw. The air amount which is smaller in the rotary and screw conveyor dryers than that in the fluidized bed dryer, reduces the energy input of the compressor.

Table 4-2. Exergy loss in each device of different biomass drying systems

	Air amount (10 ³ kg/h)	Preheating			Evaporation		Comp ressor	
		HX1	HX2,3	Ex_{avi}	HX4	Ex_{avi}		
Previous fluidized bed dryer	6.2	40.0	18.6	9.6	479.7	355	99.4	
This work		HX1,2	HX3	HX4	Ex_{avi}	HX5	Ex_{avi}	
Advanced fluidized bed dryer	6.2	8.4	1.5	97.7	58.6	189.0	122	65.4
Rotary dryer	3.1	11.7	1.8	92.7	57.2	197.2	3.9	52.0
Screw conveyor dryer	1.0	15.0	1.4	67.7	35.1	192.8	1.0	40.5

Unit of exergy loss is kW, and T_0 is the temperature of the surroundings (20 °C).

We also calculated exergy loss during the compression in different drying systems. Exergy loss of compressor increased with the increase of air amount, which were 52.0 and 40.5 kW, respectively, in the rotary and screw conveyor drying systems, and 65.4 kW in fluidized bed drying system. Another important reason for the less energy consumption in rotary and screw conveyor dryer is that, temperature difference between the cold and hot streams is closer to the minimum temperature difference in the countercurrent heat exchange dryer (rotary and screw conveyor dryers) than that in the concurrent heat exchange dryer (fluidized bed dryer), which increases the energy efficiency. Avoidable exergy losses during water evaporation were 3.9 and 1.0 kW respectively, in the rotary and screw conveyor dryers, which were much less than the 122 kW occurred in the fluidized bed dryer. Large exergy loss occurs owing to a

large temperature difference over the minimum permissible which results in unnecessary irreversibility.

To design a self-heat recuperative drying system, it is important for the heating surface of heat exchanger to form a good heat pairing and recuperate the heat in the system. Heat exchange areas in different drying systems were shown in Table 4-3. To achieve the heat exchange surface area, in the rotary dryer, about 101 tubes with 36 m length were required to be rotated axially along the dryer when the air amount was $6,200 \text{ kg h}^{-1}$. In the screw conveyor dryer, the screw flights could be considered as a fin on a heated surface, and heat exchange could through the inner surface of the screw dryer and the surface of screw flights. The screw shaft diameter is commonly 35 % of the screw diameter and screw pitch ranges 0.7 to 1.0 times the screw diameter. Heating surface area in the screw conveyor dryer was 331.5 m^2 and screw pitch was 0.45 m. On the other hand, although more energy consumption was required for the fluidized bed dryer due to blower power for the fluidization, the drying system was more compact requiring less heating surface for the same amount of product compared with the rotary and screw conveyor dryers. The main reason comes from the high heat transfer coefficient, a_t , between the tube surface and the drying materials in the fluidized bed owing to the large gas-solid surface which increases heat and mass transfer rates, which was 7 times higher than that of the rotary and screw conveyor dryers (Daud 2008; Eliaers and De Wilde 2013). Tube number increased with the increase of fluidization rate, and about 495 tubes arraying on a 45° pitch were required for heat exchange in the fluidized bed dryer at an air

velocity of $3U_{mf}$. Considering the tubes were uniformly distributed across the bed, the pinch distance among the tubes was about 0.17 m which was significantly larger than the biomass size. The immersed tubes could also improve the biomass fluidity and enhance heat transfer performance by reducing the bubble size in the fluidized bed. The relationship between energy saving from additional surfaces and the consequent capital cost needs to be investigated in a future study. Moreover, the self-heat recuperative drying process increases heat exchange surfaces and requires a compressor for heat circulation, which increases the capital cost of the drying system. However, the increased capital cost could be recovered through significant energy consumption reduction after 3–5 years' operation depending on the properties and amount of the materials to be dried.

In the following, effect of the minimum temperature difference in the heat exchanger on the energy consumption was investigated. Fig. 4-1 shows a linear correlation between the energy consumption and the minimum temperature difference. With the minimum temperature difference decreasing from 40 K to 5 K in the self-heat recuperative rotary dryer with air input amount of 3100 kg h^{-1} , energy consumption decreased by 50 %. The reason was that exergy loss due to the irreversibility of heat transfer was reduced by reducing the temperature difference during the heat exchange. A lower minimum temperature difference requires less energy consumption for the compressor, thus reduces the energy consumption in the total drying system. However, it should be mentioned that the temperature difference in the heat exchanger is limited by the increase of the capital cost.

Table 4-3. Energy consumptions of the biomass drying systems

Dryer	Conventional heat recovery dryer	Fluidized bed dryer			Rotary dryer			Screw conveyor dryer
Air amount (10^3 kg/h)		6.2	12.4	18.6	1.0	3.1	6.2	1.0
Energy Input (kW)								
Heater	2700	-	-	-	-	-	-	-
Blower	-	95	185	276	4	13	25	-
Compressor	-	529	692	854	375	467	575	375
Expander	-	-157	-270	-372	-39	-95	-169	-39
Motor	-	-	-	-	98	98	98	60
Total input	2700	449	590	726	428	483	529	396
Heating surface area (m^2)								
		135.5	162.6	186.2	236.1	279.3	341.9	331.5
Heating surface per kg of product (m^2)								
		0.022	0.026	0.030	0.038	0.045	0.055	0.053
Length of tubes (m)								
		1,438	1,726	1,977	2,506	2,965	3,629	3,519
Tube number (-)								
		360	432	495	70	83	101	-
Screw pinch (m)								
		-	-	-	-	-	-	0.45

^aNegative values mean recuperated work from the expander.

^bTube diameter is 30 mm, thickness is 2 mm and tube material is SUS444 (18 % Cr, 1.9 % Mo, 80 % Fe) with thermal conductivity, λ_t , of $26.8 \text{ Wm}^{-1}\text{K}^{-1}$.

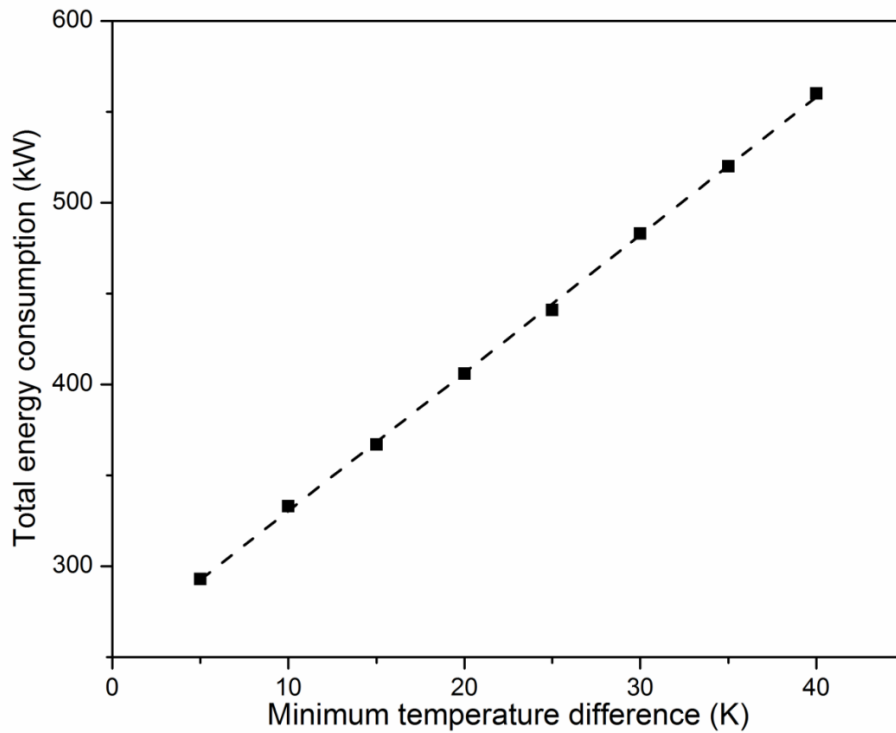


Fig. 4-1. Effect of the temperature difference on the energy consumption of the proposed drying system

The self-heat recuperative drying system is a closed system, thus the drying medium can be recirculated resulting in the broader possibility of applying an inert gas such as nitrogen or carbon dioxide as the drying medium, to avoid spontaneous combustion during drying. Energy saving potential with nitrogen or carbon dioxide as the drying medium was investigated. As shown in Fig. 4-2, the drying medium could also affect the energy consumption of the drying system, but not so dramatically. Energy consumption with nitrogen as the drying medium is a little smaller than that with air, and the energy consumption with carbon dioxide as the drying medium is the smallest. The variation in energy consumption results from the different heat capacities of the drying medium, and a low heat capacity reduces the compression work for the same temperature increase.

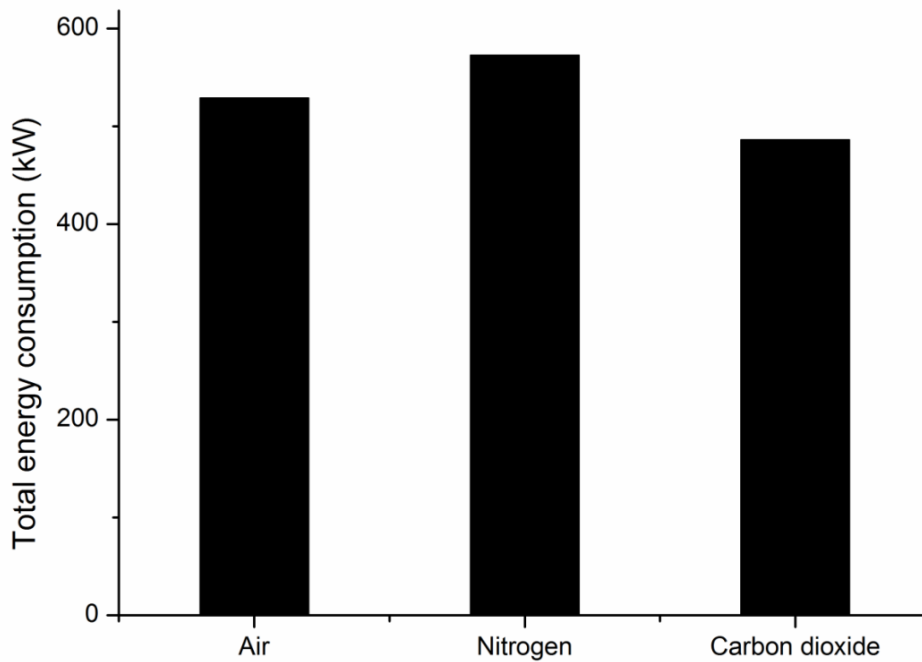


Fig. 4-2. Effect of the drying medium on the energy consumption of the proposed drying system

4.4. Conclusions

An advanced biomass drying process based on SHR technology was proposed for reducing energy consumption. Three drying systems (fluidized bed dryer, rotary dryer and screw conveyor dryer) were investigated based on SHR technology. In the new developed drying system, energy consumption was reduced to 1/7 of energy consumed by a conventional heat recovery dryer. Energy saving by applying SHR technology to the biomass drying systems mainly depends on counter/concurrent heat exchange and the minimum temperature difference between the hot and cold streams in the heat exchanger. Exergy analysis has been conducted for further energy saving solutions. Results showed that a countercurrent heat exchange and a smaller minimum

temperature difference contribute to energy saving in the biomass drying process, although the heating surface area was larger. This newly developed drying system could also use inert gas as the drying medium, and energy consumptions in the cases of nitrogen or carbon dioxide show almost the same value as that of air.

References

- "Process Design Rotary Dryer." from http://www.sbioinformatics.com/design_thesis/Terephthalic_acid/Terephthalic-2520acid_Design-2520of-2520Equipments.pdf.
- Bjork, H. and A. Rasmuson (1995). "Moisture Equilibrium of Wood and Bark Chips in Superheated Steam." Fuel **74**(12): 1887-1890.
- Borodulya, V. A., Y. S. Teplitsky, et al. (1991). "Heat-Transfer between a Surface and a Fluidized-Bed - Consideration of Pressure and Temperature Effects." International Journal of Heat and Mass Transfer **34**(1): 47-53.
- Borodulya, V. A., Y. S. Teplitsky, et al. (1989). "Heat-Transfer between a Surface and an Infiltrated Bed of Solid Particles." International Journal of Heat and Mass Transfer **32**(9): 1595-1604.
- Daud, W. R. W. (2008). "Fluidized Bed Dryers — Recent Advances." Advanced Powder Technology **19**(5): 403-418.
- Eliaers, P. and J. De Wilde (2013). "Drying of Biomass Particles: Experimental Study and Comparison of the Performance of a Conventional Fluidized Bed and a Rotating Fluidized Bed in a Static Geometry." Drying Technology **31**(2): 236-245.
- Krokida, M., D. Marinos-Kouris, et al. (2009). Rotary Drying, Handbook of Industrial Drying, CRC.
- Nonhebel G. and Moss A.A.H, Drying of solids in the chemical industry, Butterworth & Co., London, 1971.

- Pakowski, Z., B. Krupinska, et al. (2007). "Prediction of sorption equilibrium both in air and superheated steam drying of energetic variety of willow *Salix viminalis* in a wide temperature range." Fuel **86**(12-13): 1749-1757.
- Pang, S. S. and A. S. Mujumdar (2010). "Drying of Woody Biomass for Bioenergy: Drying Technologies and Optimization for an Integrated Bioenergy Plant." Drying Technology **28**(5): 690-701.
- Schlünder, E. U. (1984). "Heat transfer to packed and stirred beds from the surface of immersed bodies." Chemical Engineering and Processing: Process Intensification **18**(1): 31-53.
- Shah, M. M. (1979). "A general correlation for heat transfer during film condensation inside pipes." International Journal of Heat and Mass Transfer **22**(4): 547-556.
- Yang W.C., Fluidization, solids handling, and processing: industrial applications, Noyes Publications, Westwood, NJ, 1999.
- Waje, S. S., B. N. Thorat, et al. (2006). "An experimental study of the thermal performance of a screw conveyor dryer." Drying Technology **24**(3): 293-301.
- Waje, S. S., B. N. Thorat, et al. (2007). "Screw conveyor dryer: Process and equipment design." Drying Technology **25**(1-3): 241-247.
- Zabaniotou, A. A. (2000). "Simulation of forestry biomass drying in a rotary dryer." Drying Technology **18**(7): 1415-1431.
- Zanoelo, E. F., G. M. di Celso, et al. (2007). "Drying kinetics of mate leaves in a packed bed dryer." Biosystems Engineering **96**(4): 487-494.

CHAPTER 5

FURTHER ENERGY-SAVING BIOMASS

DRYING BASED ON SELF-HEAT

RECUPERATION TECHNOLOGY

5.1. A novel exergy recuperative drying module with superheated steam

5.1.1. Introduction

The exergy analysis study in Chapter 4 shows that a large amount of exergy loss occurred due to the existence of air, which caused the heat pairing unmatched. Thus, we changed the drying medium from incondensable gas to superheated steam to solve the above problem. Steam drying has been applied for industry use since a few decades ago. The advantages of using steam show as the improved energy efficiency due to the possibility of latent heat utilization, and the elimination of explosion and hazard risks. In this work, we firstly developed a novel drying module using superheated steam as the drying medium based on self-heat recuperation technology. Energy consumption in the exergy recuperative drying system was estimated by using a process simulator PRO/II to compare with that of the existing energy-saving drying system. Then, the exergy recuperative drying module would be applied for the biomass drying systems with a fluidized bed dryer as the evaporator.

5.1.2. Basic concept of an exergy recuperative drying module

Fig. 5-1-1 shows the basic concept of an exergy recuperative drying module. Wet sample is preheated and evaporated through sensible and latent heat exchange, successively. Water in the wet sample is converted to vapor. Thereafter it is superheated and compressed adiabatically to increase its exergy rate to provide heat for the successive drying. A heat pump module was utilized to recover the sensible heat of the dried solid for heat exchange with the inlet solid.

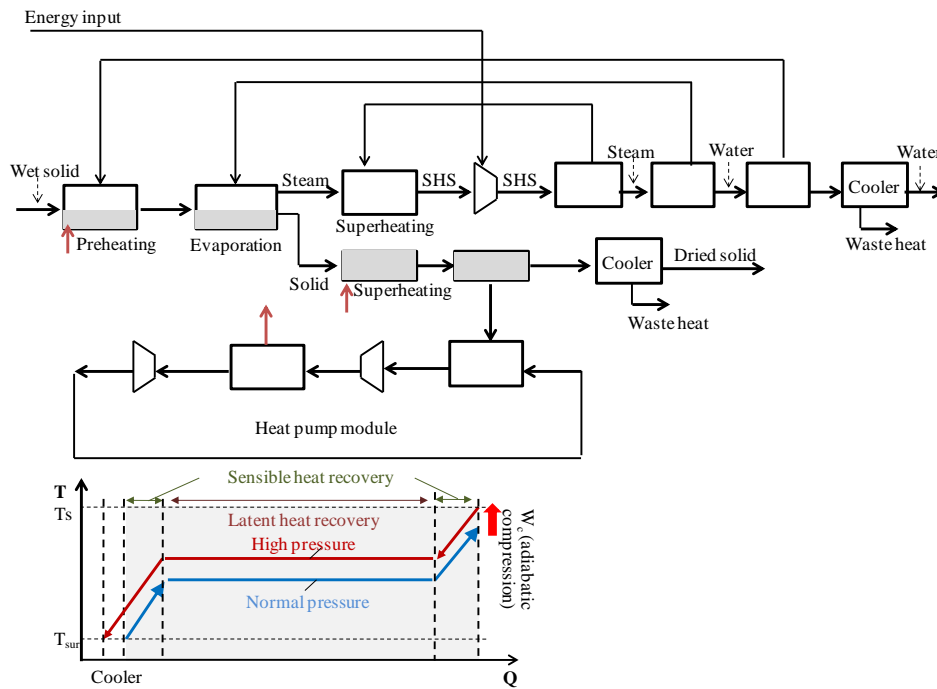


Fig. 5-1-1. Basic concept of exergy recuperative drying module

5.1.3. Design of an exergy recuperative drying system based on self-heat recuperation technology

5.1.3.1. Schematic layout of an exergy recuperative drying system

When applying the exergy recuperative drying module to an actual drying process, the existence of bound water internal to solids which requiring energy for desorption results in unmatched heat pairing. Thus, we divided the drying process into three continuous stages: preheating period, constant drying period for unbound water removal and falling rate drying period for bound water removal. Fig. 5-1-2 shows the schematic layout of the exergy recuperative drying system using superheated steam as the drying medium. Since the drying rate is controlled by the heat and mass transfer in the constant drying period, a fluidized bed dryer increases the drying rate and makes the equipment more compact. For the falling rate drying period, we chose a screw conveyor dryer with a countercurrent type, and the reason will be explained in Section 5.1.3.2.3.

Initially, the wet solid receives heat from the heat exchanger HX1 for preheating to the boiling point. Subsequently, it is fed to a fluidized bed dryer (HX2) where the unbound water is evaporated by the heat supplied from the compressed steam flowing inside the heat exchangers immersed in the bed. Then, the exhausted steam is split into the recycled and purged superheated steams. The purged superheated steam equivalent to the water evaporated from the wet solid is compressed and recirculated as the heat source for evaporation (HX2) and preheating (HX1). Then, the wet solids with the bound water are fed to the screw conveyor dryer (HX3) for the remaining water evaporation. The evaporated water is compressed and recycled to the screw conveyor dryer to increase the drying medium temperature. As a result, the relative pressure of superheated steam decreases to improve water holding capacities for water removal. Finally, the dried solid is cooled to the surrounding temperature.

5.1.3.2. Energy balance in the exergy recuperative drying system

5.1.3.2.1. Zone of preheating period

In the preheating period, the wet solid is preheated from the surrounding temperature (T_{sur}) to the boiling temperature, 373 K (T_{trs}), without water evaporation. Energy input for preheating is given by:

$$H_{preheat} = (m_w C_{pw} + m_{ps} C_{ps})(T_{trs} - T_{sur}) \quad (5-1-1)$$

where m_w and m_{ps} represent the amount of water and solid particles in wet solid particles, respectively. C_{pw} and C_{ps} are the constant pressure heat capacities of the water and the solid, respectively.

5.1.3.2.2. Zone of constant drying period

Following the preheating period, the constant drying period appears until the water

amount in the solid falls to m_{0w} . The bulk water on the particle surface and water in the macropores can be removed with slightly superheated steam. The energy consumption in this period is mainly due to the latent heat for water evaporation and the sensible heat supply for removing water from the macropores by superheating. The desorption heat for water in macropores is negligible compared with the evaporation heat. Thus, the amount of heat transferred to the wet solid can be calculated by:

$$H_{\text{FBD}} = (m_w - m_{0w})L_e + (m_w C_{pw} + m_{ps} C_{ps})(T_0 - T_{\text{trs}}) \quad (5-1-2)$$

where L_e is the water evaporation enthalpy, and T_0 is the fluidized bed temperature.

5.1.3.2.3. Zone of falling rate drying period

When the exposed surface water is removed, the water in the solid is mostly bound water. The drying rate decreases rapidly as the drying rate is governed by the water diffusion in the solid particle. To separate bound water from the solid, energy is required for both the latent heat of evaporation and the desorption heat which increases with progressing drying. Thus, the zone of the falling rate drying period may be considered to be divided into subzones numbered 1, 2, ..., n with m_{1w} , m_{2w} , ..., m_{nw} , and m_{nw} being the final dried solid water content. The heat transferred to the solid can be divided into three parts: latent heat of the water evaporation, water desorption heat and sensible heats of both water and solid particles from superheating. Energy consumption in each subzone is:

$$H_n = (m_{n-1w} - m_{nw}) \left[L_e + \Delta H_n + C_{pw}(T_n - T_{n-1}) \right] + m_{ps} C_{ps}(T_n - T_{n-1}) \quad (5-1-3)$$

Finally, the total heat transfer amount from the compressed steam to the solid in the falling rate drying period could be calculated as:

Water desorption heat can be derived from the Clausius-Clapeyron equation:

$$\Delta H = -\frac{R}{M_v} \left[\frac{\partial(\ln \frac{p}{p_{\text{sat}}})}{\partial(T_{\text{sorp}}^{-1})} \right]_v \quad (5-1-4)$$

where p/p_{sat} is the ratio of equilibrium pressure to saturated vapor pressure. R is the universal gas constant. M_v is the water molecular weight, and T_{sorp} is the desorption temperature. Thus, the total energy input for solid drying in the proposed system is

$$H_{\text{tot}} = H_{\text{preheat}} + H_{\text{FBD}} + H_{\text{SCD}} \quad (5-1-5)$$

5.1.4. Process simulation

We chose brown coal as an investigated sample in this research, which commonly contains a high water content of 45–70 wt% (wb). The properties of brown coal used in the calculation are shown in Table 5-1-1. The energy consumption of the proposed drying system (SHR) is compared with the existing energy-saving drying systems for brown coal drying.

Table 5-1-1. Prosperities of brown coal (Aziz et al. 2012)

Properties	Value
Type	Yallourn, seam Y
Initial moisture (wt% wb)	65
Volatile matter <i>V</i> (wt% db)	51.1
Ash (wt% db)	1.7
Carbon <i>F</i> (wt% db)	66.7
Hydrogen <i>H</i> (wt% db)	4.7
Sulfur <i>S</i> (wt% db)	0.3
Oxygen <i>O</i> (wt% db)	26
Max. vitrinite reflectance (%)	0.32
Bulk density (kg m ⁻³)	900
Molecular weight (-)	10660.5
Average particle diameter (m)	2.0×10 ⁻³
Voidage at min. fluid. <i>e_{mf}</i>	0.57
Sphericity	0.63

5.1.4.1. Sorption isotherm of brown coal

To decide the operation conditions of a drying process, it is necessary to have an understanding of solid–water interactions. Hence, sorption isotherms are required to determine the driving force which is the relative vapor pressure at different drying temperatures. The equilibrium moisture contents of Yallourn brown coal at different drying temperatures are calculated from Eq. 5-1-6 proposed by Chen et al. (2001) based on the experimental work conducted by Allardice and Evans (1971) as shown in Fig. 5-1-3.

$$\frac{P}{P_{\text{sat}}} = 1 - \exp \left[-2.53(T_b - 273)^{0.47} \left(\frac{M}{100 - M} \right)^{1.58} \right] \quad (5-1-6)$$

where T_b is the drying temperature, and M is the water content of the dried brown coal. The drying temperature is initially near 373 K until 37 wt% (wb). The temperature increases gradually as the water content drops from 37 to 20 wt% (wb), to provide a low relative vapor pressure to remove water in the macropores. Thereafter, the drying temperature increases significantly, and the remaining water is considered as the bound water.

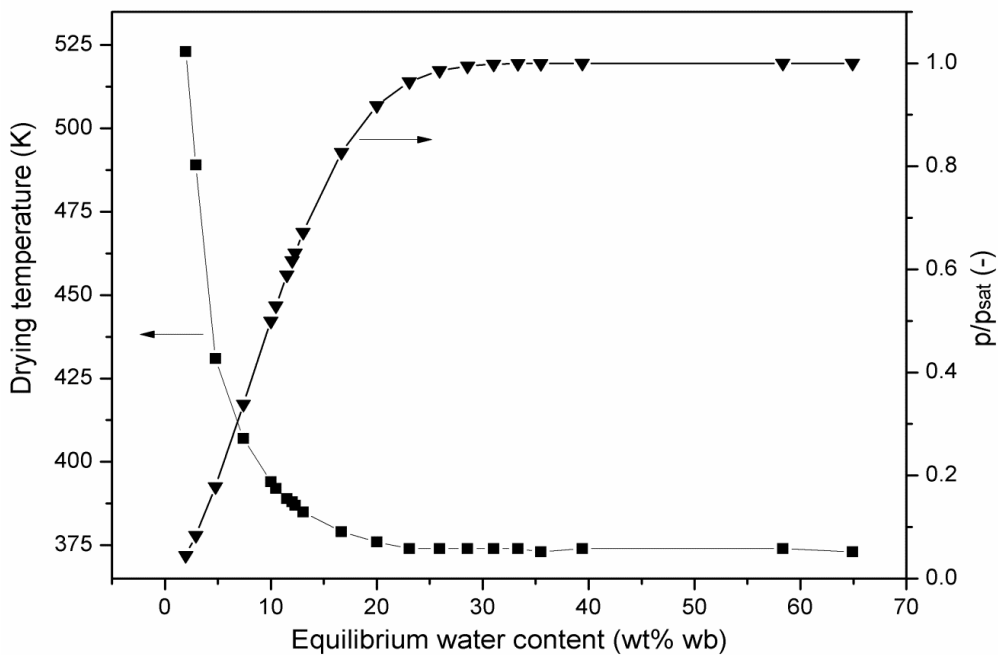


Fig. 5-1-3. Equilibrium moisture content of Yallourn brown coal at different drying temperatures and relative vapor pressures

5.1.4.2. Simulation conditions

To compare the energy consumption of different drying systems, we chose a fluidized bed dryer as the evaporator for different energy-saving drying systems. The minimum fluidization velocity for fluidization of brown coal particles can be derivated from the equation recommended by Chitester et al. (1984) for coarse particle involving the

correction factor for wet coal particles proposed by Pata et al. (1988).

$$U_{mf} = \frac{\mu_g \left\{ \left[(28.7)^2 + 0.0494Ar \right]^{1/2} - 28.7 \right\}}{\rho_g \left[1.182d_p - 5.65 \times 10^{-4} + \frac{7.413 \times 10^{-2}}{M^{1.58}} \right]} \quad (5-1-7)$$

The blower work to compensate the pressure loss Δp_f in the fluidized bed is calculated according to the equation proposed by Kunii and Levenspiel (1991) as follows:

$$\Delta p_f = \Delta p_b + \Delta p_d \quad (5-1-8)$$

where Δp_b and Δp_d are pressure drops across the bed and distributor, respectively, and they could be calculated as

$$\Delta p_b = (1 - \varepsilon_{mf})(\rho_p - \rho_g)H_b \frac{g}{c} \quad (5-1-9)$$

$$\Delta p_d = 0.4\Delta p_b \quad (5-1-10)$$

The mechanical energy input of the screw conveyor dryer is available in the previous work (Jangam et al., 2011; Waje et al., 2007). The simulation conditions for brown coal drying using the PRO/II ver. 9.0 software (Invensys Corp.) are as follows. (1) The wet brown coal inlet flow rate is 200 t h^{-1} and the initial moisture content is 65 wt% (wb); (2) drying is conducted to a water content of 10 wt% (wb) which requires brown coal particles finally heated to 393 K based on the sorption isotherm of brown coal shown in Fig. 5-1-3; (3) the adiabatic efficiencies of the compressor and blower are 80%; (4) drying is performed under atmospheric conditions; (5) thermodynamic calculations employ the Soave-Redlich-Kwong (SRK) method; (6) the fluidized bed dryer and screw conveyor dryer with internal heat exchangers can exist as a mixer, heat exchanger and separator; (7) the heat exchange is concurrent in the fluidized bed dryer and countercurrent in other heat exchangers including the screw conveyor dryer; (8) the

minimum temperature difference in each heat exchanger is assumed to be 10 K; (9) no heat loss is assumed from the drying system to the surroundings.

5.1.4.3. Simulation results

5.1.4.3.1. Energy consumption in the exergy recuperative drying process

Fig. 5-1-4 shows the energy consumption in different drying systems. Results showed that the energy consumption of the SHR is reduced to 1/7–1/12 that of the CHR. The MVR and MSD consume 1/4–1/7 and about 1/2 that of the CHR consumption, respectively. The variation in energy consumption of each drying system results from the blower work increase. This follows the increase in fluidization velocity as a result of the increase in volumetric amount of the drying medium. The CHR could recover about 15% of the input energy of the drying process.

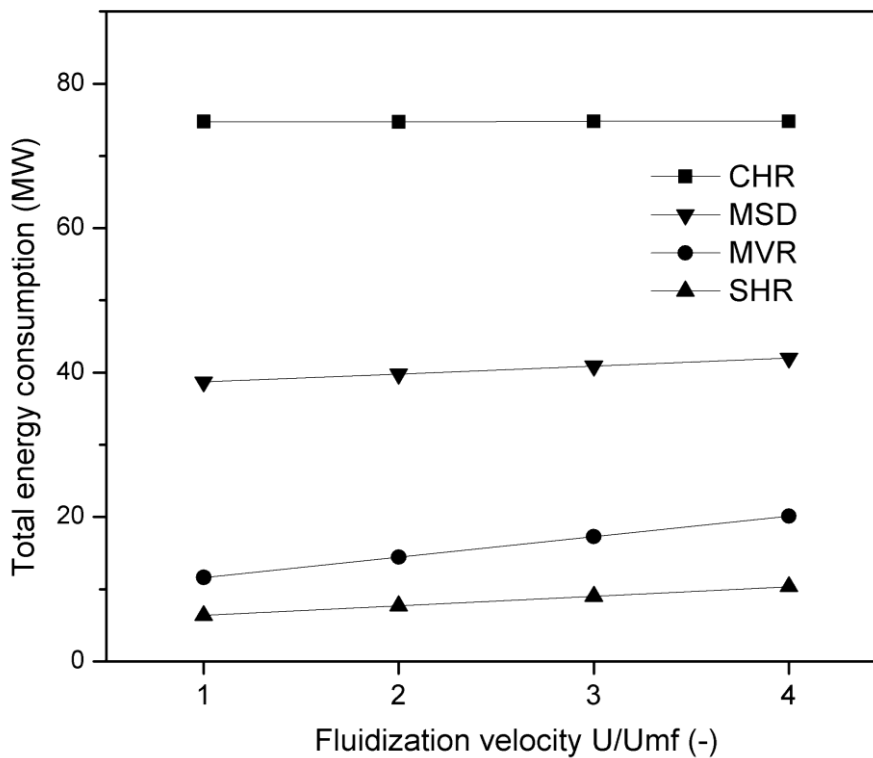


Fig. 5-1-4. Comparison of energy consumptions in different drying systems.

The energy consumption in the SHR can be further reduced by more than 40% compared with that of the MVR. The decrease in energy consumption results from good heat pairing in the newly designed drying process (Fig. 5-1-5) compared with that in the MVR. It should be noticed that, in the SHR and MVR dryers, electrical energy is required by the compressor; while in the CHR and MSD dryers, system energy is supplied by the combustion heat of fossil fuel in the boiler. To compare the two forms of energy, electrical energy is converted to primary energy by the given equation;

$$H = E/f \quad (5-1-11)$$

where H is thermal energy, E is electrical energy and f is electricity generation efficiency which is 36.6% in Japan. Thus, the equivalent primary energy use in the SHR and MVR can be reduced to 23% and 55% of that in the CHR, respectively.

The good heat pairing was described by the energy and material flow diagram of the exergy recuperative drying system shown in Fig. 5-1-6. The boxes represent units, the lines represent the flow of material or energy and the red arrows show the energy input in the drying system. We assumed that a heat exchanger can be divided into a self-heat transmitter and a self-heat receiver. Wet brown coal was preheated in self-heat receivers (2; 12.7 MW) (3; 0.5 MW) and evaporated in the self-heat receiver (4; 70.9 MW), pairing with sensible and latent heat of the purged superheated steam compressed by a compressor (5; 3.15 MW). The brown coal with bound water received heat from the self-heat receiver (6; 3.79 MW) to be dried to the desired water content. However, it should be mentioned that the proposed drying system added a screw conveyor dryer for bound water removal which may increase the investment cost. In addition, the increased number of dryers and compressors makes the drying system more complex. Such a complex system normally requires a more sophisticated control system to form the heat

pairing in each heat exchanger for energy saving.

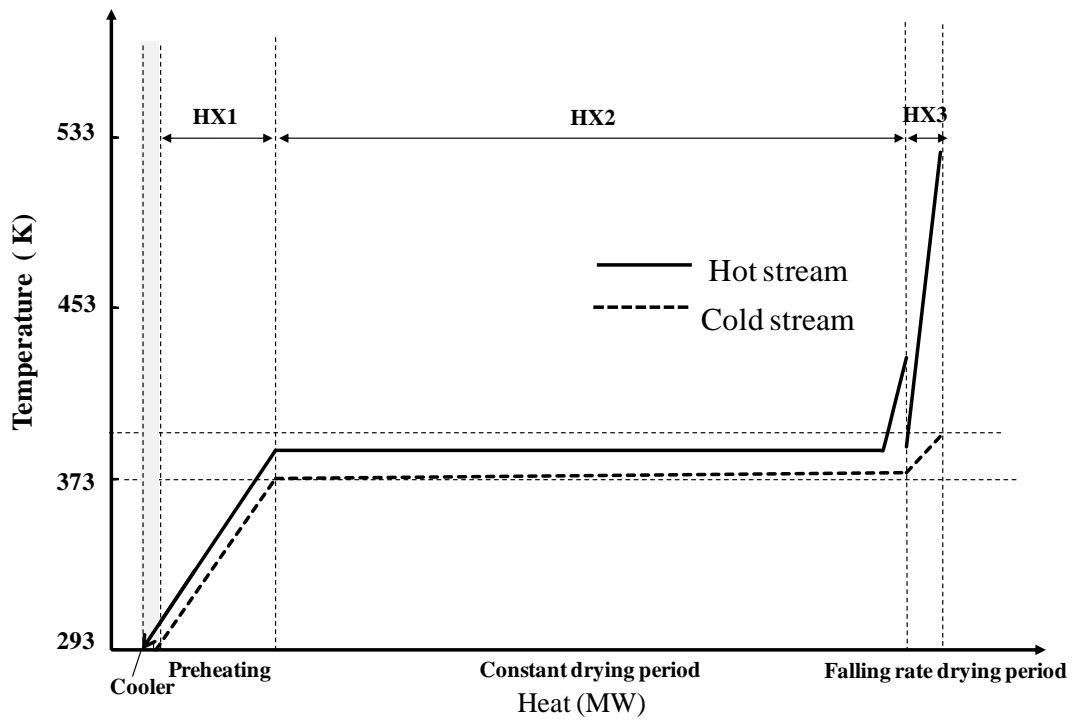


Fig. 5-1-5. Temperature and heat diagram of the exergy recuperative drying process.

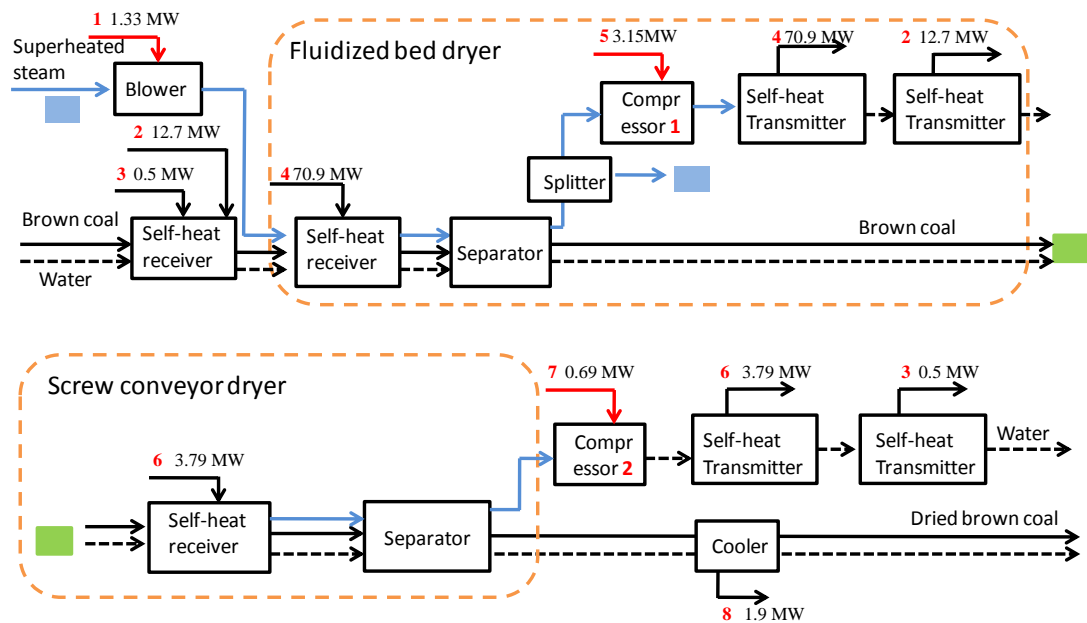


Fig. 5-1-6. Energy and material flow diagram of the exergy recuperative drying system.

5.1.4.3.2. Effect of final water content on energy consumption of the exergy recuperative drying system

We qualified the effect of final water content of the dried brown coal on the energy consumption of the drying system. As shown in Fig. 5-1-7, energy consumption in the MVR increased to more than two times when the final water content decreased from 17.5 to 7.5 wt% (wb). However, the energy consumption change in the SHR was not apparent compared with that in the MVR. Actually, the additional energy input is almost equal to the increase of desorption heat of the bound water. In addition, the energy consumption difference between the MVR and the SHR was not apparent when drying brown coal to high water content; however, it increased when the water content of the dried brown coal was low. This is because it requires a higher drying temperature to remove more bound water. In the MVR, water evaporation occurs in one heat exchanger (fluidized bed dryer), therefore, the entire bed temperature should be maintained at the final water desorption temperature for the intense particles mixing in the fluidized bed dryer. A large energy input for the compressor is required to increase the superheated steam condensation temperature for heat exchange to achieve the high bed temperature in the MVR. On the other hand, in the SHR, the negative effect of bound water on the heat pairing was reduced through separation of the unbound water and bound water removal in the fluidized bed dryer and screw conveyor dryer, respectively. In the screw conveyor dryer for bound water removal, the solid temperature gradually increases through the heat exchanger due to the countercurrent heat exchange. Meanwhile, bound water desorbs from smaller pores in the solid particle with the solid movement. Increased energy savings can be predicted owing to a small temperature difference which is near to ΔT_{\min} during the heat exchange in SHR compared with that in MVR.

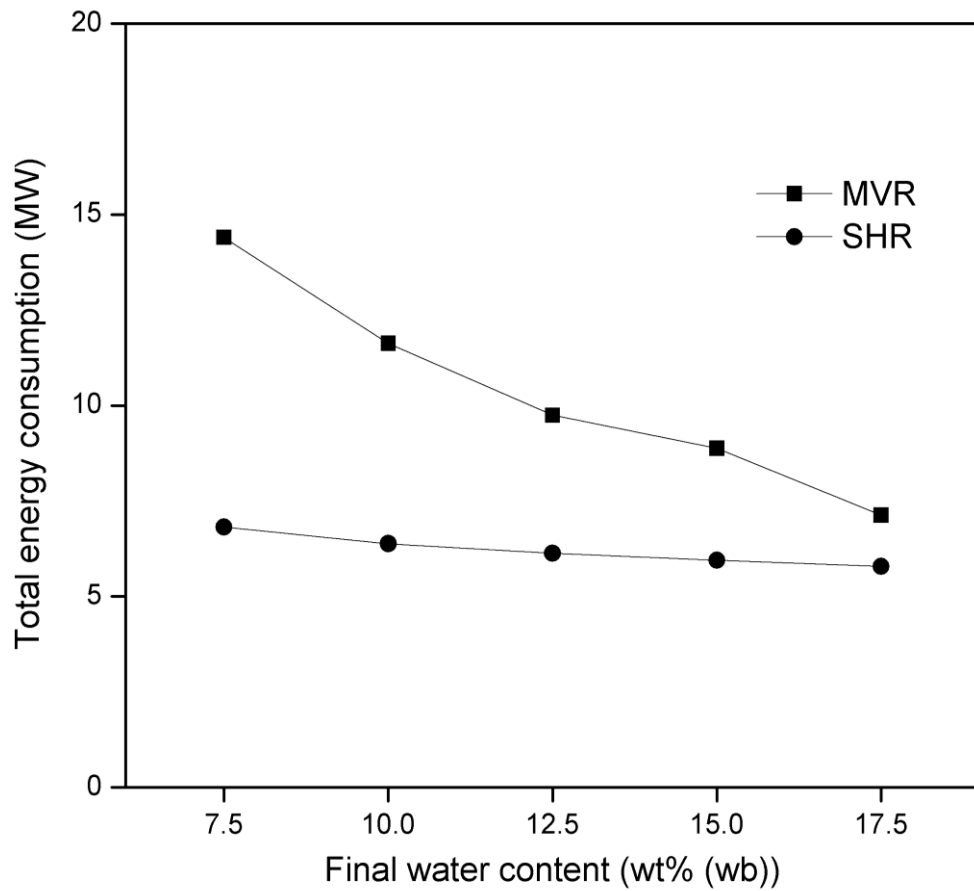


Fig. 5-1-7. Relationship between final water content of dried sample and energy consumption of the drying system.

5.1.4.3.3. Effect of compressor adiabatic efficiency on the energy consumption of the exergy recuperative drying system

Fig. 5-1-8 shows the compressor adiabatic efficiency effect on total energy consumption of the exergy recuperative drying system at different fluidization velocities. With the increase of the compressor adiabatic efficiency, total energy consumption of the drying system was found to be reduced. With the adiabatic efficiency of the compressor CP1 increasing from 50% to 90%, the total energy input decreased by approximately 20–30% at different fluidization velocities. Heat exchange in the

fluidized bed dryer is concurrent, and to utilize the latent heat of the evaporated water from the brown coal, the purged steam has to be compressed to such a pressure that its condensation temperature exceeds the bed temperature over ΔT_{\min} . Thus, the outlet pressure of superheated steam from CP1 should be maintained constant at different adiabatic efficiencies. Low adiabatic efficiency results in more electric energy changed into heat instead of compression work and the heat would be finally purged to the surroundings based on the energy balance. There was almost no significant difference regarding the energy input of CP2 in all evaluated adiabatic efficiencies. This is because a part of the input work for the adiabatic pressure change was transformed into additional heating for the required energy of bound water desorption. Thus, the adiabatic efficiency of CP1 had a slight effect on the total energy consumption, while the adiabatic efficiency of CP2 did not affect the total energy consumption.

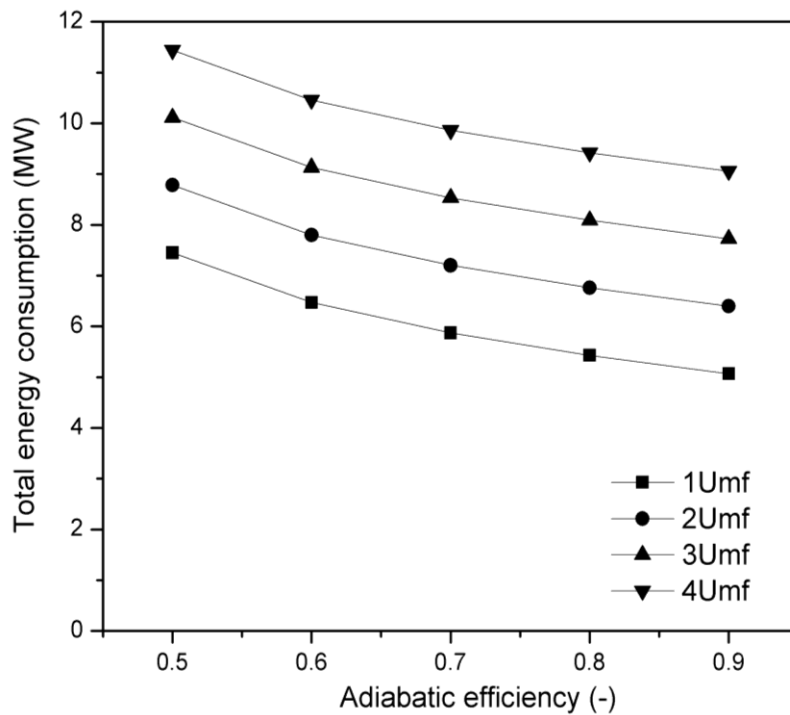


Fig. 5-1-8. Adiabatic efficiency effect on total energy consumption of the exergy recuperative drying system.

5.1.4.3.4. Exergy loss in the proposed drying process

To separate water from the solid particles during the drying process, a large amount of energy has to be added to act as a driving force for mass transfer. Usually, the driving force is much larger than required resulting in additional exergy loss. Cussler and Dutta (2012) compared the free energy increase affected by separation with the minimum work required for separation processes to explore the maximum possible efficiency for isothermal chemical separations (absorption, liquid-liquid extraction and membrane separations). However, exergy loss from a large irreversibility in the drying process becomes a predominant factor causing a huge amount of energy consumption and should be taken into account. Thus, we compared the theoretical minimum input exergy (W_{\min}) with the total input exergy of the drying process to clarify the reduced potential for exergy input of the designed process. W_{\min} includes both the minimum exergy required for bound water desorption (W_{sorp}) and irreversibility during heat exchange ($W_{\text{sen}} + W_{\text{lat}}$):

$$\begin{aligned}
 W_{\min} &= W_{\text{sorp}} + W_{\text{sen}} + W_{\text{lat}} \\
 &= \sum_{n=1}^n (m_{n-1w} - m_{nw}) \Delta H_n + (m_{ps} \Delta S_{ps} + m_l \Delta S_w) \Delta T_{\min} + (m_w + m_{nw}) \frac{L_e}{T_{\text{trs}}} \Delta T_{\min}
 \end{aligned}
 \tag{5-1-12}$$

where ΔS_{ps} and ΔS_w are the entropy changes of brown coal and water during the heating process, respectively. Table 5-1- 2 shows the exergy loss in the proposed drying process. The additional input energy arises from: 1) a 897 kW exergy loss occurred during the constant drying period resulting from the adiabatic efficiency of CP1 which was 0.8, and the temperature difference during the heat exchanger which was slightly higher than ΔT_{\min} in the fluidized bed dryer, and 2) a 200 kW exergy loss occurred in the falling rate drying period caused by the bound water desorption.

Table 5-1-2. Exergy loss in the proposed drying process

	Theoretical minimum exergy input	Exergy input in the proposed process	Exergy loss
Exergy loss during free water remove	$2267 = 534 (W_{sen}) + 1733 (W_{lat})$	3164	897
Exergy loss during bound water remove	$553 = 384(W_{sorp}) + 169(W_{lat})$	753	200
Total energy input	$2820 (W_{min})$	3854	1097

Note the unit of each value is kW. The total energy does not include the energy consumption for the blower to compensate for the pressure loss in the fluidized bed dryer.

5.1.4.3.5. Comparison with previous work

Based on self-heat recuperation technology, Aziz et al. have developed an energy-saving drying process with air as the drying medium for both biomass and brown coal drying, which showed a good energy-saving potential (Aziz et al., 2011a; Aziz et al., 2011b). In this drying system, the wet sample is heated initially in the preheating stage and enters the fluidized bed dryer for evaporation. The mixture of air and steam exhausted from the fluidized bed dryer is compressed to increase its exergy rate so that it can be used as a heat source for evaporation. The air-steam mixture is separated because of the temperature drop during the heat exchange and expansion in the expander. The separated dry air is then recycled for the subsequent drying process. We investigated energy consumption for drying the same amount of brown coal under the same simulation conditions with air as the drying medium. Results showed that energy consumptions were 21.3, 25.3, 29.1 and 32.8 MW at a fluidization velocity of 1, 2, 3 and $4U_{mf}$, respectively, which were more than three times the energy consumption

of the newly designed system in this work. Reasons for the reduced energy consumption of the proposed drying process are: (i) a good heat pairing formation compared with the unmatched heat pairing in the previous work for the existence of air (Liu et al., 2012); (ii) less compression work required for the superheated steam drying system by compressing the pure steam unmixed with the air, and (iii) no additional work required for the separation of air.

5.1.5. Conclusions

As drying is one of the intensive energy-consuming systems, it is necessary to develop a low energy consumption drying technology. In this work, an exergy recuperative module for energy-saving drying with superheated steam has been proposed and applied to design an exergy recuperative drying system. Simulation results show that energy consumption in the exergy recuperative drying process could be reduced to 1/7–1/12 that of the CHR, less than 1/4 that of the MSD and near 1/2 that of the MVR. Factors affecting energy consumption of the proposed system have been investigated. Results indicate that energy consumption of the exergy recuperative drying process would increase slightly with the decrease in the final water content of the dried brown coal. The adiabatic efficiency of the compressor affects the total energy consumption reduction slightly. The exergy loss in the proposed system was investigated by comparing with the theoretical minimum input exergy, which is shown as high exergy efficiency. Finally, energy consumptions of the superheated steam and gas drying systems were compared, both of which were developed based on self-heat recuperation technology. It was found that energy consumption in the proposed process could be reduced to below 1/3 that of the previous process.

References

- Allardic, D.J., Evans, D.G., 1971. The Brown Coal/Water System: Part 2. Water Sorption Isotherms on Bed-Moist Yallourn Brown Coal. *Fuel* 50, 236-253.
- Aziz, M., Kansha Y., Kishimoto A., Kotani Y., Liu Y., Tsutsumi A., 2012. Advanced energy saving in low rank coal drying based on self-heat recuperation technology. *Fuel Processing Technology* 104, 12-16.
- Aziz, M., Fushimi, C., Kansha, Y., Mochidzuki, K., Kaneko, S., Tsutsumi, A., Matsumoto, K., Hashimoto, T., Kawamoto, N., Oura, K., Yokohama, K., Yamaguchi, Y., Kinoshita, M., 2011a. Innovative energy-efficient biomass drying based on self-heat recuperation technology. *Chemical Engineering & Technology* 34, 1095-1103.
- Aziz, M., Kansha, Y., Tsutsumi, A., 2011b. Self-heat recuperative fluidized bed drying of brown coal. *Chemical Engineering and Processing* 50, 944-951.
- Brammer, J.G., Bridgwater, A.V., 1999. Drying technologies for an integrated gasification bio-energy plant. *Renewable & Sustainable Energy Reviews* 3, 243-289.
- Brousse, E., Claudel, B., Jallut, C., 1985. Modeling and Optimization of the Steady-State Operation of a Vapor Recompression Distillation Column. *Chemical Engineering Science* 40, 2073-2078.
- Chen, Z., Agarwal, P.K., Agnew, J.B., 2001. Steam drying of coal. Part 2. Modeling the operation of a fluidized bed drying unit. *Fuel* 80, 209-223.
- Chitester, D.C., Kornosky, R.M., Fan, L.S., Danko, J.P., 1984. Characteristics of Fluidization at High-Pressure. *Chemical Engineering Science* 39, 253-261.
- Cussler, E.L., Dutta, B.K., 2012. On separation efficiency. *AIChE Journal* 58,

3825-3831.

- Djaeni, M., Bartels, P., Sanders, J., van Straten, G., van Boxtel, A.J.B., 2007. Multistage zeolite drying for energy-efficient drying. *Drying Technology* 25, 1053-1067.
- Darwish, M.A., ElDessouky, H., 1996. The heat recovery thermal vapour-compression desalting system: A comparison with other thermal desalination processes. *Applied Thermal Engineering* 16, 523-537.
- Ewers, J., Klutz, H.J., Renzenbrink, W., Scheffknecht, G., 2003. The development of pre-drying and BoA-plus technology, VGB Conference, Cologne.
- Fyhr, C., Rasmuson, A., 1996. Mathematical model of steam drying of wood chips and other hygroscopic porous media. *AIChE Journal* 42, 2491-2502.
- Groenewold, H., Tsotsas, E., 2007. Drying in fluidized beds with immersed heating elements. *Chemical Engineering Science* 62, 481-502.
- Hugget, A., Sebastian, P., Nadeau, J.P., 1999. Global optimization of a dryer by using neural networks and genetic algorithms. *AIChE Journal* 45, 1227-1238.
- Jangam, S.V., Karthikeyan, M., Mujumdar, A.S., 2011. A Critical Assessment of Industrial Coal Drying Technologies: Role of Energy, Emissions, Risk and Sustainability. *Drying Technology* 29, 395-407.
- Kakaras, E., Ahladas, P., Syrmopoulos, S., 2002. Computer simulation studies for the integration of an external dryer into a Greek lignite-fired power plant. *Fuel* 81, 583-593.
- Kansha, Y., Tsuru, N., Fushimi, C., Shimogawara, K., Tsutsumi, A., 2010. An innovative module of heat circulation for fractional distillation. *Chemical Engineering Science* 65, 330-334.
- Kansha, Y., Tsuru, N., Sato, K., Fushimi, C., Tsutsumi, A., 2009. Self-heat recuperation

- technology for energy saving in chemical processes. *Industrial & Engineering Chemistry Research* 48, 7682-7686.
- Kemp, I.C., 2012. Fundamentals of Energy Analysis of Dryers, in: Tsotsas, E., Mujumdar, A.S. (Eds.), *Modern Drying Technology, Energy Savings*. Wiley-VCH, pp. 1-45.
- Kemp, I.C., 2005. Reducing dryer energy use by process integration and pinch analysis. *Drying Technology* 23, 2089-2104.
- Kishimoto, A., Kansha, Y., Fushimi, C., Tsutsumi, A., 2011. Exergy Recuperative CO₂ Gas Separation in Post-Combustion Capture. *Industrial & Engineering Chemistry Research* 50, 10128-10135.
- Kunii, D., Levenspiel, O., 1991. *Fluidization Engineering*, second ed. Butterworth-Heinemann, Washington.
- Linnhoff, B., Hindmarsh, E., 1983. The Pinch Design Method for Heat-Exchanger Networks. *Chemical Engineering Science* 38, 745-763.
- Liu, Y., Aziz, M., Fushimi, C., Kansha, Y., Mochidzuki, K., Kaneko, S., Tsutsumi, A., Yokohama, K., Myoyo, K., Oura, K., Matsuo, K., Sawa, S., Shinoda, K., 2012. Exergy Analysis of Biomass Drying Based on Self-Heat Recuperation Technology and Its Application to Industry: a Simulation and Experimental Study. *Industrial & Engineering Chemistry Research*, 51, 9997-10007.
- Lynd, L.R., Grethlein, H.E., 1986. Distillation with Intermediate Heat-Pumps and Optimal Sidestream Return. *AIChE Journal* 32, 1347-1359.
- Pata, J., Carsky, M., Hartman, M., Vesely, V., 1988. Minimum Fluidization Velocities of Wet Coal Particles. *Industrial & Engineering Chemistry Research* 27, 1493-1496.
- Potter, O.E., Keogh, A.J., 1981. Drying High-Moisture Coals before Liquefaction or

Gasification. Fuel Processing Technology 4, 217-227.

Potter, O.E., Li, X.G.A., Georgakopoulos, S., Mao, Q.M., 1990. Some Design Aspects of Steam-Fluidized Steam Heated Dryers. Drying Technology 8, 25-39.

Strumillo, C., Jones, P.L., Zylla, R., 2009. Energy Aspects in Drying, Handbook of Industrial Drying. CRC.

Syahrula, S., Hamdullahpurb, F., Dincerc, I., 2002. Exergy analysis of fluidized bed drying of moist particles. Exergy, An International Journal 2, 87-98.

Waje, S.S., Thorat, B.N., Mujumdar, A.S., 2007. Screw conveyor dryer: Process and equipment design. Drying Technology 25, 241-247.

Wang, Z.H., Chen, G.H., 2000. Heat and mass transfer in batch fluidized-bed drying of porous particles. Chemical Engineering Science 55, 1857-1869.

5.2. Fluidized Bed Drying of Biomass with Superheated steam based on Self-Heat Recuperation Technology

5.2.1. Introduction

A novel exergy recuperative drying module was developed in Section 5.1, and in this section, we try to apply this module for the biomass drying process. Water in the biomass could be divided as free water which includes the surface water on the particle surface and capillary water captured by the capillary force and bound water. The equilibrium moisture content of biomass depends on the water activity a_w for both gas and superheated steam (SHS) drying (Bjork and Rasmuson 1995). For gas drying, water activity is the ratio of partial pressure of water vapor to the saturation pressure at the same temperature. For SHS drying, water activity is defined as the ratio of actual pressure of SHS to the saturation pressure at the SHS temperature as Eq.5-2-1:

$$a_w = \frac{P}{P_{\text{sat}}} \quad (5-2-1)$$

Thus, it is possible that one generalized equation could predict moisture equilibrium both in gas and superheated steam drying processes (Pakowski et al. 2007). We calculated the sorption isotherm of biomass at different water activities (Fig. 5-2-1) based on the modified Karlsson-Soininen equation (Karlsson, 1982):

$$a_w = \exp \left[\frac{T \exp(-32.591X + 14.229\sqrt{X} - 6.167)}{-\exp(-14.261X + 2.057\sqrt{X} + 0.785)} \right] \quad (5-2-2)$$

where a_w is the water activity, T is drying temperature and X is the moisture content of biomass (kg/kg, dry basis). The free water could be defined as the equilibrium moisture content in an environment of 0.99 water activity. From Fig. 5-2-1, free water is 32.4 wt%

(wb) when a_w is equal to 0.99, and the equilibrium drying temperature is calculated as 100.3 °C. The drying temperature increases gradually for the remaining water removal. The drying process includes a constant drying stage and a falling-rate drying stage. The constant drying stage is for free water removal, and the falling rate drying stage is for the removal of bound water which is adsorbed or chemically bounded with the biomass. Thus, even if the drying temperature achieves to the boiling point of water, the bound water is not possible to be removed. To remove the bound water, superheating is required to provide a low relative vapor pressure to overcome the binding force. The superheating temperature is determined by the final water content of the biomass and increases with the decrease of the final water content of biomass.

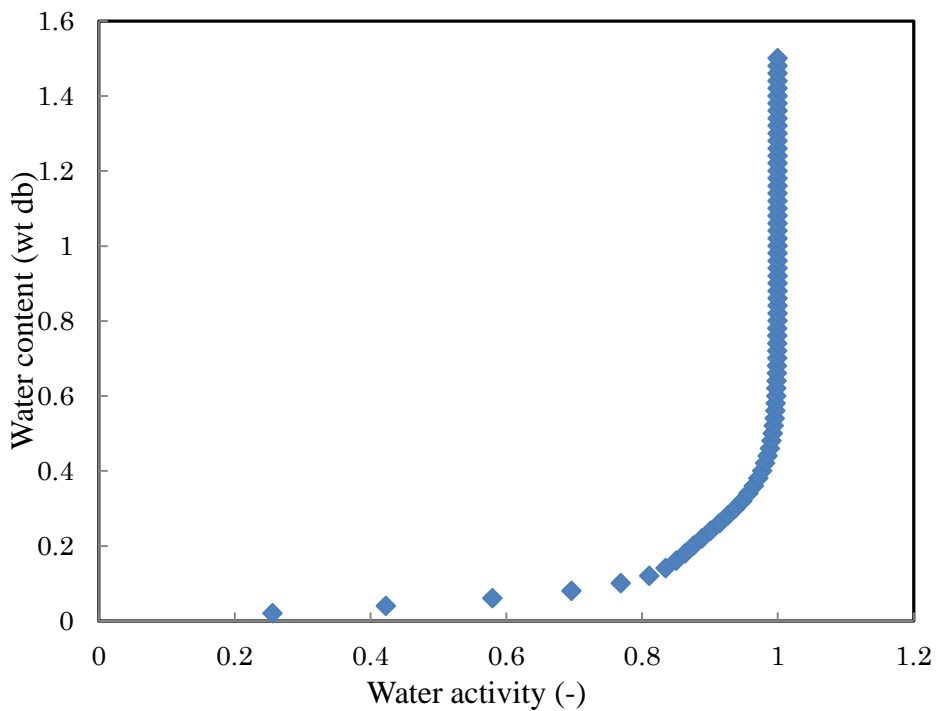


Fig. 5-2-1. Equilibrium moisture content of biomass at different water actives

We used fluidized bed dryer for biomass drying because fluidized beds generally require less drying time for the large contact surface area between solids and gas for the rapid transfer of heat and moisture between solids and gas. In this research, the exergy recuperative drying module was applied for biomass drying considering free water and bound removal. Self-heat recuperative biomass drying processes were developed for free water and bound water removal, respectively, and energy consumption in each drying process was calculated and compared through the simulation software. Furthermore, an economical multi-stage exergy recuperative fluidized bed dryer was developed.

5.2.2. Exergy recuperative biomass drying process

For biomass free water removal, a process diagram for biomass drying based on self-heat recuperation technology is designed as shown in Fig. 5-2-2. Initially, the wet biomass receives heat from the heat exchanger HX1 for preheating biomass to the boiling point. Subsequently, biomass is fed to a fluidized bed dryer (HX2) where the free water is evaporated by the heat supplied from the compressed steam flowing inside the heat exchangers immersed in the bed. Then, the exhausted steam is split into the recycled and purged superheated steams. The purged superheated steam equivalent to the water evaporated from the wet solid is compressed and recirculated as the heat source for evaporation (HX2) and preheating (HX1). The process is more concise without gas-liquid separators and an expander compared with the self-heat recuperative drying process with gas as the drying medium as shown in Chapter 2. In this work, only steam exists inside the dryer without air contamination inside the dryer and water activity of superheated steam correlates directly to the dryer temperature. Thus, the bed

temperature is fixed to the equilibrium drying temperature to achieve to certain moisture content at a constant pressure. Water evaporation also requires a large amount of energy input, and energy required for free water evaporation could be calculated as

$$H_f = m_{\text{biomass}} (X_{\text{int}} - X) \Delta H_{\text{water}} \quad (5-2-3)$$

where H_{water} is the water evaporation enthalpy, and X_{int} and X are the initial and final moisture content of biomass on dry basis, respectively.

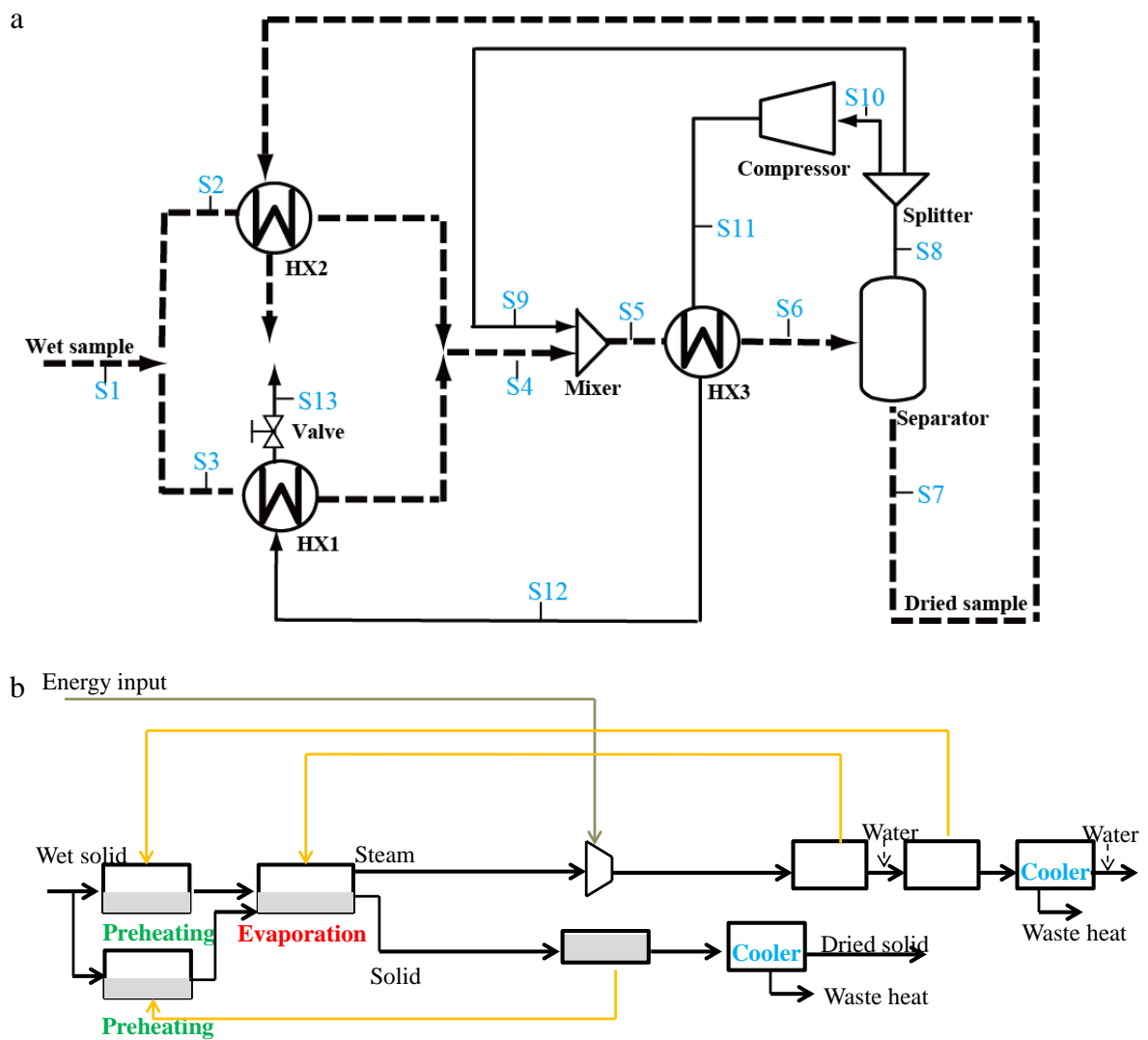


Fig. 5-2-2. a) Biomass drying with superheated steam based on self-heat recuperation, and b) Energy and materials flow diagrams of the self-heat recuperative drying process.

For both free and bound water removal in the fluidized bed dryer, drying temperature should be over 100 °C due to the bound water absorbed in the cavities of the biomass. Energy required for bound water evaporation could be calculated as (Perre P., 2012):

$$H_s(X) = 0.4\Delta H_{v(T)} \left(\frac{X_{fsp} - X}{X_{fsp}} \right) \quad (5-2-4)$$

$$H_s = \int_x^{X_{fsp}} H_s(X) dX = \frac{0.4\Delta H_{v(T)}}{X_{fsp}^2} \left(\frac{2X_{fsp}^2}{3} - X_{fsp} \cdot X + \frac{X^3}{3} \right) \quad (5-2-5)$$

When biomass was dried lower than the critical water content, both free water and bound would be evaporate from the biomass. In this work, free water and bound water were removed from biomass separately for energy saving and a multi-stage fluidized bed dryer was adopted to make the device more compact and to reduce the capital cost. Multi-stage fluidized bed is favor to further reduce the energy consumption in the falling rate stage by comparing Fig. 5-2-3a with Fig. 5-2-3b and c. Exergy loss from the heat transfer could be reflected from the space area between the hot and cold streams lines. As shown in Fig. 5-2-3b and c, multi-stage fluidized bed could make a better heat pairing which could reduce the minimum temperature difference between the superheated steam and wet biomass. On the other side, it also increased energy input from the multiple compressions and duty for the blower. The relationship between energy consumption and number of fluidized bed stages would be investigated in Section 3.2.4.2.

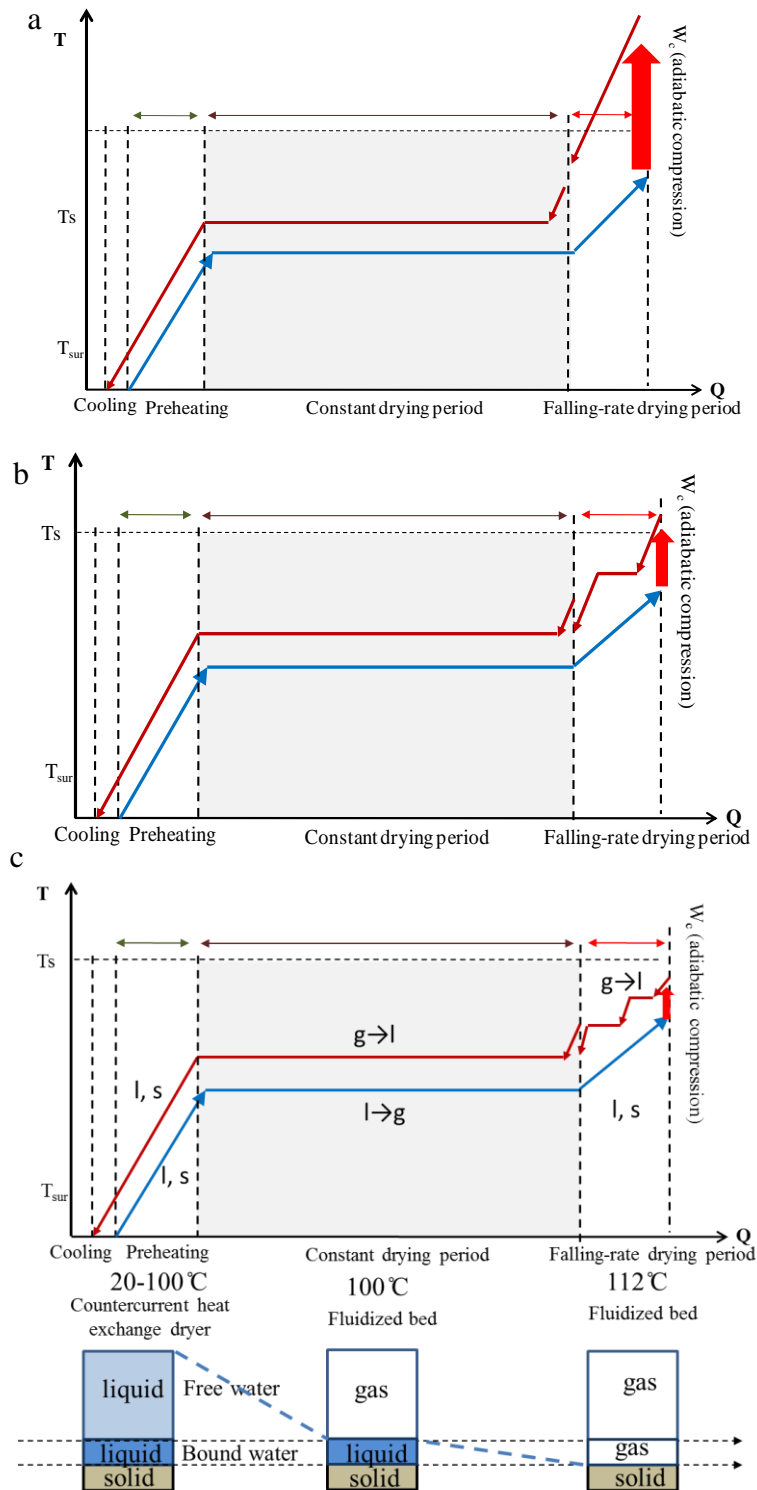


Fig. 5-2-3. Temperature and heat diagram of the exergy recuperative drying processes for free and bound water removal: a) single stage fluidized bed dryer, b) two-stage fluidized bed dryer and c) three-stage fluidized bed dryer.

5.2.3. Simulation Conditions

The simulation conditions for biomass drying using the PRO/II ver. 9.1 software (Invensys Corp.) are as follows: (1) The wet biomass inlet flow rate is 5000 kg h^{-1} and the initial moisture content is 75 wt% (wb); (2) the adiabatic efficiencies of the compressor and blower are 80%; (3) drying is performed under atmospheric conditions; (4) thermodynamic calculations employ the Soave-Redlich-Kwong (SRK) method; (5) the fluidized bed dryer with internal heat exchangers can exist as a mixer, heat exchanger and separator; (6) the heat exchange is concurrent in the fluidized bed dryer; (7) the minimum temperature difference in each heat exchanger is assumed to be 10 K; (8) no heat loss is assumed from the drying system to the surroundings.

5.2.4. Results and discussion

5.2.4.1. Energy consumption in the exergy recuperative drying process for free water removal

Based on Fig. 5-2-1, drying temperature should be kept over $100.3 \text{ }^{\circ}\text{C}$ for free water removal in which water content dropped from 75.0 to 31.5 wt% (wb). Through Fig. 5-2-4, we could find a dramatic energy-saving potential in the exergy recuperative drying system with superheated steam which was less than 1/20 of conventional heat recovery drying process and 1/5 of the self-heat recuperative drying system with air. Energy consumptions in the CHR, SHR-air and SHR-steam could be divided as three parts: the minimum exergy loss for biomass drying, the blower duty for biomass fluidization and additional exergy input due to the higher temperature difference between hot and cold streams in the heat exchanger compared to the ΔT_{\min} and the compressor adiabatic efficiency which is 80 %. In the three systems, the minimum

exergy loss for biomass drying was the same, and blower work did not change significantly for the same amount of biomass fluidization. The minimum exergy loss for biomass drying could be calculated from the following equation.

$$W_{\min} = E_{\text{sensible}} + E_{\text{latent}} \\ = \left(m_{\text{ps}} \Delta S_{\text{ps}} + m_1 \Delta S_w \right) \Delta T_{\min} + (X_{\text{int}} - X) m_{\text{biomass}} \frac{\Delta H_{\text{water}}}{T_{\text{trs}}} \Delta T_{\min} \quad (5-2-9)$$

where W_{\min} was the minimum exergy required for irreversibility during heat exchange ($E_{\text{sensible}} + E_{\text{latent}}$) and calculated as 63.5 kW for free water removal.

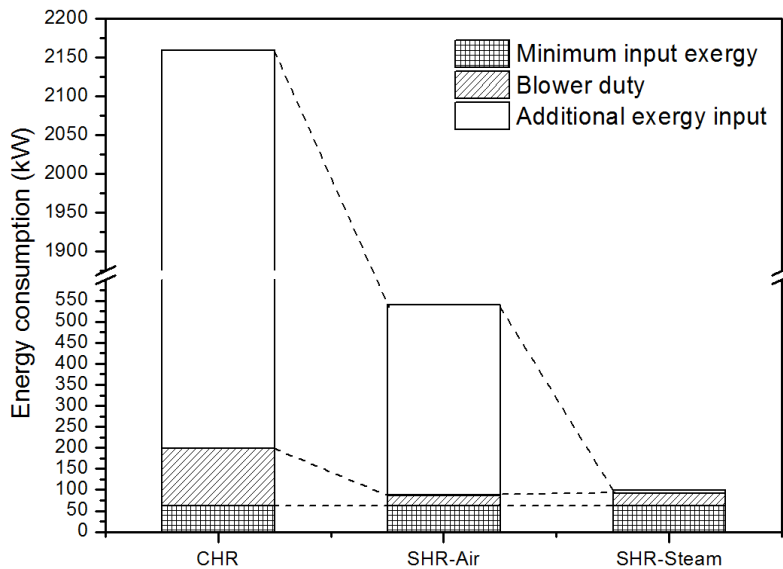


Fig. 5-2-4. Energy consumption in different drying systems

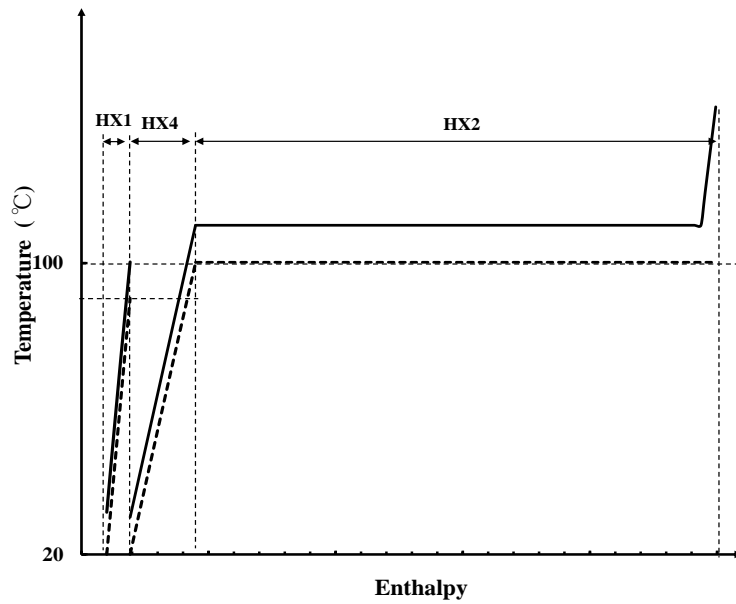


Fig. 5-2-5. Temperature and heat diagram of the exergy recuperative drying process.

The big difference among the three systems was the additional exergy loss which mainly came from the exergy loss during the heat exchange between the compressed steam in the heat exchange tubes with the biomass. In the conventional heat recovery drying process, a large amount of exergy loss still occurred due to the fuel combustion for the steam generation. In the self-heat recuperative drying system with air, heat exchange temperature difference between the hot and cold streams was high, because the hot stream temperature would greatly increase as the air-steam mixture was compressed. In the self-heat recuperative drying system with steam, energy consumption could be dramatically decreased due to the good heat pairing in the drying process (Fig. 5-2-5). The existence of air in the steam also increased the duty of compressor. Energy consumption for the drying processes with air and steam as the drying medium could be calculated respectively:

$$W_{c-gas} = m_{steam} C_{p,steam} \Delta T_{v+s} + m_1 C_{p,g} \Delta T_g \quad (5-2-10)$$

$$W_{c-steam} = m_{steam} C_{p,steam} \Delta T_{steam} \quad (5-2-11)$$

where m_{steam} and m_{gas} are the flow rates of the steam and gas, respectively. C_{vs} and C_{vg} are the constant volume heat capacities of steam and air, respectively. ΔT_1 and ΔT_2 is the temperature difference between the outlet and inlet of the compressor for gas and steam drying. ΔT_1 is much high than ΔT_2 due to the significant temperature increase as gas is compressed. For drying the same amount of wet sample, m_{steam} is the same at the two drying systems while additional energy input will be required for the compression of drying medium gas. Therefore, gas drying consumes more energy than steam drying system. In addition, for the exergy recuperative drying with gas, the existence of non-condensable gas in the compressed vapor inside the heat exchanger tubes potentially reduces the heat transfer rate in the heat exchange. As a result, larger heat-transfer surface is required to provide an equivalent heat amount with superheated steam drying. Specific chemical exergy of biomass could be calculated by the following calculation:

$$e = 1812.5 + 297.241C + 615.788H + 20.356O + 20.652N + 99.738S - T_0 S_{OM}^0 + E_{ash}^{\text{CH}} - T_0 S_{ash}^0 \quad (5-2-12)$$

and the specific chemical exergy of biomass is 19.9 MJ kg^{-1} . The water evaporation heat is 2270 kJ kg^{-1} . For 5000 kg h^{-1} biomass with the water content of 75.0 wt % (wb), the effective energy could be calculated as 16363 MJ h^{-1} and the effective energy in the dried biomass was 23477 MJ h^{-1} . Energy consumption is 100.2 kW which is 360 MJ h^{-1} . The results shows that compared with the energy held by the dried biomass, the input energy for drying was relatively low which was about 1.5 % of the energy in the biomass.

5.2.4.2. Free water and bound water removal

In this work, we studied energy consumption of different stages fluidized bed dryer

when drying the biomass to 7.5 wt% (wb). Thus, the biomass particles should be finally heated to 111 °C for the bound water removal based on Fig. 5-2-1. For exergy recuperation in the falling rate drying stage, the generated vapor coming from the bound water would be compressed for the energy supply of the subsequent bound water removal. Simulation results of fluidized bed dryer with different stages were presented in Fig. 5-2-6. When the number of fluidized bed increased from single stage to two stages, system energy consumption decreased by 37.8 %. With stage number further increased, energy consumption was further decreased by 4.8 %. On the other side, the increase of stage number will increase duty of blower due to the pressure loss caused by the distributor of fluidized bed. Thus, two-stage fluidized bed was necessary in case of biomass drying for both free and bound water removal. Compared with the conventional heat recovery drying process, energy consumptions in the self-heat recuperative drying process with 1, 2 and 3 stages could be reduced to 1/10, 1/17 and 1/18, respectively. Biomass superheated steam drying with steam recompression has currently be conducted in a closed loop pneumatic conveying type manufactured by GEA Barr-Rosin, Co, with a compression ratio of 10–20 for inlet superheated steam preheating (Superheated steam dryer, GEA Barr-Rosin, Co.). Energy consumption (150–200 kWh/ton evaporated water) was 4–5 times higher than that in our process.

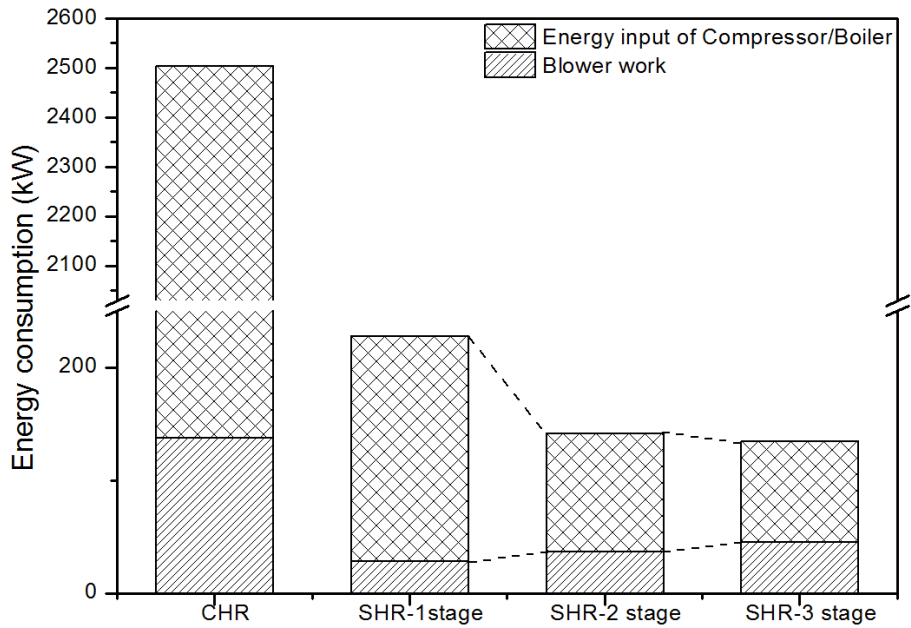


Fig. 5-2-6. Energy consumptions in the heat-recuperative fluidized bed dryer with different stages. Energy input for drying biomass to 7.5 wt% (wb).

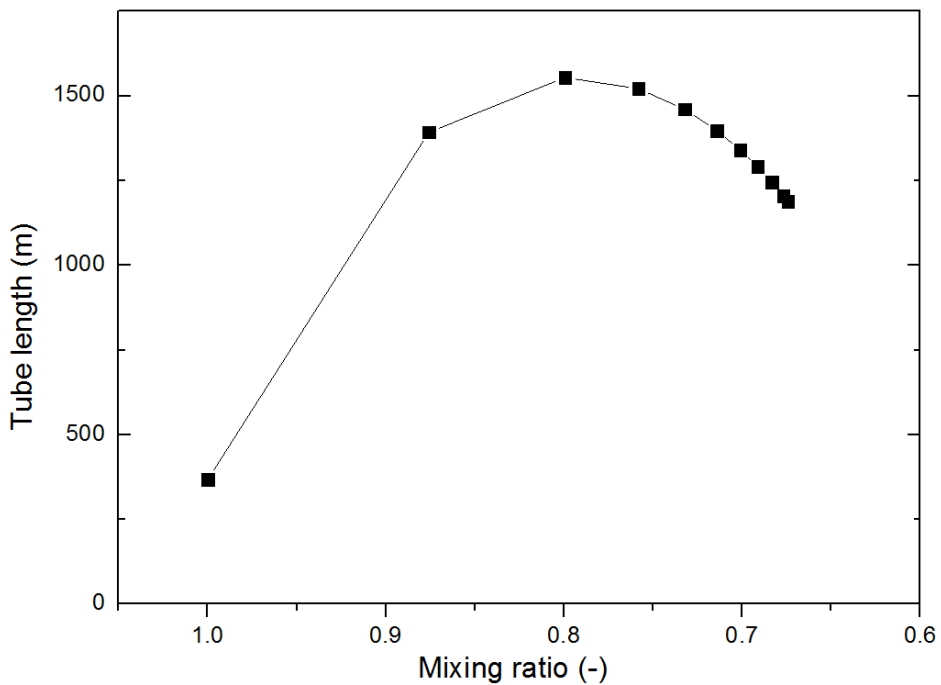


Fig. 5-2-7. Length of heat transfer tubes in the fluidized bed dryer. Mixing ratio=mass of steam/total steam mass

Fig. 5-2-7 shows the effect of mixing ratio on the length of heat transfer tubes in the fluidized bed dryer. The outer diameter of the tube is 20 mm with inner diameter of 16 mm. The material of the tube was SUS316. Results shows that the length of heat transfer tubes was short when the stream in pure vapor and increased with the mixture ratio (steam/air) decreasing. Thus, the total surface areas of the heat-exchange tubes immersed in the FBD could be reduced by increasing the heat transfer rate during condensation of water. About 182 tubes were required for the heat transfer during the drying process when the stream in the heat transfer tube is pure vapor. Thus, it is feasible for the design of the fluidized bed dryer from the aspect of the arrangement of the heat transfer tubes.

5.2.5. Conclusions

The exergy recuperative module was applied for the biomass drying system. For biomass drying, free water and bound water were considered. For the free water removal, the proposed drying process could save energy consumption to 1/20 of the conventional heat recovery drying system. For the free and bound water removal, energy consumption was saved to the 1/17 of conventional heat recovery drying system in the self-heat recuperative fluidized bed dryer with 2 stages.

References

- Bjork, H. and A. Rasmuson. 1995. Moisture Equilibrium of Wood and Bark Chips in Superheated Steam. *Fuel*, 74(12), 1887-1890.
- Chitester, D. C., R. M. Kornosky, et al. 1984. Characteristics of Fluidization at High-Pressure. *Chemical Engineering Science*, 39(2), 253-261.
- Karlsson M, Soininen M. The drying characteristics of a paper machine. In: 3rd international drying symposium; 1982. p. 351-62.
- Kunii, D. and O. Levenspiel (1991). *Fluidization Engineering*. Washington, Butterworth-Heinemann.
- Pakowski, Z., B. Krupinska, et al. 2007. Prediction of sorption equilibrium both in air and superheated steam drying of energetic variety of willow *Salix viminalis* in a wide temperature range. *Fuel*, 86(12-13), 1749-1757.
- Perre P., Almeida G., and Colin J., Energy issues of drying and heat treatment for solid wood and other biomass sources. In *Modern Drying Technology, Energy Savings*, Tsotsas, E.; Mujumdar, A. S., Eds. Wiley-VCH: 2012; pp 245-289.
- van der Ham, L. V. and S. Kjelstrup. 2010. Exergy analysis of two cryogenic air separation processes. *Energy*, 35(12), 4731-4739.
- Superheated Steam Drying, GEA Barr-Rosin Co,
<http://www.barr-rosin.com/products/super-heated-steam-drying.asp>

5.3. Biomass drying in the exergy recuperative fluidized bed dryer with superheated steam

5.3.1. Introduction

For the biomass steam drying in the fluidized bed dryer, we found a dramatic energy-saving performance of the proposed self-heat recuperative drying process based on the simulation results. However, for the actual drying performance, it was hard to predict from the simulation software. To our knowledge, there is very little report about the biomass drying with steam in a fluidized bed dryer (Fyhr and Rasmuson, 1996; 1997). Tatemoto et al. (2007) investigated drying characteristics of suspended samples in the fluidized bed dryer with superheated steam; however, the change of fluidization behavior during the drying process could not be detected. To confirm the drying performance, we conducted the sawdust drying in the fluidized bed dryer in this section. Wet sawdust was used as the drying material in this work. Silica sand was mixed with sawdust for sawdust particles at all moisture contents were poorly fluidized in a single component system. Mixing and fluidization performance were firstly investigated in the fluidized bed dryer with air as the drying medium. Based on the results, an optimal weight ratio and diameter of silica sand to sawdust was determined for the batchwise and semi-continuous experiments with steam as the drying medium. Drying characteristic of sawdust in the fluidized bed dryer was investigated. System stability of heat exchange was also checked in the fluidized bed with semi-continuous operation.

5.3.2. Experimental setup

A laboratory-scale fluidized bed dryer for the biomass drying was set up as shown in Fig. 5-3-1, and its main body was made of stainless steel. Some inspection windows

were located to observe the internal fluidization of particles. Biomass was preheated to the boiling point and added from the top of the fluidized bed dryer. Cross-section of the fluidized bed dryer is square with a side length of 0.2 m and a 1.0 m height. A steam generator (OSG-150T, Osaka Denki Co. Japan) was added to generate steam as the fluidization medium. The generated steam would be heated with a heater at the entrance of the fluidized bed dryer to achieve a desired temperature and the flow rate of steam could be read from the steam flow meter. On the other side, to simulate the compressed steam from the moisture in the biomass, another steam generator (OSG-40, Osaka Denki Co. Japan) was added to produce compressed steam which went through heat transfer tubes in the fluidized bed dryer to provide evaporation heat for biomass drying. At the outlet of heat transfer tubes, the condensed water was separated from steam after heat exchange with biomass in the fluidized bed dryer. At the outlet of each steam generator, a gas-liquid separator was added to separate the condensed water in the saturated steam from the steam generator. Phenolic foam insulation was fixed around the surface of the fluidized bed to prevent heat loss from the bed to the environment. The temperature of the bed surface could be kept between 100 °C and 120 °C with an accuracy of 1 °C by covering the ribbon heaters around the drying chamber to prevent heat loss from the bed. Pressure and temperature at each pipe and in the fluidized bed dryer were measured and recorded by a data logger (NR1000 Keyence, Co. Japan). To inhibit the steam leakage during the sampling and flash evaporation when biomass contacting with air, a special outlet was designed for the fluidized bed dryer as shown in Fig. 5-3-2. The door at the outlet could slide from one side to the other side to determine the sampling time for the semi-continuous experiment. A special sampler could plug in the fluidized bed through the sampling port to detect at sawdust moisture content during

the drying process.

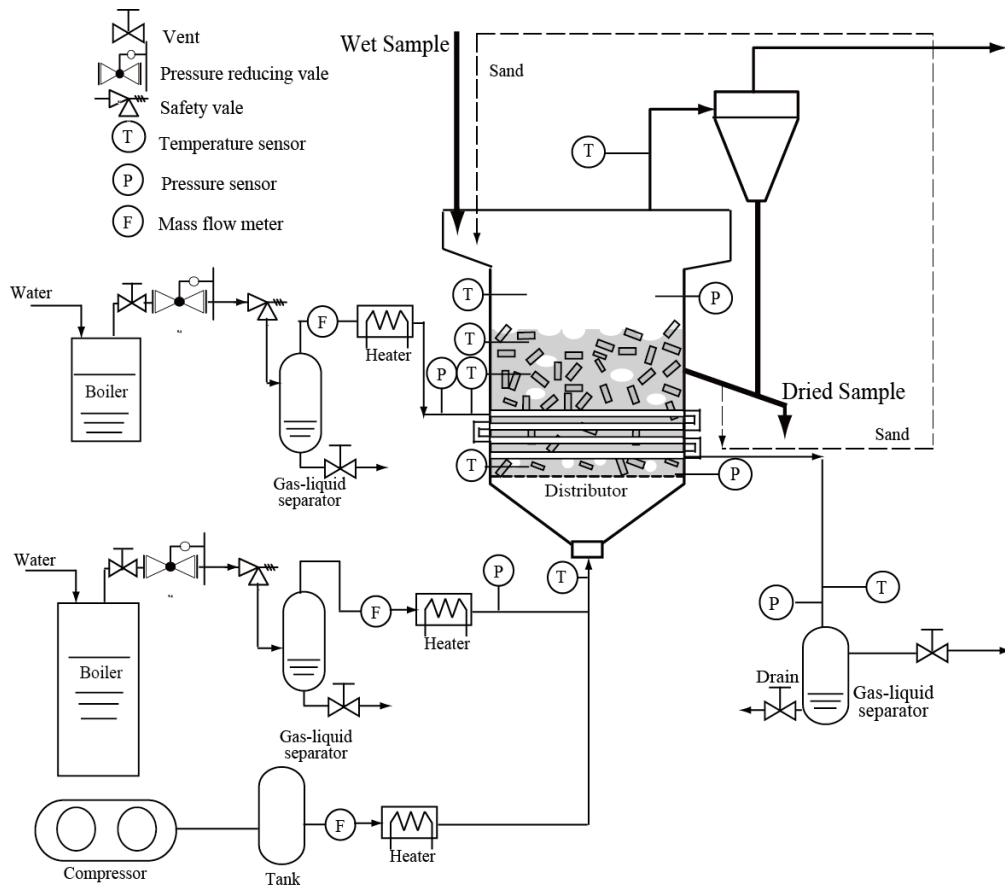


Fig. 5-3-1. Schematic diagram of an experimental fluidized bed dryer

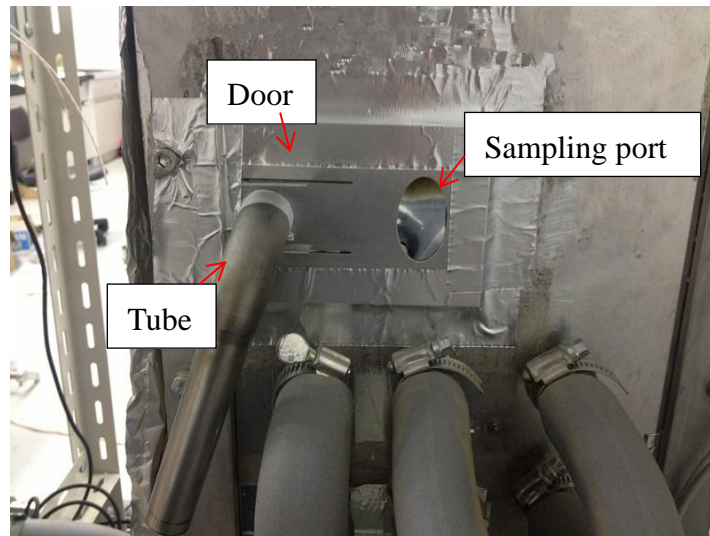


Fig. 5-3-2. Outlet of the steam fluidized bed dryer

5.3.3. Experimental procedure

We first tried to investigate the mixing and fluidization performance of silica sand and sawdust for a stable operation in the fluidized bed dryer. The mixture of sawdust and silica sand with different diameters, shown in Table 5-3-1, at various mixing ratios (weight of sawdust to total weight) was fluidized in the fluidized bed dryer. Pressure drops in the fluidized bed were investigated at different gas velocities for the determination of the minimum fluidization velocity of silica sand and sawdust mixture. In adequate fluidization a bubbling regime is observed without the formation of channels at increasing gas velocities (Clarke et al. 2005). With mixing ratio further increasing, experiment was stopped when the poor fluidization occurred which was determined visually and pressure drop across the bed.

Table 5-3-1. Some relevant properties of the solids used in this study

	Diameter d (mm)	Density ρ (g/cm ³)	U_{mf} (cm/s)
Sand (No.7)	0.10	2.62	1.16
Sand (No.6A)	0.15	2.62	3.03
Sand (No.6)	0.34	2.59	8.78
Sawdust	0.34~0.5	0.28	-

Then, both the batchwise and semi-continuous drying experiments for sawdust were conducted in the fluidized bed dryer with superheated steam as the drying medium. Before the steam experiment, the fluidized bed was preheated to over 100 °C with hot air as the fluidization medium to avoid steam condensation during the preheating process and remove possible moisture in the silica sand. Then, the fluidization medium was changed from air to steam. In the batchwise experiment, fluidizing medium was pre-heated initially to the bed temperature before entering the FBD. As drying process progresses, the water owned by sawdust sample evaporates in the fluidizing/drying medium. In batchwise experiments, three sheathed heaters (diameter 6 mm, length 120 mm) were installed inside the FBD at a height of 25 mm above the distributor to mock the compressed steam that was used as a heat source for drying. After sampling was completed, the sawdust was separated from the sand through sieving and weighed before moved an oven. Then the sample was heated for 24 h at 103 °C. After that, the heated sample was weighted again and the moisture content of the sawdust, M , could be calculated as followed:

$$W_{\text{wet}} = \frac{M_1 - M_2}{M_1} \times 100\% \quad (5-3-1)$$

In the semi-continuous experiment, 150 g sawdust with a water content of 61.8 wt% (wb) was fed intermittently to the FBD with an interval of 8 min. Meanwhile, the dried sawdust is discharged together with the silica sand from the tube with an interval of 15 min at the outlet as shown in Fig. 5-3-1. Compressed steam from a steam generator (OSG-40, Osaka Denki Co. Japan) with a pressure of 190 kPa at 119 °C flowed through the heat exchange tubes (as shown in Table 5-3-2) in the fluidized bed and supplied steam condensation heat for water evaporation. The sampling time could be controlled by opening and closing the door at the outlet. Condensed water was collected through a tank and weighted after the drying process completed. Discharged sand-sawdust mixture is moved to the oven. The moisture content of the dried sawdust is measured based on ASTM D4442-07. Drying experiment is conducted for 180 min, but it was stopped in the case of poor fluidization which is determined visually and by temperature distribution across the bed.

Table 5-3-2. Properties of heat transfer tubes immersed inside FBD and steam

<i>Tube Properties</i>	<i>Values</i>
Tube material	SUS316 (18% Cr, Ni 12%, Mo 2.5%, 67.5% Fe)
Thermal conductivity (W mK ⁻¹)	16.7
Inner diameter (mm)	8
Outer diameter (mm)	10
Arrangement	Horizontal
Pitch distance (mm)	50
<i>Compressed steam</i>	
Inlet temperature (°C)	119
Inlet pressure (kPa)	190

5.3.4. Results and discussion

5.3.4.1. Mixing and fluidization performance of silica sand and sawdust

We investigated three different diameters of silica sand to test the hydrodynamic performance when cofluidization with wet sawdust. Results showed that the diameter of silica sand had an important effect on the fluidization performance. Minimum fluidization velocity of silica sand and sawdust mixture at different mixing ratios was shown in Fig. 5-3-3. The minimum fluidization velocity was determined from the relationship between the velocity of the drying gas and pressure loss in the bed. Good mixing and fluidization performance was shown in each diameter of silica sand when the mixing ratio was between 0 and 0.5. However, channeling occurred in mixture of sawdust and silica sand ($d = 0.1$ mm) when the weight ratio increased to 0.7, signified by a tough in the pressure drop curve as shown in Fig. 5-3-4. The pressure the bed does not return to a packed bed and continues to exhibit channeling until the gas velocity is zero. In the case of silica sand ($d = 0.34$ mm), sawdust and silica sand could co-fluidized well at a low mixing ratio, however, when the mixing ratio increased to larger than 0.5, the binary mixture was difficult to be co-fluidized because the fluidization velocity was not large energy for the capability of the blower in our experimental device. In the case of silica sand ($d = 0.154$ mm), the mixing and fluidization performance showed well even at a high mixing ratio. Based on the above results, silica sand with a diameter of 0.154 mm will be used in future steam drying experiment. In the case of silica sand diameter of 0.154 mm, the minimum fluidization velocity of the mixture of sand and wet biomass has also been calculated from equations recommended by Bilbao et al. (Bilbao et al, 1987) as:

$$u_{vf} = u_{pk} - (u_{pk} - u_f) X_f ; \quad (5-3-2)$$

$$u_{pk} = 50d_{pk}^{0.84} ; \quad (5-3-3)$$

$$X_f = \frac{x_f}{x_f + (\rho_f / \rho_{pk})(1 - x_f)} ; \quad (5-3-4)$$

where, d_{pk} is particle size of packed component, u_{vf} is superficial velocity of gas where both components in a binary mixture are fluidized, and x_f is weight fraction of fluid and packed component in binary mixture. Results in Fig. 5-3-5 showed the approximate values of the calculated value and experimental value by defining a higher value of u_{pk} of 0.71.

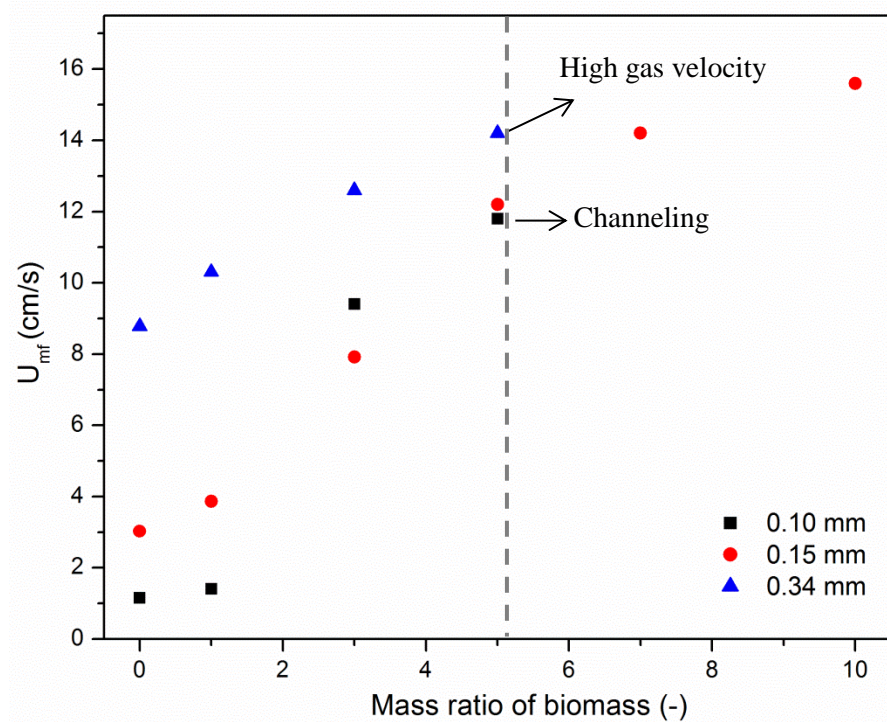


Fig. 5-3-3. Minimum fluidization velocity of silica sand and sawdust mixture at different mixing ratios

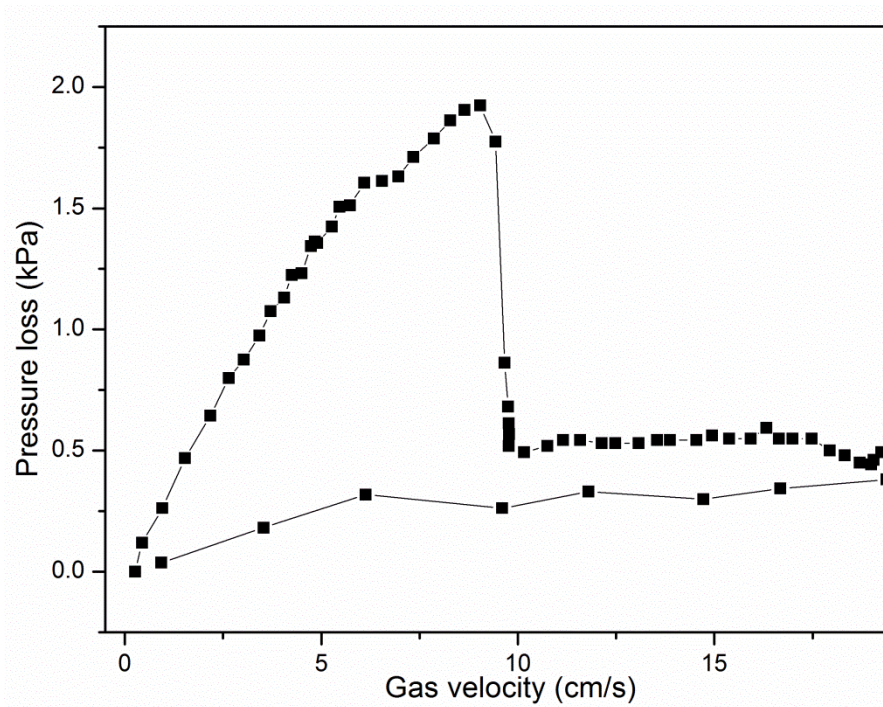


Fig. 5-3-4. Pressure drop across the bed at different gas velocities in the fluidized bed, sawdust with silica sand ($d = 0.1$ mm) ratio of 0.7.

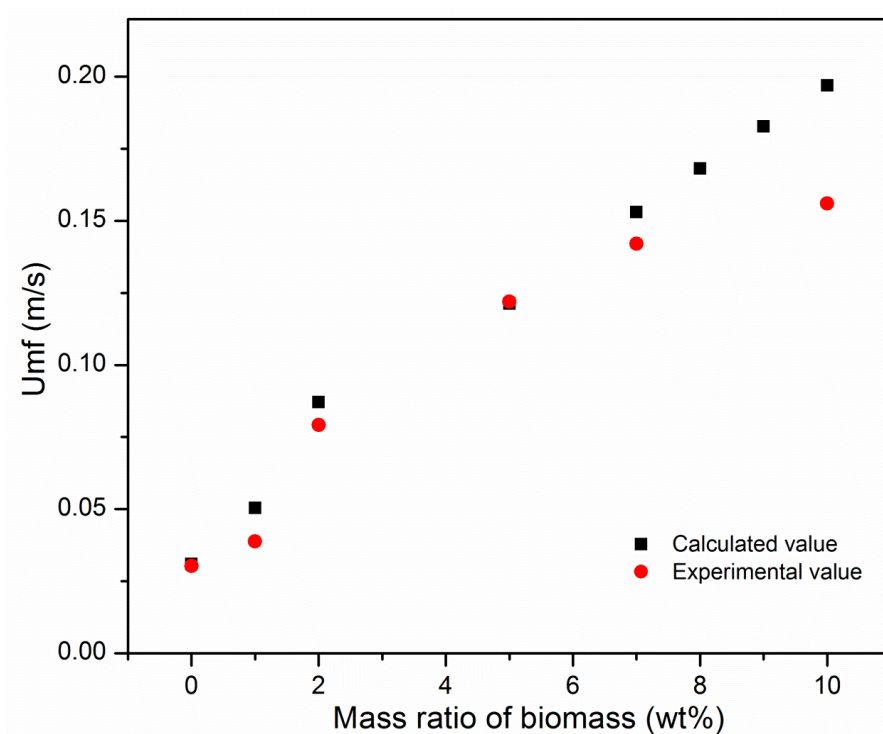
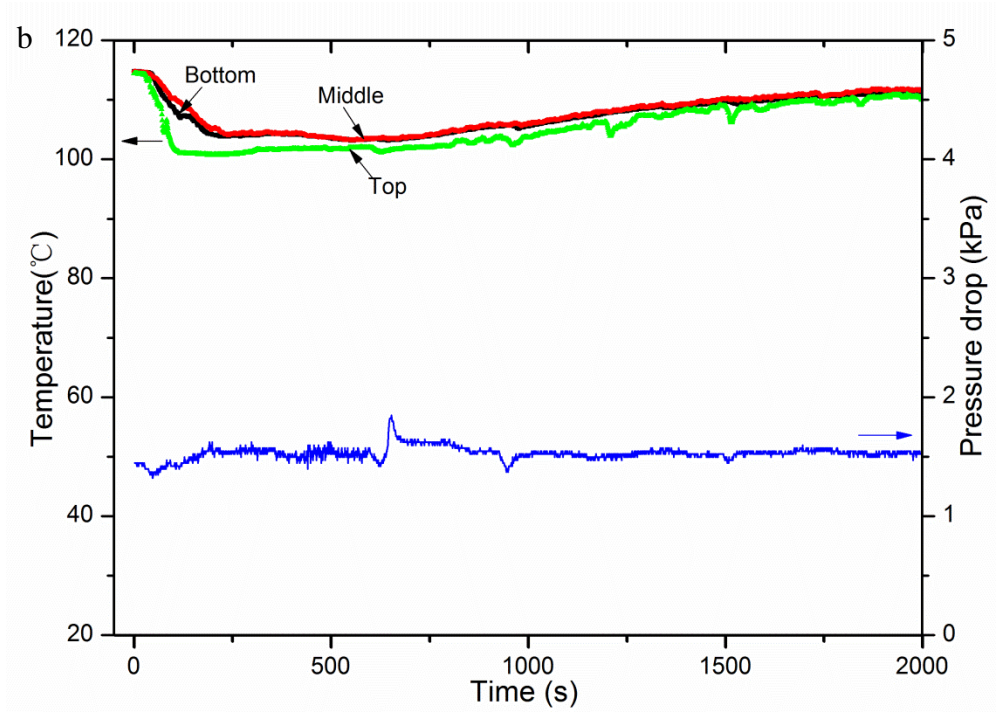
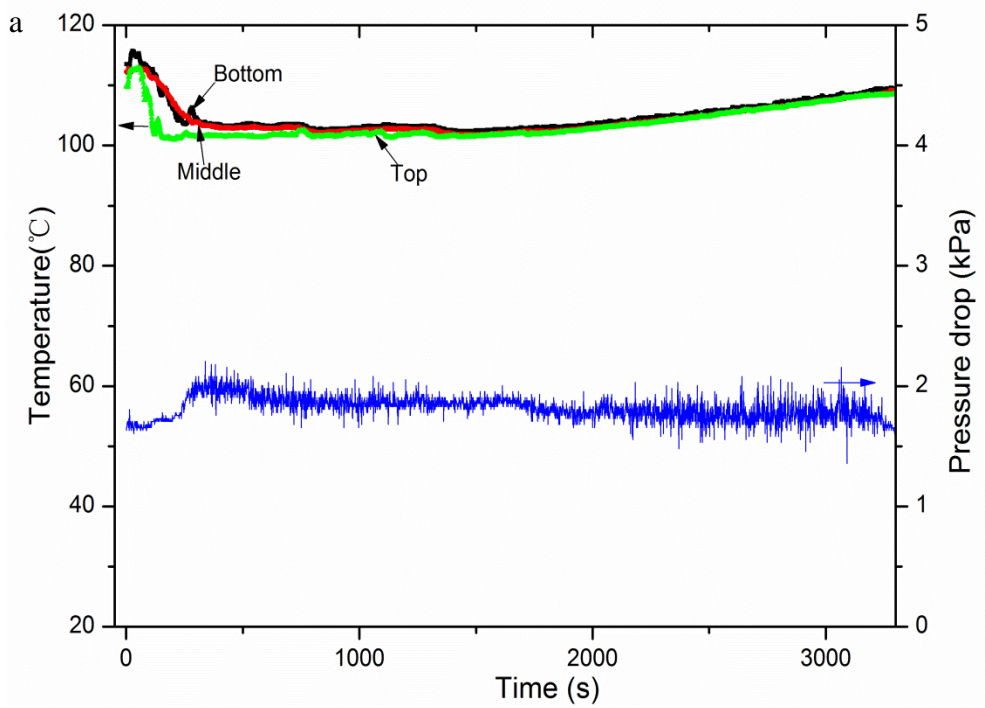


Fig. 5-3-5. Comparison of experimental minimum fluidization velocity in this study and predicted value from Bilbao et al. (1987)

5.3.4.2. Batchwise experiment for biomass drying

Wet sawdust was input into the steam fluidized bed dryer. Sawdust was preheated to 80 °C to avoid the steam condensation on the sawdust surface leading to an increased drying time when sawdust was put into the fluidized bed dryer. The steam flow rate was 4.1 kg h⁻¹ with a velocity of 7.79 cm s⁻¹. Steam inlet temperature was 120 °C with an absolute pressure of 160 kPa. The top, middle and bottom of the fluidized bed were investigated during the drying process. The temperature difference among the top, middle and bottom levels was very small, indicating a homogenous state in the fluidized bed. As shown in Fig. 5-3-6a, in our system, biomass could be fluidized and dried at a very low temperature which was 101.5 °C without steam condensation. The low bed temperature could reduce exergy loss during the heat exchange process which has been proved in Section 3.2. The bed temperature dropped from 112 °C to 101.5 °C when the sawdust was put into the bed and bed temperature continued to be 101.5 °C for 27 min for the free water removal. The energy supply was used as the heat for water evaporation thus, the bed temperature kept constant during the free water drying process. The bed temperature began to increase for the removal of bound water adsorbed or chemically bounded with the biomass. The bed temperature was a little higher than the boiling point of water due to the temperature difference existence for heat transfer from the sand to biomass particles. Furthermore, energy input amount increased to 240 W, and the time for constant drying stage was shortened from 27 min to 12.6 min (Fig. 5-3-6b). Drying time could be shortened through increasing the number of heaters. In the case of indirect steam fluidized dryer, energy supply was from the steam condensation, thus, increasing the number of heaters in this experiment could be achieved by increasing the heat exchange surfaces in the indirect steam fluidized bed

dryer. When the energy input amount increased to 360 W, the constant drying rate period almost disappeared for the large amount of heat supply (Fig. 5-3-6c). Water content of dried biomass was also investigated during the drying process. Sawdust water content dropped rapidly from 61.8 to 2.5 wt% (wb) during the first 10 min, and further reduced to 1.5 wt% (wb) at 20 min. The moisture content was kept to be 1.6 wt% (wb), after then, which meant the equilibrium water content had already been achieved. This could be achieved easily through the electric heater which has a high surface temperature, but requires a higher energy input for the compressor to generate a higher steam pressure to have heat exchange with the fluidized bed with a higher bed temperature in the indirect steam fluidized bed dryer. In the fluidization bed dryer, the mass and heat transfer rates were high; thus, the surface water in the biomass was removed quickly. For the bound water removal, the physical properties of the sample such as water diffusivity and thermal conductivity and so on affected the drying performance. Thus, it took almost the same time for bound water removal as that of free water removal, although the amount of bound water was less than half of the free water. The constant rate period was significantly affected by the energy input into the dryer, as compared to its effect on the fall rate period. The bound water removal time also decreased with the increased input energy amount, however, not so dramatic compared to the free water removal stage.



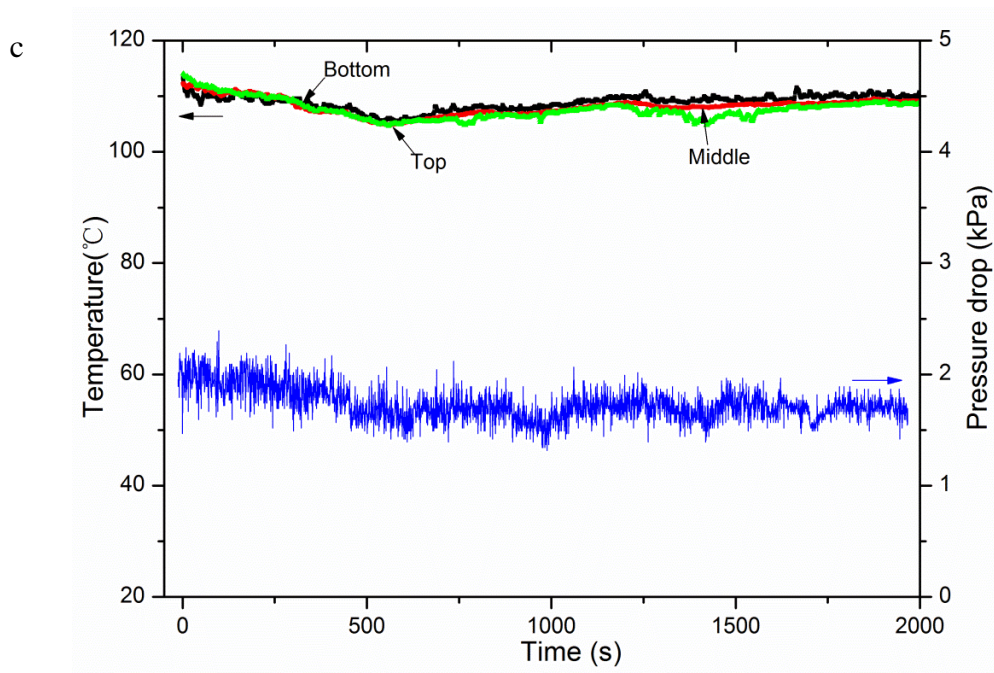


Fig. 5-3-6. Temperature distribution and pressure drop in the fluidized bed dryer with steam as fluidization medium., a) energy input from sheathed heater 120 W, b) energy input from sheathed heater 240 W and c) energy input from sheathed heater 360 W.

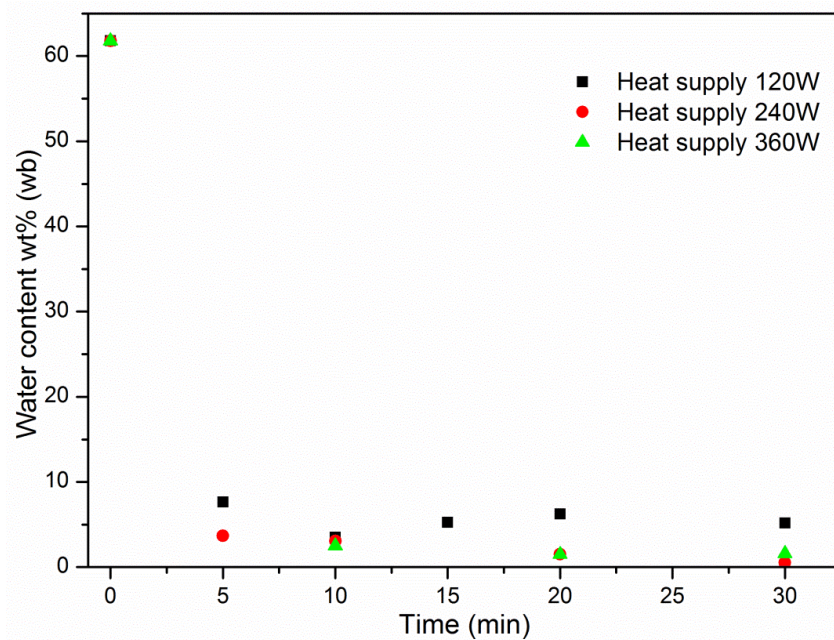


Fig. 5-3-7. Water content of sawdust in the fluidized bed dryer with steam as the drying medium at different amount of heat supply.

5.3.4.3. Comparison with drying performance with air and superheated steam

To compare the drying performance of sawdust drying with superheated steam and air. The energy input from sheathed heater was both 120 W, and the other conditions were the same with that of superheated steam drying except for the drying medium. Results showed that fluidized bed drying with air had a higher drying rate at the same condition. Water content of sawdust decreased to 4.4 wt% (wb) at the first 5 min which it took more than 20 min for the case of steam drying. The water content further dropped to less than 1.0 wt% (wb) from 10 min. This was because the air had a low relative humidity compared with that of the superheated steam thus, had a greater driving force. The change of bed temperature was more significant in the fluidized bed dryer with air, the bed temperature dropped to less than 80 °C when the wet biomass was input into the fluidized bed dryer as shown in Fig. 5-3-7. The top of the bed temperature dropped as the separated silica sand from the sawdust recirculated into the fluidized bed. However, the duration at this temperature was short indicating that the surface water was removed in a short time. The mass transport to the surface was lower than the evaporation rate on the biomass surface and the period of constant drying rate disappeared. The bed temperature then increased due to the additional heat supply. In the case of superheated steam drying, Fig. 5-3-6a showed that the bed temperature during the period of constant drying rate remained near to the boiling point at the operation pressure (about 104 kPa), and the period of constant drying rate was longer than that in the case of the air drying. This was mainly due to the fast moving rate of the internal water to the surface for the higher bed temperature than the case of air drying and the weaker driving force of the superheated steam. However, the big drop of the bed temperature for the water evaporation generated more exergy loss for heat transfer for the fluidized bed dryer with

air. In the superheated steam the bed temperature kept constant near to the boiling point at the constant rate drying period, and thus caused a minimum exergy loss during the heat transfer process.

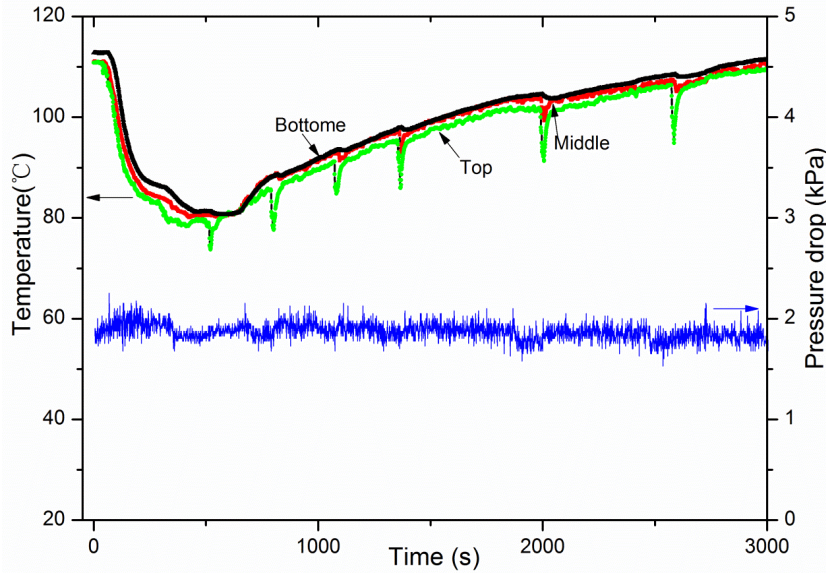


Fig. 5-3-8. Temperature distribution and pressure drop in the fluidized bed dryer with air as the fluidization medium.

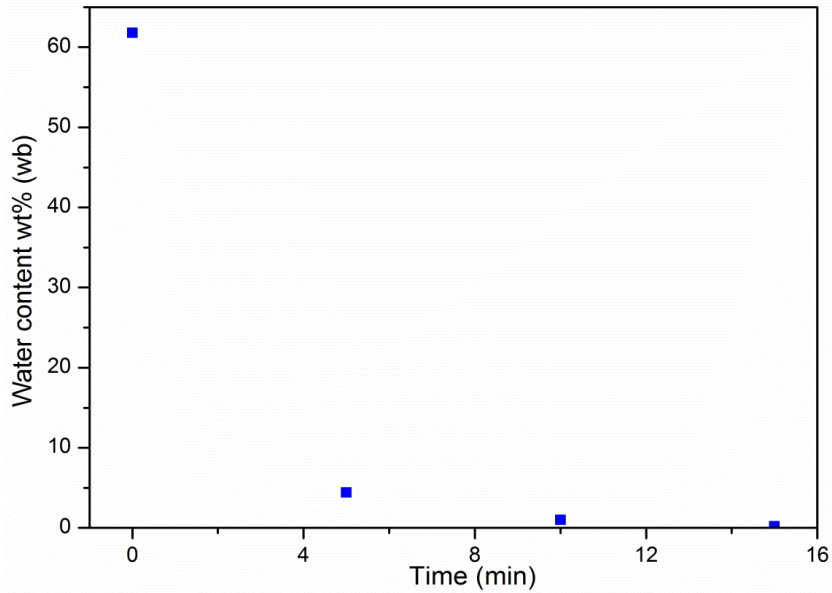


Fig. 5-3-9. Water content of sawdust in the fluidized bed dryer with air as the drying medium

5.3.4.4. Semicontinuous experiment for sawdust drying

Fig. 5-3-10 shows that the temperatures in the bed dropped near to the boiling point at the time of wet biomass feeding for its free water evaporation. Afterward, the temperature soon returned to the mean temperature owing to the good mixing in the fluidized bed. The temperature difference among the top and bottom levels was very small, indicating a homogenous state in the fluidized bed. The water evaporation energy was supplied from the condensed water inside heat exchange tubes. Consistent temperature and pressure of the air-steam mixture at the outlet of heat-exchange tubes were confirmed and shown in Fig. 5-3-11. The mean values of the outlet absolute pressure and temperature of the steam were about 182 kPa and 118 °C, respectively, indicating a stable heat exchange between the immersed tubes and the fluidized bed. The drops in pressure and temperature through the 18 immersed tubes during the heat exchange were about 8.0 kPa and 1.0 K, respectively, owing to the consistent heat exchange with the wet biomass. Moisture content of dried rice straw was constant as 2.5 wt% (wb). Sawdust was sampled and water content was investigated every 15 min. Fig. 5-3-12 shows that water content was constant during the drying process which was kept at a low value of 2.5 wt% (wb). Condensed water was collected in the tank (Fig. 5-3-13) and weighted as 1040 g and the evaporated water in the biomass was 1092 g. This means almost the evaporation heat was supplied from the water condensation heat and shows a good heat pairing actually formed in the fluidized bed dryer. The other energy was supplied by the fluidization medium (superheated steam) which was 120 °C.

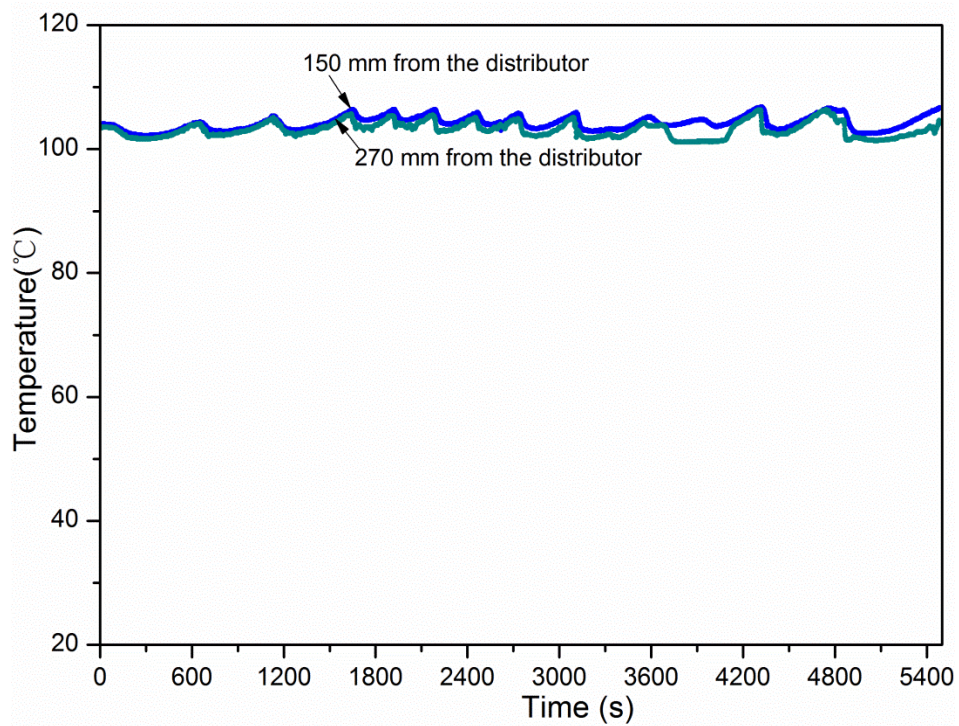


Fig. 5-3-10. The bed temperature distribution in the FBD

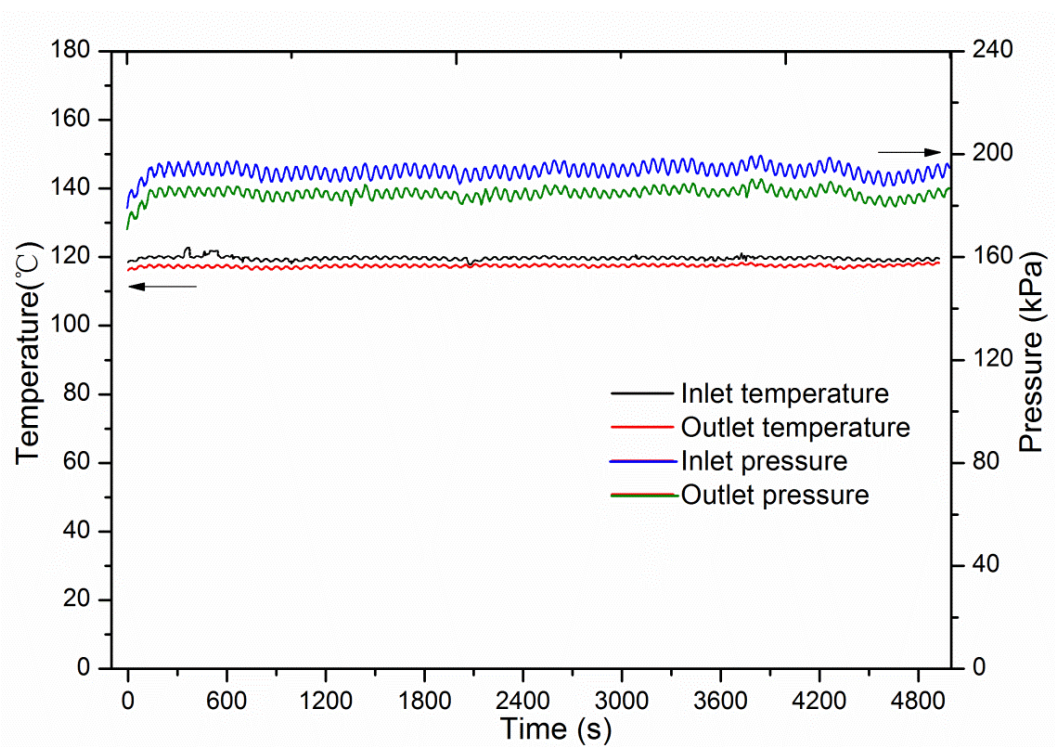


Fig. 5-3-11. Temperature and pressure of the compressed steam at the inlet and outlet of the FBD

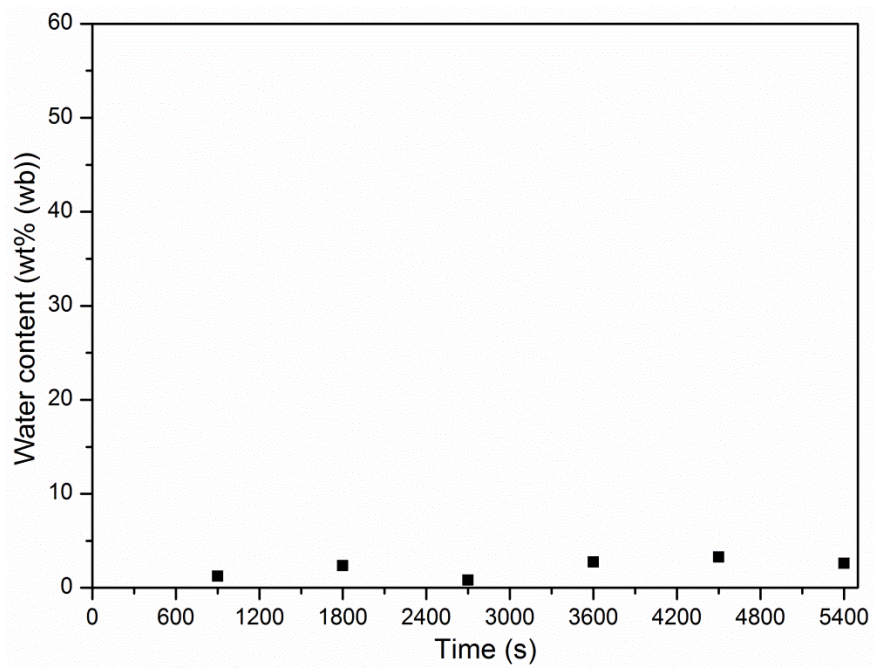


Fig. 5-3-12. Water content of dried sawdust during the drying process.

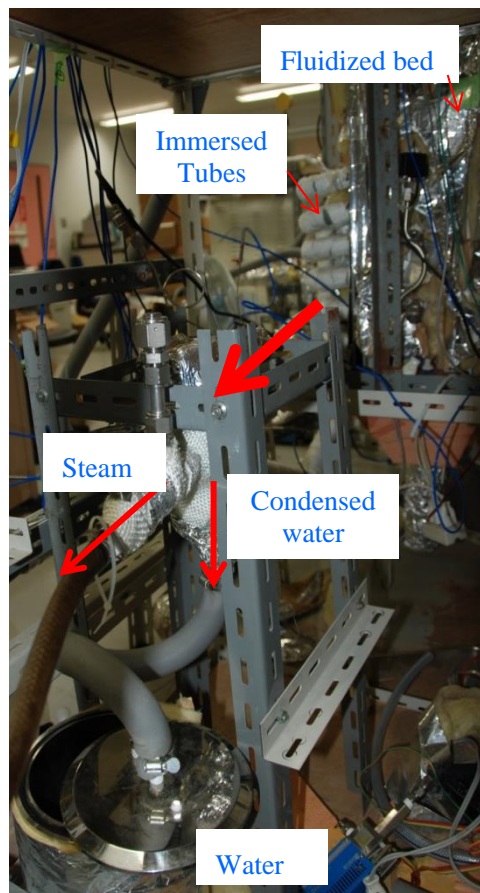


Fig. 5-3-13. Condensed water collection device

5.3.5. Conclusions

A good stability in fluidized bed dryer based on simulation conditions is confirmed. Silica sand with a diameter of 0.15 mm was chosen for the following steam drying experiments. The batchwise experiment showed that biomass could be dried with steam at near to the boiling point at the operation pressure in the fluidized bed dryer with a high drying rate. More energy supply through increasing the heat exchange surfaces could shorten the drying time to less than half of the drying process especially for the constant drying period. Sawdust drying with air in the fluidized bed dryer has also been investigated which had a higher drying rate compared with superheated steam drying, however, it caused more exergy loss during the drying process. Heat exchange stability in the fluidized bed was good. Almost the evaporation heat was supplied from the water condensation heat, and a low and constant water content of dried sawdust was achieved.

References

- Bilbao, R., J. Lezaun and J.C. Abanades, 1987. Fluidization velocities of sand/straw binary mixtures. *Powder Technol.*, 52: 1-6.
- Clarke, K. L., T. Pugsley, et al. 2005. Fluidization of moist sawdust in binary particle systems in a gas-solid fluidized bed. *Chemical Engineering Science*, 60(24), 6909-6918.
- Fyhr, C. and A. Rasmuson. 1996. Mathematical model of steam drying of wood chips and other hygroscopic porous media. *AIChE Journal*, 42(9), 2491-2502.
- Fyhr, C. and A. Rasmuson. 1997. Steam drying of wood chips in pneumatic conveying dryers. *Drying Technology*, 15(6-8), 1775-1785.
- Tatemoto, Y., Sugita, K., Yano, S., Mawatari, Y., Noda, K., Nobuyuki K., Drying Characteristics of Porous Materials in Superheated Steam Fluidized Bed under Reduced Pressure, *Journal of chemical engineering of Japan* 38(12), 983-989.

5.4. Novel fluidized bed dryer for biomass drying

5.4.1. Introduction

Through Chapters 2 and 3, we found the biomass could be dried under the simulation conditions. However, the main disadvantage of the current biomass fluidized bed dryer was that biomass particles could not be fluidized alone without adding silica sands or mechanical assistance which would increase the blower energy consumption or capital cost. Thus, we further developed a novel fluidized bed dryer for biomass drying in this chapter.

In Chapter 1, it is known that Many kinds of drying systems have been developed for biomass drying such as the conveyor dryers, rotary dryer of single or multiple passes, and the fixed and moving bed dryers, among which rotary dryers are the most common (Waje et al. 2006; Waje et al. 2007; Zabaniotou 2000; Zanoelo et al. 2007). However, because of their operating conditions, horizontal configuration, and low-heat transfer rate, existing biomass dryers are usually large and occupy a large footprint (Fagernas et al. 2010). To improve the economy of biomass-based processes prior to transport, it is desirable to have a compact and economical dryer. Fluidized beds have a high heat transfer rate and exhibit excellent solid mixing and uniform temperature distribution (Daud 2008; Law & Mujumdar 2009). The fluidized bed dryer could thus be a potential compact dryer for biomass drying. Unfortunately, one of the challenges for biomass drying in fluidized beds is to achieve good gas-solid contact and bed stability. Because of their peculiar shape and low density, biomass particles are subject to extensive channeling and slugging and cannot be fluidized properly in normal fluidized beds even at high gas velocities (Clarke et al. 2005; Cui and Grace 2007; Moreno et al. 2006). An inert material such as silica sand, glass spheres, alumina, or calcite is usually used to

facilitate fluidization of the biomass particles, which are present only in a small fraction (Rao and Bheemarasetti 2001). The introduction of inert particles into the fluidized bed may contaminate the dried biomass product and increase the pressure drop through the bed. Mechanically assisted fluidized beds such as vibrated or agitated and pulsed fluidized beds have been used for biomass drying without the addition of inert particles (Puspasari et al. 2013; Reyes et al. 2008). However, the increased equipment complexity may result in operational problems and increase the cost of the device. Biomass could also be dried in spouted beds at high gas velocities (Olazar et al. 2012); however, the heat transfer rate decreases because of the inefficient gas-solid contact compared with fluidized beds (Klassen and Gishler 1958).

The aim of this work is to explore a compact and economical dryer for biomass drying by using the advantages of high mass and heat transfer rates in the fluidized bed. A new fluidized bed dryer was proposed for biomass drying with inclined micro-jet distributor design. During drying, the fluidization behavior of the pure biomass particles would be affected by evaporating and wet regions on the surface of the particles and the inter-particle capillary forces. In addition, during the drying process, the fluidization behavior may be altered as the moisture content decreasing. Thus, the fluidization performance needs to be examined during the drying process. The biomass drying rate also had to be investigated to confirm the drying performance in the proposed fluidized bed dryer. In this work, the effects of air velocity and drying temperature were investigated to evaluate the performance of the fluidized bed dryer.

5.4.2. Materials and methods

5.4.2.1. Materials and experimental equipment

The sawdust sample, obtained from RONA lumber store in Vancouver, Canada, is a mixture of spruce and fir, with spruce as the main component. The sample was separated into two size fractions of 250–355 and 355–500 μm , respectively, using a Ro-Tap RX94 sieving device (W.S. TYLER Co. Ohio, USA). The solid density of the sawdust measured using a multi-pycnometer (Quantachrome Instruments Co. Florida, USA) was 1388 kg m^{-3} . The bulk density of wet sawdust with 60 wt% (wb) moisture content was 282 kg m^{-3} .

Batch runs for drying the sawdust were conducted in a stainless steel fluidized bed dryer, 1.5 m tall and 50 mm in diameter, as shown in Fig. 5-4-1a. A gas distributor with 30° vertically inclined orifices was designed to achieve a good solid circulation. Twelve holes were located around the peripheral region and two holes in the center with an inclined angle opposite the outer region. As a result, a solid circulation pattern was established with sawdust particles rising in the center, passing through a fountain region and then moving down slowly along the wall. This kept the entire bed of particles in motion as shown in Fig. 5-4-1b. Three K-type thermocouples (T1, T2, and T3) with diameter of 1.6 mm were used to measure the temperatures of the inlet gas, fluidized bed, and reactor wall and control the electric heater by means of a proportional integral derivative controller. The pressure drop across the fluidized bed was measured by the pressure difference between the pressure transducer P1 before and after the sawdust input. Dry air from an air cylinder was preheated to the desired temperature before being fed into the fluidized bed. The air flow was measured using a rotameter. As the drying progressed, water in the sample evaporated into the air. A hygrometer (HUMICAP, Vaisala, Finland, with precision of 1.0 %) was installed at the fluidized bed dryer outlet to monitor the relative humidity and temperature of the humid air

simultaneously. The wall surface of the fluidized bed dryer was maintained at a certain temperature by an electric heater surrounding the outer wall of the fluidized bed. The reactor was insulated to prevent heat loss from the bed to the environment.

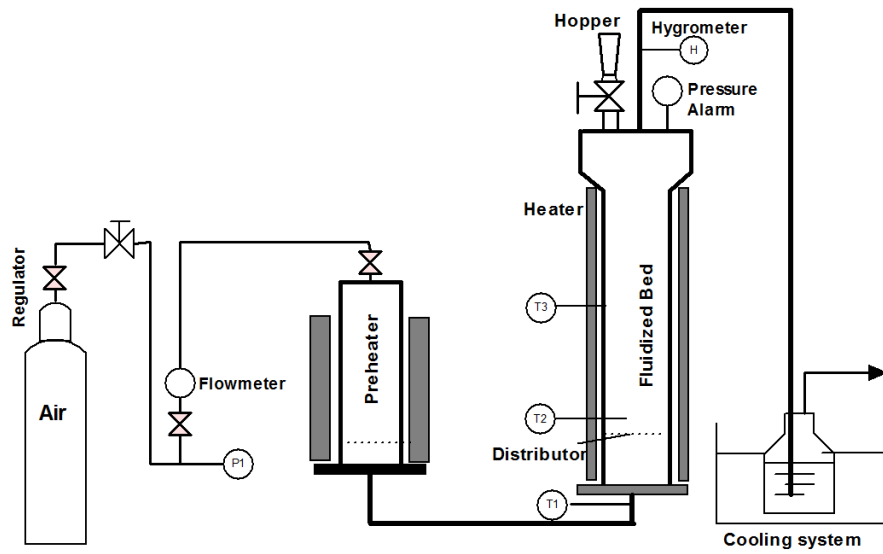


Fig. 5- 4-1a. Schematic of the fluidized bed drying unit.

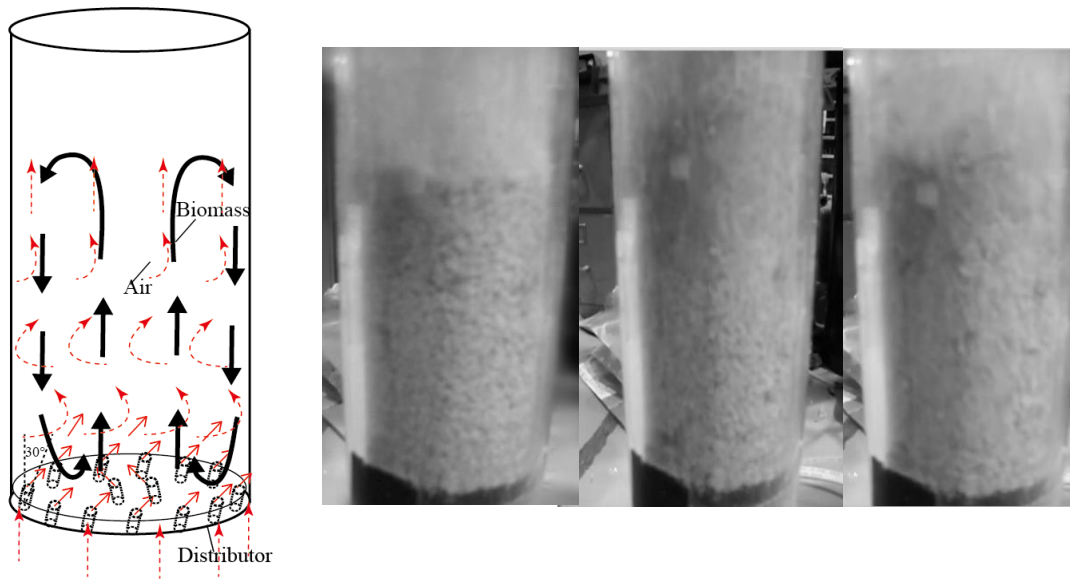


Fig. 5-4-1b. Left: Solid circulation pattern in the new fluidized bed dryer; right: sawdust (255-500 μm) fluidization in the cold model.

5.4.2.2. Experimental procedure

The fluidized bed dryer was heated up to the targeted drying temperature slowly and kept stable for at least 10 min. Wet sawdust with certain moisture content was weighted by a balance with a precision of 0.1 mg, and fed from the top of the fluidized bed immediately. After then, the sample was fluidized by air with predetermined flow and desired residence time. During the drying process, water was transferred from the wet sawdust to air. As it was difficult to investigate the weight change of sawdust in the stainless steel fluidized bed during the drying process, weight loss of wet sawdust, W_{loss} , was calculated through the water amount carried by air.

$$W_{\text{loss}} = w_n - w_m = m_g \sum_{i=m}^n Y_i \quad [\text{g-water}] \quad (5-4-1)$$

where w_n and w_m are the weight of wet sawdust at different time. Then, drying rate, R_w , can be determined as Eq. 5-4-2:

$$R_w = \frac{dw}{dt} = \frac{m_g \sum_{i=m}^n Y_i}{t_n - t_m} = \frac{m_g (Y_m + Y_{m+1} + \dots + Y_i)}{t_n - t_m}, \quad [\text{g-water/min}] \quad (5-4-2)$$

where m_g is the amount of air, and Y is the specific humidity which is the ratio of mass of water vapour per unit mass of dry air, which could be calculated by

$$Y = 0.622 \left(\frac{p_s}{p - p_s} \right) . \quad [\text{g-water/kg-air}] \quad (5-4-3)$$

The water vapour saturation pressure was calculated by the Wagner-Pruss equation (Wagner and Pruss 1993),

$$\ln \left(\frac{p_s}{22.064e6} \right) = 647.096 / T_k (-7.85951783 v + 1.84408259 v^{1.5} - 11.7866497 v^3 + 22.6807411 v^{3.5} - 15.9618719 v^4 + 1.80122502 v^{7.5}) \quad (5-4-4)$$

where,

$$v = 1 - T / 647.096 . \quad (5-4-5)$$

T is absolute air temperature (K). At the conclusion of the drying cycle, dried samples were collected and their final moisture content, W_{wet} , was determined according to the ASTM D4442-07 standard by heating the sample at 103 °C for 24 h in an oven, with the moisture content given by

$$W_{\text{wet}} = \frac{M_1 - M_2}{M_1} \times 100\% , \quad [\text{wt\% wb}] \quad (5-4-6)$$

where M_1 is the initial sampled dried sawdust and M_2 is final weights of the samples after drying in the oven for 24h, respectively.

5.4.3. Results and discussion

5.4.3.1 Fluidization behavior in the fluidized bed dryer

Biomass has a typical moisture content of over 50 wt% (wb), which is expected to have a strong effect on the fluidization behavior of biomass particles. We first investigated the effect of sawdust moisture content on fluidization performance. The fluidization behavior is assessed from the pressure drop across the fluidized bed, which is believed to be an important indicator (Bai et al. 1999; Bi et al. 2000), reflecting changes in the fluidization behavior in the fluidized bed (Wormsbecker and Pugsley 2008). In this study, we investigated the pressure loss across the fluidized bed through change of pressure drop during the sawdust drying. Drying rates at different operating conditions were also investigated to link the hydrodynamic characteristics to the mechanisms of drying. The change in drying rate could reflect the fluidization conditions in the fluidized bed indirectly because the drying rate was high under good fluidization conditions. Prior to drying, the minimum fluidization velocities of dry sawdust of different sizes were determined in a cold model unit, and a velocity of 0.32 m s⁻¹ was found to give a stable fluidization of 20 g sawdust sample.

Fig. 5-4-2 shows the drying curves of 20 g sawdust at an initial moisture content of 60, 40, and 20 wt% (wb). Three different water contents of sawdust were chosen to investigate the effect of moisture content on fluidization behavior. To dry sawdust with a moisture content of 60 wt% (wb), pressure drop P1 was approximately at 4 kPa initially and increased to 10 kPa after 4 min drying when the sawdust moisture content dropped to 50.1 wt% (wb). The drying rate increased initially during the preheating period and decreased as the drying progressed. It rose again when the sawdust moisture content further decreased and then decreased until the drying completed. When drying

sawdust with a moisture content of 40 and 20 wt% (wb), the drying rate increased initially during the preheating period and then decreased gradually as the inner moisture was transported to the surface by diffusion. Different from the case with initial moisture content of 60 wt% (wb), P1 increased initially by 10 and 8 kPa, respectively, and then remained almost constant with a decrease of 1–2 kPa once the drying had been completed because of the mass loss. Once the moisture content of the sawdust had dropped to less than 40 wt% (wb), the wet sawdust could be fully fluidized. The low initial moisture content of the input sawdust allowed it to reach full fluidization because of the weak capillary forces between the biomass particles.

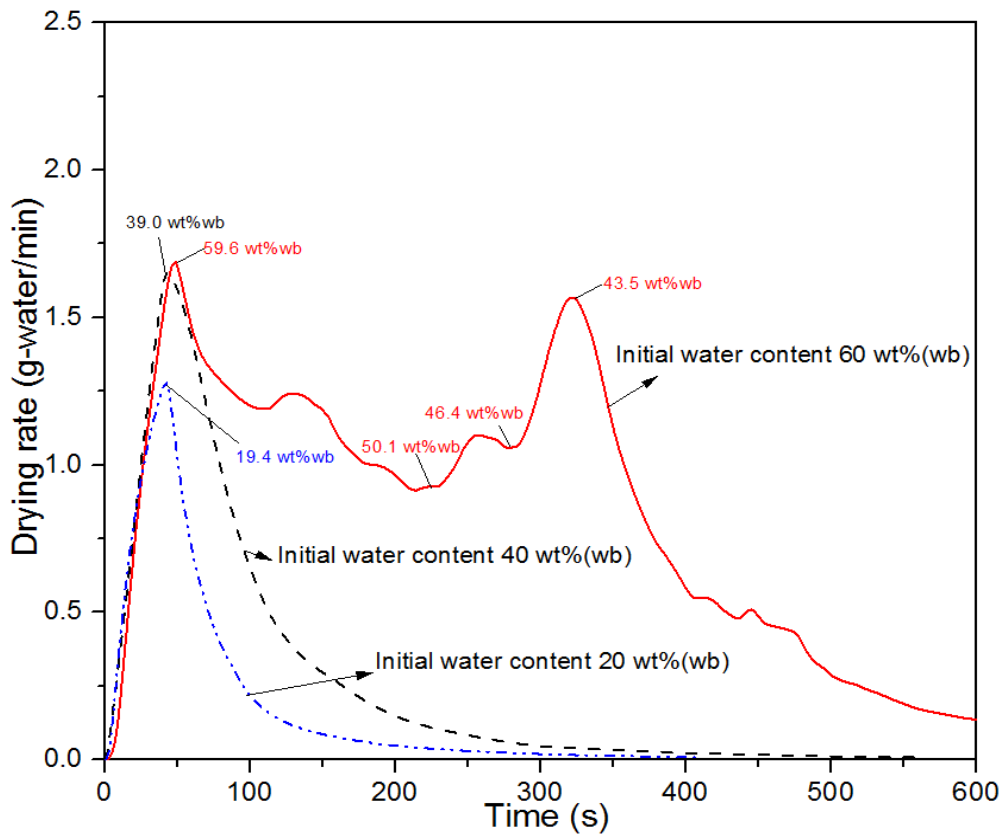


Fig. 5-4-2. Effect of initial moisture content of sawdust on the sawdust drying rate. Bed and air temperature were both 90 °C. Air velocity was 0.32 m s⁻¹.

The effect of bed height to diameter (H/D) ratio on the fluidization performance was investigated next. Fig. 5-4-3a shows the drying rate at different H/D values of 0.5, 1.0, and 2.0 with sawdust loadings of 10, 20, and 30 g, respectively. In the initial drying period, water evaporated from the biomass surface and a fast drying rate was achieved in all cases. With the decrease in surface water ratio, the drying rate began to decrease. For H/D values of 1.0 and 2.0, the drying rate rose again at similar moisture contents of 50.1 and 51.7 wt% (wb), respectively, likely due to the improved fluidization quality. With further surface water removal, the internal diffusion rate controlled the drying process, causing the drying rate to drop again at a moisture content of 43.5 and 42.5 wt% (wb), respectively. For an H/D value of 0.5, the stable fluidization was achieved initially for the small loading of sawdust. A small trough was found after the peak in the drying curve which was suspected to correspond to the onset of full fluidization following partial fluidization. Water in the sawdust occurs in three forms as surface, capillary, and bound water. Surface water on the biomass surface has the same properties as free liquid water. Capillary water in the cell cavities is more difficult to evaporate because of the strong capillary forces. Bound water requires energy to break free from the polymer chains in the cell wall. Fig. 5- 4-3b shows the drying rate as a function of sawdust moisture content and helps explain the relationship between fluidization behavior and sawdust moisture content. The fluidization behavior can be divided into three stages indicated by numbers 1, 2, and 3 on the drying curve. Point 1 is the starting point, point 2 is the transition point from partial to full fluidization with increasing drying rate, and point 3 is the transition point from full fluidization with an increasing drying rate to full fluidization with a decreasing drying rate. During partial fluidization (1–2), sawdust particles were partially fluidized, most likely due to the agglomeration of those high

moisture content sawdust particles. With progressing drying, part of the surface water was removed and capillary forces between the particles became weakened. Full fluidization with an increasing drying rate (2–3) was reached in which the whole bed became fluidized and the drying rate increased because of the increased mass and heat transfer rates. After the surface water had been removed, full fluidization with a decreasing drying rate (3–) occurred when internal water diffusion became the limiting factor.

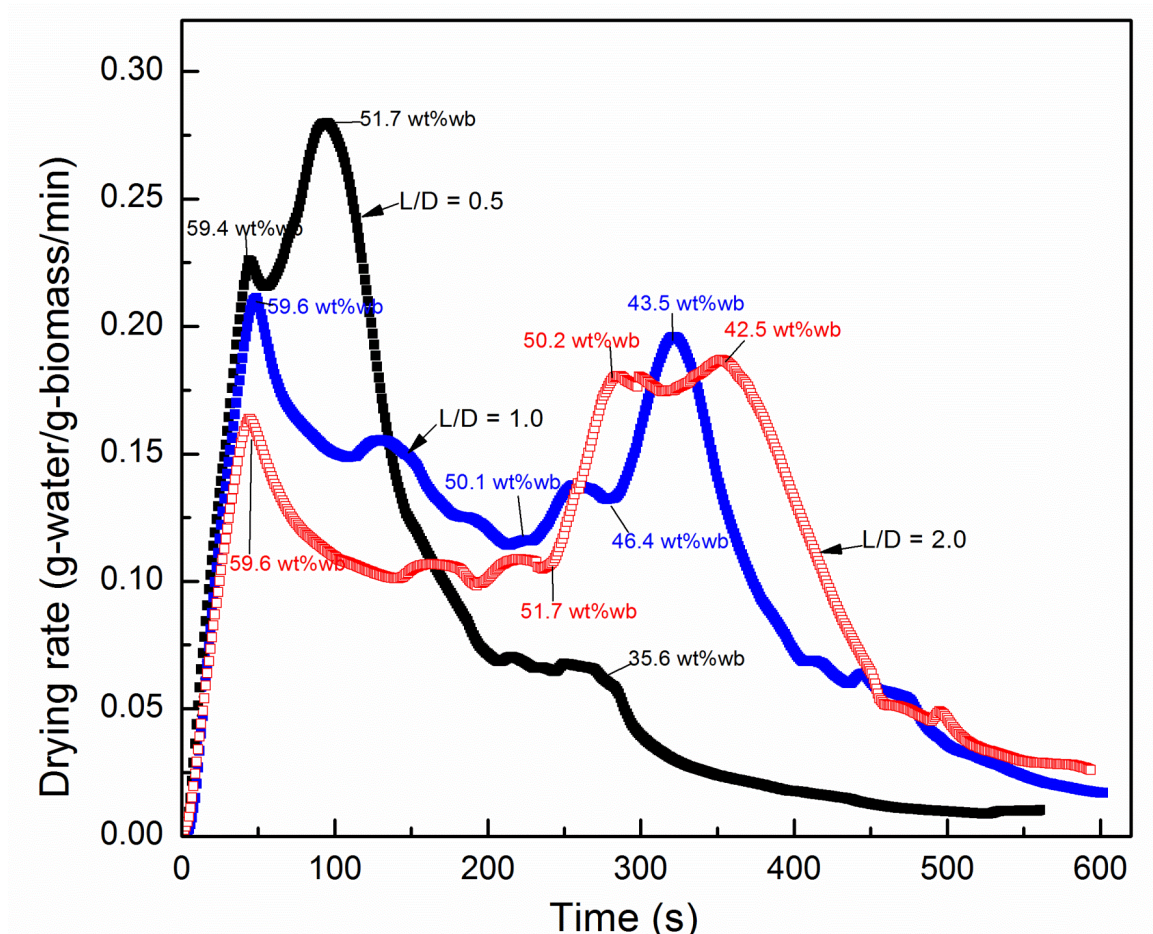


Fig. 5-4-3a. Sawdust drying rate at different H/D values. Initial moisture content of sawdust was 60 wt% (wb), and bed and air temperature were both 90 °C. Air velocity was 0.32 m s⁻¹.

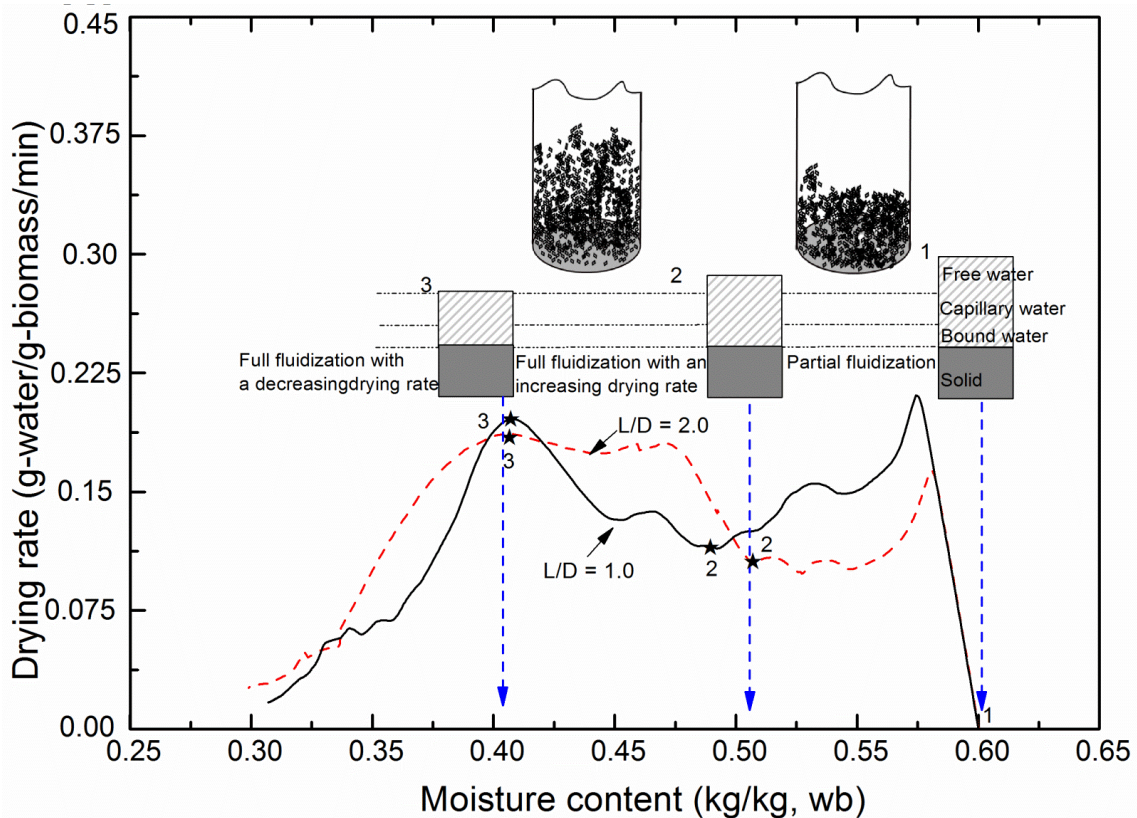


Fig. 5-4-3b. Sawdust drying rate as function of moisture content at different H/D values. Initial moisture content of sawdust was 60 wt% (wb), and bed and air temperature were both 90 °C. Air velocity was 0.32 m s⁻¹.

Figs. 5-4-4a and 4b show the drying rates as a function of sawdust moisture at various air velocities and bed temperatures. With the exception of the air velocity of 0.14 m s⁻¹ in which the packed bed formed, in the other cases, three drying stages existed during the drying process. The moisture content at point 2 was lower when the sawdust was dried at a higher drying temperature or air velocity. The thin liquid film over the particle surface had to be removed to eliminate capillary forces and full fluidization could only occur once the overall particle surface water had been removed. This resulted in lower moisture content at point 2, because more water could be

removed during the partial fluidization drying period at a higher temperature or gas velocity. This could also lower the moisture content at point 3 for the same reason. A study of the relationship between moisture content and fluidization behavior provides critical information for the stable drying of sawdust particles such as in a continuous fluidized dryer. The maximum feeding rate of wet sawdust for continuous operation could also be determined in the current fluidized bed dryer.

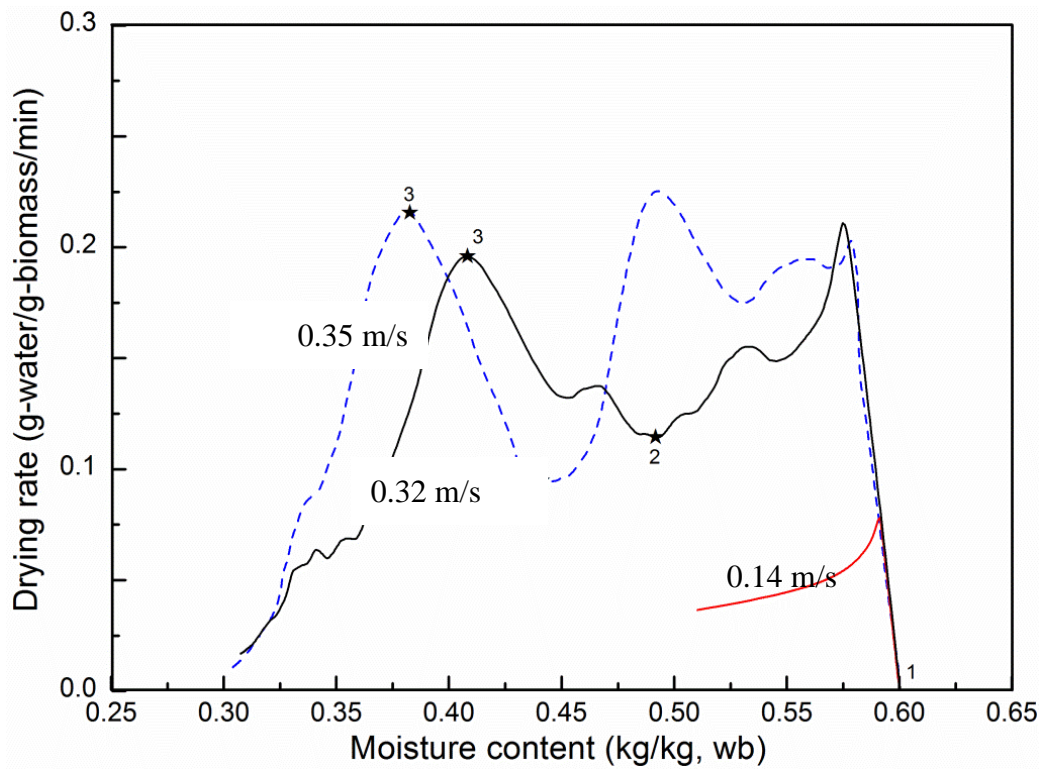


Fig. 5-4-4a. Effect of air velocity on the sawdust fluidization behaviour. Initial moisture content of sawdust was 60 wt% (wb), and bed and air temperature were both 90 °C.

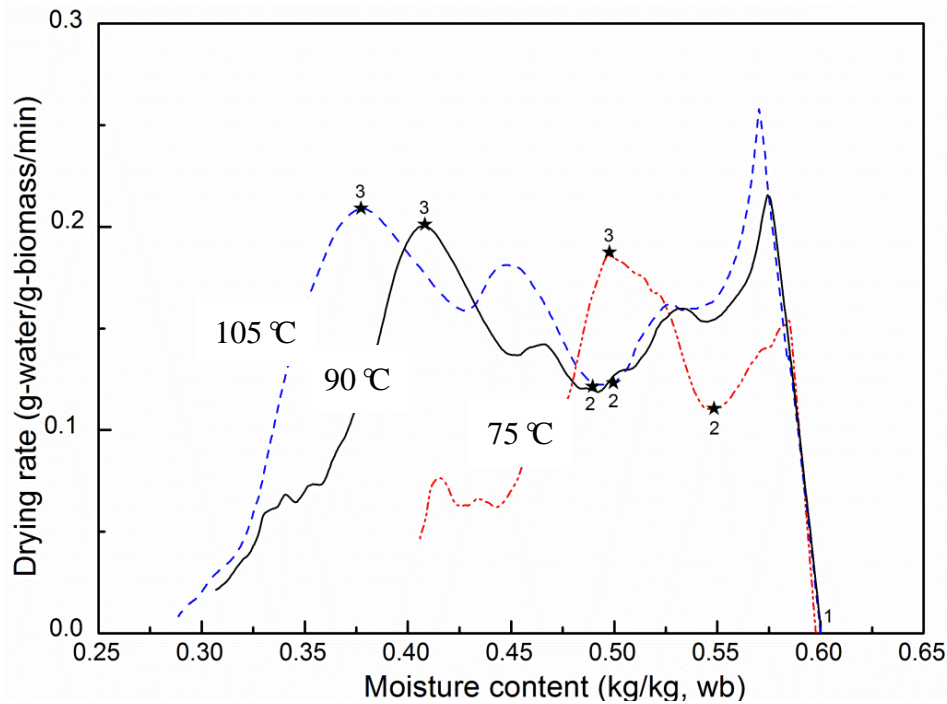


Fig. 5-4-4b. Effect of bed temperature on the sawdust fluidization behaviour. Initial moisture content of sawdust was 60 wt% (wb), and air temperature was 90 °C. Air velocity was 0.32 m s⁻¹.

5.4.3.2. Drying kinetics in the fluidized bed dryer

Results from the drying kinetics in the fluidized bed dryer show that increasing the air velocity from 0.14 to 0.32 m s⁻¹ could enhance the drying rate significantly (Fig. 5-4-5a). This occurs because a low air velocity would not sufficient to fluidize biomass particles and the bed stayed in a fixed state. When the air velocity increased over 0.32 m s⁻¹, stable fluidization resulted. The wall-to-bed heat transfer rate in the fluidized bed was much higher than that of the fixed bed because of bubble-induced bed-material refreshment along the heated wall (Kuipers et al. 1992). As a result, the moisture content of the sawdust could be decreased by 10 wt% (wb) in the first 3 min at an air velocity of 0.32 m s⁻¹, while it took more than 10 min at an air velocity of 0.14 m s⁻¹.

When the air velocity increased to 0.35 m s^{-1} , the drying rate increased slightly compared with that at 0.32 m s^{-1} because of the increased external mass transfer rate. At the air velocities of 0.32 and 0.35 m s^{-1} , the drying rates were both significantly high during the first 6 min when surface water was evaporated. The drying rate then dropped as capillary water was removed. The air velocity increases the external water diffusion rate and the drying rate in the constant rate drying period is affected significantly by the velocity of the drying medium compared with the falling rate period. At the air velocity was 0.14 m s^{-1} , the drying rate decreased gradually because of the decrease in surface water ratio as the drying progressed.

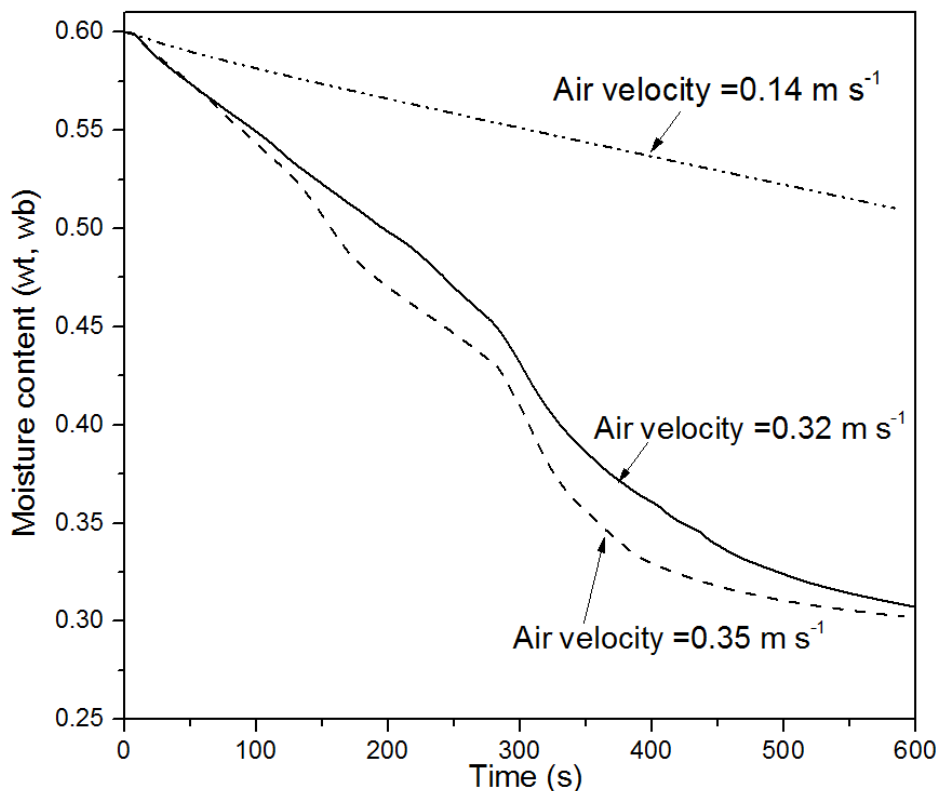


Fig. 5-4-5a. Effect of air velocity on the sawdust drying rate.

The heat provided for water evaporation comes mainly from the heated wall surface of the fluidized bed while air mainly plays a role as the drying medium. Thus, it is important to investigate the effect of bed temperature on drying rate. Fig. 5-4-5b shows the sawdust drying rate at three temperatures of 75, 90, and 105 °C. A high bed temperature increased the drying rate. This occurs because an increase in bed temperature decreases the relative humidity of the air and increases the mass transfer driving force for water removal from inside the particle. Another important effect of the high bed temperature is to lower the final moisture contents result in the dried sawdust. At high temperature, water molecules become activated to higher energy levels. They become less stable and break away from the water binding sites of the material. This decreases the equilibrium moisture content (Palipane and Driscoll 1993). The drying rate of sawdust at two size fractions, 250–355 and 355–500 µm, was also investigated. The particle size was reported to have an effect on drying rate in both the constant and falling rate drying periods because of a larger specific surface area and shorter diffusion paths for smaller particles. As expected, the drying rate of the 250–355 µm sawdust was slightly higher than that of the 355–500 µm fraction because of the increased internal and external moisture diffusion. However, the particle size did not have a significant effect on drying rate as shown in Fig. 5-4-5c, likely because the overall transfer process is controlled by external diffusion, as observed by other researchers (Chandran et al. 1990; Olazar et al. 2012). Based on these investigations, the drying rate was believed to be affected mainly by air velocity and bed temperature for a given particle size and biomass loading. The initial moisture could affect the initial fluidization quality.

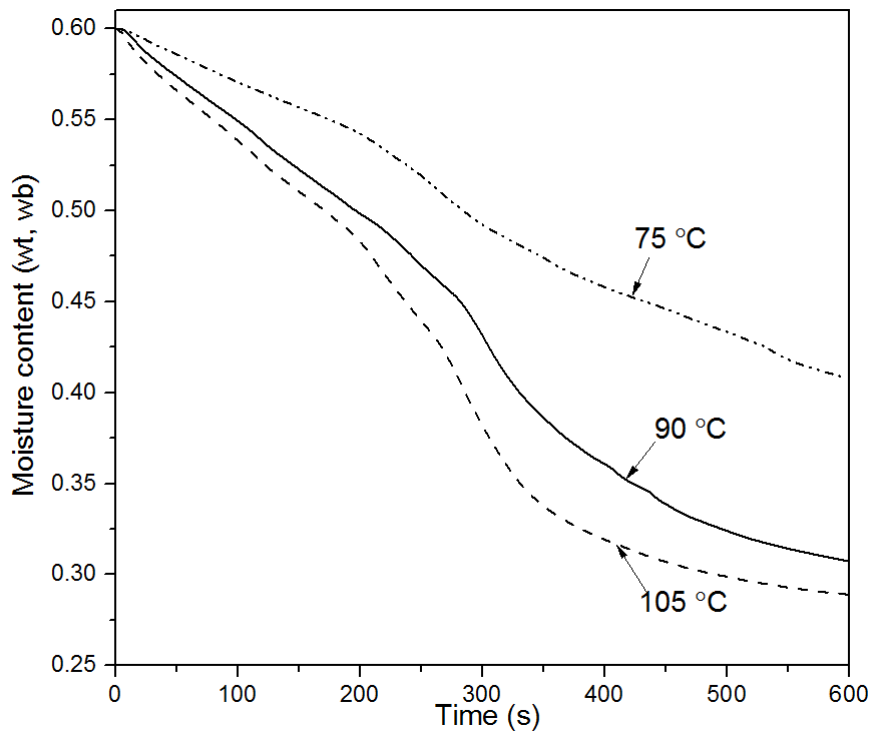


Fig. 5-4-5b. Effect of bed temperature on the sawdust drying rate.

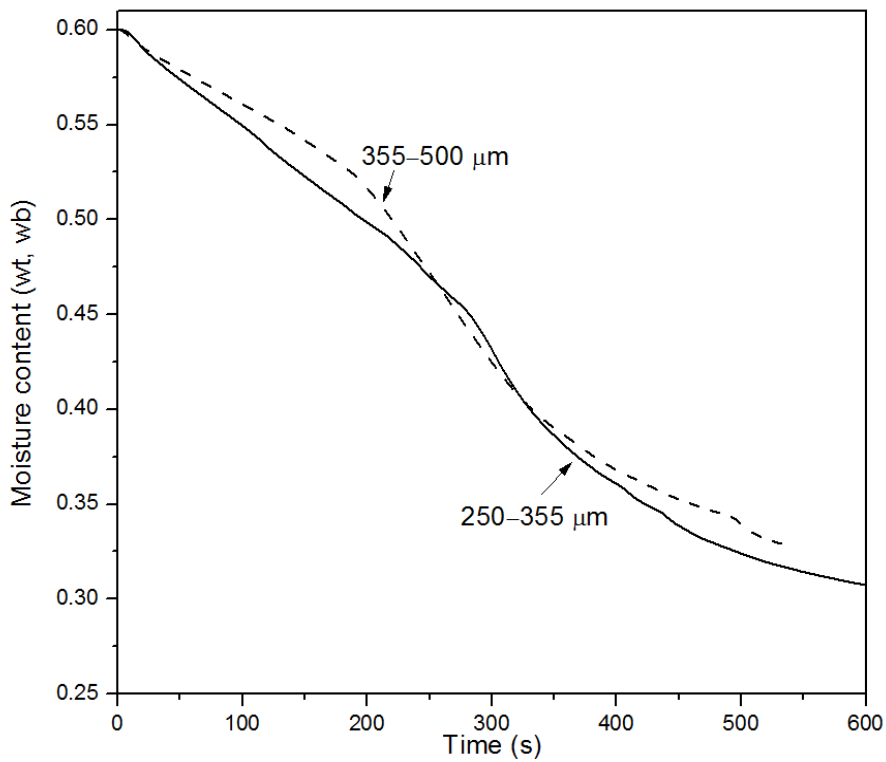


Fig. 5-4-5c. Effect of particle diameter on the sawdust drying rate.

5.4.3.3 Drying of binary mixture particles

Binary mixture of biomass and sand particles are often used for fluidized bed biomass combustion and gasification. Although drying kinetics of binary mixtures of homogeneous materials have been studied recently, drying kinetics have not been frequently reported on (Srinivas and Pydi Setty 2013). To evaluate the drying performance of the current fluidized bed dryer, we conducted sawdust drying with a sintered metal distributor at the same drying conditions as the newly designed dryer (see Fig. 5-4-6a). Silica sand ($d_p = 0.1$ mm) was added to co-fluidize with the sawdust. The mass ratio of wet sawdust to silica sand of the binary mixture in the fluidized bed dryer was 9.0 wt%, which made it easy to fluidize even at the presence of high moisture content sawdust. Sheathed heaters were installed inside the fluidized bed dryer to maintain a constant bed temperature. When the bed temperature reached the desired temperature, sawdust with a moisture content of 63 wt% (wb) was fed from the top of the dryer. The final moisture content of the dried samples was measured in an oven based on the ASTM D4442-07 standard.

To compare the drying performance in the two drying systems, the specific drying rate, R_{sp} , was defined as the ratio of drying rate to mass of dried biomass, M_{dry} .

$$R_{sp} = \frac{1}{M_{dry}} \frac{dw}{dt} = \frac{R_w}{M_{dry}}, \quad [\text{g-water/g-biomass/min}] \quad (5-4-7)$$

Fig. 5-4-6b shows the average specific drying rates for drying times of 5 and 15 min. The specific drying rates, R_{sp} , were almost the same in the two drying systems, which illustrates that the two systems had a similar drying rate for the same amount of biomass. In the binary mixture fluidized bed dryer, the input inert particles would enhance the heat transfer rate by filling the space between the biomass particles. In the new fluidized

bed dryer, high coefficients of interfacial mass and heat transfer were achieved because of the high gas-solid slip velocity. Table 5-4-1 lists the final moisture contents of the dried sawdust in the two drying systems. The final moisture content which was 8.90 wt% (wb) in the new fluidized bed dryer was almost the same as that in the conventional fluidized bed dryer (8.88 wt%, wb). However, without inert particle addition, the new fluidized bed dryer had a higher biomass particle density and required no separation of dried sawdust from the sand. This makes the system more compact and economical.

Table 5-4-1. Final moisture content of sawdust in the new fluidized bed dryer and a binary mixture fluidized bed dryer.

Properties	Binary mixture fluidized bed dryer	New fluidized bed dryer
Initial moisture content (wt% wb)	63	60
Sawdust weight (g)	635	20
Silica sand weight (g)	6350	0
Air flow (Nm ³ h ⁻¹)	9.6	2.26
Air velocity (m s ⁻¹)	0.17	0.32
Bed materials volume (×10 ⁻³ m ³)	5.2	0.071
Bed height (cm)	13.0	5.1
Final moisture content (wt% wb)	8.88	8.90

The final moisture content of sawdust drying was tested in 15 min in each batch operation. Bed and inlet air temperature were 105 and 55 °C, respectively, in both drying systems.

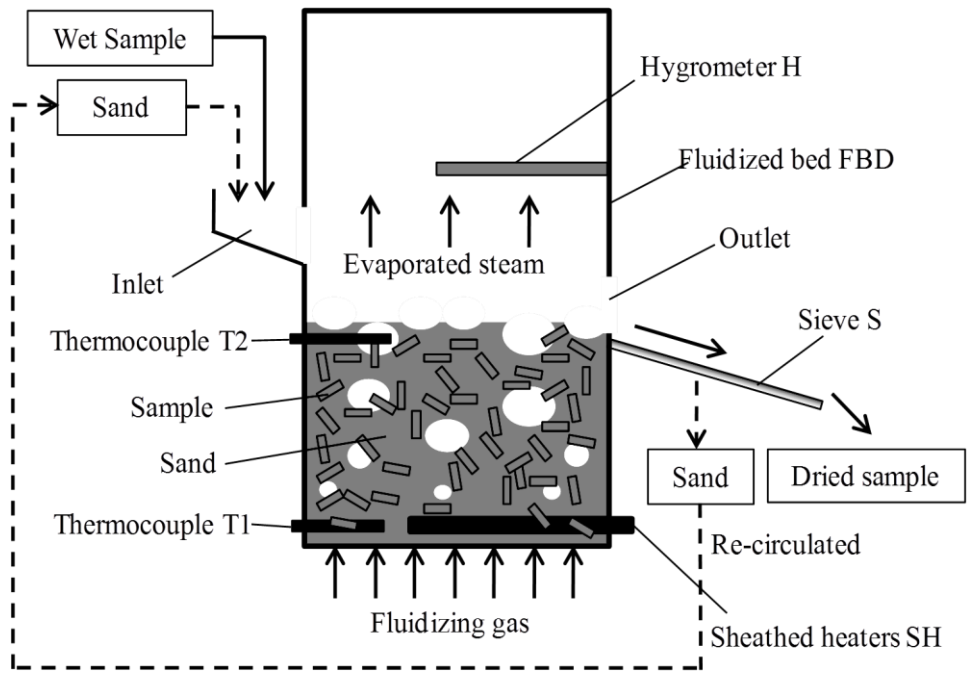


Fig. 5-4-6a. Schematic of the binary mixture fluidized bed dryer for biomass drying.

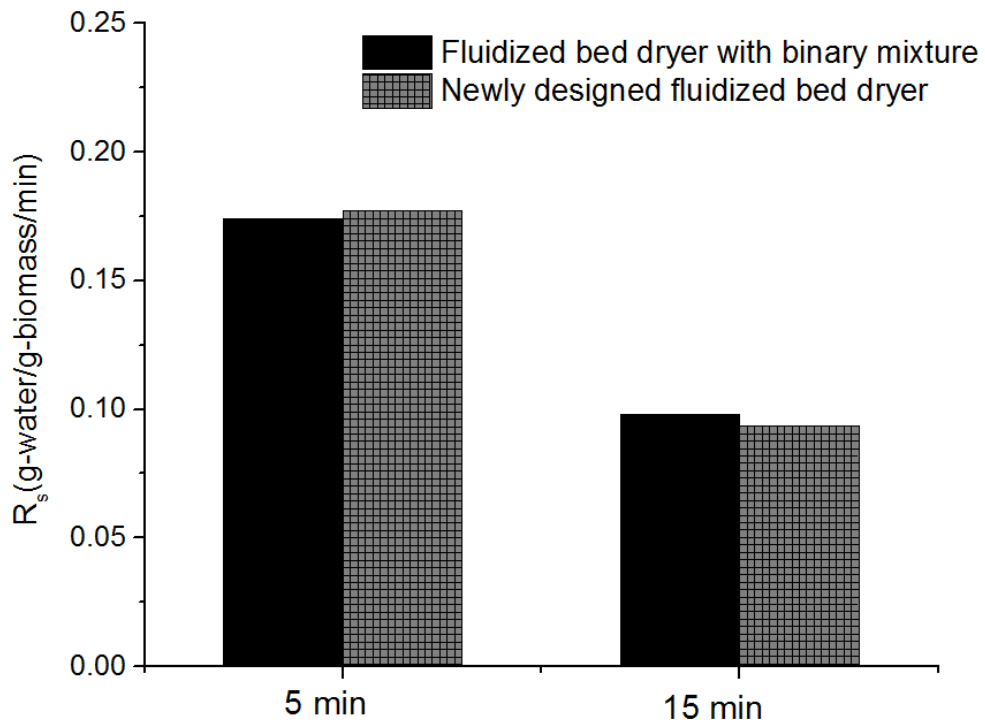


Fig. 5-4-6b. Specific drying rates in the fluidized bed dryer with binary mixture and newly designed fluidized bed dryer

5.4.4. Conclusions

A newly designed fluidized bed dryer for biomass drying was proposed and evaluated on its hydrodynamic and drying performance. Initial moisture content of sawdust had a critical impact on the fluidization behavior. For sawdust of low moisture content, full fluidization could be easily established right at the beginning. While for the drying of sawdust of high moisture content, the fluidization behavior could be divided into three stages: partial fluidization, full fluidization with an increasing drying rate and full fluidization with a decreasing drying rate. Moreover, the H/D value, air velocity and bed temperature had impacts on the sawdust fluidization behavior. At an H/D value of 0.5, the bed could be fluidized at the beginning. The fluidization behavior changed slightly as the H/D value varied from 1.0 to 2.0. A higher air velocity or higher bed temperature could decrease the critical moisture content corresponding to the full fluidization. A high drying rate was confirmed in the fluidized bed dryer when air velocity was over 0.32 m s^{-1} and a high bed temperature. The relationship between moisture content and fluidization behavior provides the critical information for the stable drying operation of sawdust particles in a continuous fluidized dryer. The new fluidized bed dryer had a similar drying rate with a conventional fluidized bed dryer of binary mixture, but was more compact and did not require biomass separation from inert particles. Heat transfer between the pure biomass particles and immersed surface would be studied in the future for the design and scaling up of the new fluidized bed dryer.

References

- ASTM Standard D4442-07, 2003. *Standard Test Methods for Direct Moisture Content Measurement of Wood and Wood-Base Materials*. ASTM International, West Conshohocken, PA, 2003. ed.
- Bai, D., A. S. Issangya, et al. 1999. Characteristics of gas-fluidized beds in different flow regimes. *Industrial & Engineering Chemistry Research*, 38(3), 803-811.
- Bi, H. T., N. Ellis, et al. 2000. A state-of-the-art review of gas-solid turbulent fluidization. *Chemical Engineering Science*, 55(21), 4789-4825.
- Chandran, A. N., S. S. Rao, et al. 1990. Fluidized-Bed Drying of Solids. *AIChE Journal*, 36(1), 29-38.
- Clarke, K. L., T. Pugsley, et al. 2005. Fluidization of moist sawdust in binary particle systems in a gas-solid fluidized bed. *Chemical Engineering Science*, 60(24), 6909-6918.
- Cui, H. P. and J. R. Grace. 2007. Fluidization of biomass particles: A review of experimental multiphase flow aspects. *Chemical Engineering Science*, 62(1-2), 45-55.
- Daud, W. R. W. 2008. Fluidized Bed Dryers — Recent Advances. *Advanced Powder Technology*, 19(5), 403-418.
- Fagernas, L., J. Brammer, et al. 2010. Drying of biomass for second generation synfuel production. *Biomass & Bioenergy*, 34(9), 1267-1277.
- Kaliyan, N. and R. V. Morey. 2009. Factors affecting strength and durability of densified biomass products. *Biomass & Bioenergy*, 33(3), 337-359.
- Klassen, J. and P. E. Gishler. 1958. Heat transfer from column wall to bed in spouted fluidized and packed systems. *The Canadian Journal of Chemical Engineering*,

36(1), 12-18.

Kuipers, J. A. M., W. Prins, et al. 1992. Numerical-Calculation of Wall-to-Bed Heat-Transfer Coefficients in Gas-Fluidized Beds. *AIChE Journal*, 38(7), 1079-1091.

Maciejewska, A., H. Veringa, et al. Co-firing of biomass with coal: constraints and role of biomass pre-treatment. http://ie.jrc.ec.europa.eu/publications/scientific_publications/2006/EUR22461EN.pdf.

McKendry, P. 2002. Energy production from biomass (part 2): conversion technologies. *Bioresource Technology*, 83(1), 47-54.

Moreno, R., G. Antolin, et al. 2006. Quality of fluidisation for the drying of forestry Biomass particles in a fluidised bed. *Biosystems Engineering*, 94(1), 47-56.

Olazar, M., G. Lopez, et al. 2012. Drying of Biomass in a Conical Spouted Bed with Different Types of Internal Devices. *Drying Technology*, 30(2), 207-216.

Palipane, K. B. and R. H. Driscoll. 1993. Moisture Sorption Characteristics of in-Shell Macadamia Nuts. *Journal of Food Engineering*, 18(1), 63-76.

Puspasari, I., M. Z. M. Talib, et al. 2013. Fluidization characteristics of oil palm frond particles in agitated bed. *Chemical Engineering Research & Design*, 91(3), 497-507.

Rao, T. R. and J. V. R. Bheemarasetti. 2001. Minimum fluidization velocities of mixtures of biomass and sands. *Energy*, 26(6), 633-644.

Reyes, A., R. Vega, et al. 2008. Drying sawdust in a pulsed fluidized bed. *Drying Technology*, 26(4), 476-486.

Srinivas, G. and Y. Pydi Setty. 2013. Drying behavior of uniform and binary mixture of solids in a batch fluidized bed dryer. *Powder Technology*, 241(0), 181-187.

- Wagner, W. and A. Pruss. 1993. International Equations for the Saturation Properties of Ordinary Water Substance - Revised According to the International Temperature Scale of 1990 (Vol 16, Pg 893, 1987). *Journal of Physical and Chemical Reference Data*, 22(3), 783-787.
- Waje, S. S., B. N. Thorat, et al. 2006. An experimental study of the thermal performance of a screw conveyor dryer. *Drying Technology*, 24(3), 293-301.
- Waje, S. S., B. N. Thorat, et al. 2007. Screw conveyor dryer: Process and equipment design. *Drying Technology*, 25(1-3), 241-247.
- Wang, L., C. L. Weller, et al. 2008. Contemporary issues in thermal gasification of biomass and its application to electricity and fuel production. *Biomass & Bioenergy*, 32(7), 573-581.
- Wormsbecker, M. and T. Pugsley. 2008. The influence of moisture on the fluidization behaviour of porous pharmaceutical granule. *Chemical Engineering Science*, 63(16), 4063-4069.
- Zabaniotou, A. A. 2000. Simulation of forestry biomass drying in a rotary dryer. *Drying Technology*, 18(7), 1415-1431.
- Zanoelo, E. F., G. M. di Celso, et al. 2007. Drying kinetics of mate leaves in a packed bed dryer. *Biosystems Engineering*, 96(4), 487-494.

CHAPTER 6
SUMMARY AND FUTURE WORK

6.1. Summary

Biomass is a promising sustainable energy; however, its current application for energy supply was limited and its high moisture content was one of the main reasons. Drying could reduce its moisture content but consumes a large amount of energy, and current biomass dryers (rotary dryer and conveyor dryer) are large. To solve the above problems, in this research we developed biomass drying processes based on SHR technology to reduce the energy consumption for biomass drying. We also succeed to apply the fluidized bed dryer for biomass drying which is more compact and efficient.

At the beginning, energy analysis was performed in the existing energy-saving drying processes and the unmatched heat pairing was found as the main reason for the large amount of energy consumption in the existing energy-saving processes. Heat pairing concept was introduced to apply SHR technology for the drying process. Exergy analysis was conducted to investigate exergy loss in an initial design of fluidized bed dryer based on SHR technology. A large amount of exergy loss occurred in the evaporator coming from the unmatched heat pairing due to the existence of air which has only sensible heat. By solving the above problem, SHR technology was succeeded to be applied to the fluidized bed dryer. The energy consumption could be saved to 1/6 of the conventional heat recovery dryer. A lab-scale fluidized bed dryer was built to investigate if simulation conditions of the proposed self-heat recuperative drying process are feasible for the actual biomass drying. A good stability in the fluidized bed dryer for biomass drying and high drying rate was found through the experimental results. SHR technology has also been applied to other types of biomass dryer which also showed a good energy-saving potential, however, with a large footprint. Existence of air was found for the exergy loss in the drying process, thus we changed the drying

medium from air to superheated steam.

Energy consumption could be dramatically decreased to 1/12 of conventional heat recovery drying process in the exergy recuperative drying system with superheated steam for biomass drying. Different from air drying system, in the superheated steam drying system, free water and bound water should be removed from biomass separately for good heat pairing. This was the main reason of still large energy consumption in the existing mechanical vapor recompression drying process which failed to consider heat pairing in the drying system. A high drying rate and a stable heat exchange was found through the experimental results. The main disadvantage of the current biomass fluidized bed dryer was that biomass particles could not be fluidized alone without adding silica sands or mechanical aids which increases the blower energy consumption or capital cost. Thus, we further developed a new fluidized bed dryer in which pure biomass particles succeeded to be fluidized. This made the dryer more compact with a high drying performance. This research would promote biomass application by reducing pretreatment cost which was currently limiting the biomass utilization through reducing drying energy consumption and size of drying device.

In Chapter 2, exergy loss was investigated in the drying process and heat pairing concept was developed to apply SHR technology for the drying process. Energy analysis was performed in the existing energy-saving drying processes and the unmatched heat pairing was found as the main reason for the large amount of energy consumption in the existing energy-saving processes. Initial design was proposed for biomass drying in a fluidized bed dryer which saved energy consumption to 1/4 of the conventional heat recovery drying process. Exergy analysis showed that the exergy loss

was greater in the fluidized bed dryer than in other units due to the sensible heat of air was paired with the latent heat of water evaporation.

In Chapter 3, SHR technology was succeeded to be applied to the fluidized bed dryer. The energy consumption could be saved to 1/6 of the conventional heat recovery dryer due to the good heat pairing. In the experiment, we investigated the hydrodynamic behavior inside the fluidized bed dryer with silica sand as the fluidizing particles and immersed heating elements as a heat source. The results showed that good solid mixing, as well as a uniform temperature across the bed, could be achieved under the condition that the fluidization velocity was at least three times the minimum fluidization velocity of sand and a good drying performance could be also achieved in this situation. Furthermore, a stability investigation of the fluidized bed dryer was conducted.

In Chapter 4, the other biomass drying systems (rotary dryer and screw conveyor dryer) were investigated based on SHR technology. Energy consumption can be reduced to 1/7 of that of a conventional heat recovery dryer. Effects of the heat exchange type, ratio of air to product, minimum temperature difference between the hot and cold streams in the heat exchanger, and drying medium on the system energy consumption were evaluated when applying self-heat recuperation technology to a biomass drying system. Energy saving by applying SHR technology to the biomass drying systems mainly depended on the minimum temperature difference between the hot and cold streams in the heat exchanger.

In Chapter 5, an exergy recuperative module for energy-saving drying with superheated steam has been proposed and applied to design an exergy recuperative drying system. Simulation results show that energy consumption in the exergy recuperative drying process could be reduced to 1/7–1/12 that of the CHR, less than 1/4

that of the MSD and near 1/2 that of the MVR. Energy consumption of the exergy recuperative drying process would increase slightly with the decrease in the final water content and the adiabatic efficiency of the compressor affects the total energy consumption reduction slightly. The exergy recuperative module was applied for the biomass drying system. Furthermore, a steam fluidized bed dryer was built in our lab. Hydrodynamic study, drying kinetics of sawdust and heat transfer stability in the fluidized bed dryer with steam were investigated. Biomass could be dried at near to the boiling point in the fluidized bed dryer with a high drying rate. More energy supply through increasing the heat exchange surfaces could shorten the drying time especially for the constant drying period. In Section 5.4, a new fluidized bed dryer was proposed for biomass drying. Biomass particles could form a good solid circulation in the fluidized bed without adding inert particles and mechanical aids. Results showed that initial moisture content of input sawdust affected on the sawdust fluidization performance. For sawdust of high moisture content drying, the fluidization behavior could be divided into three stages: partial fluidization, full fluidization with an increasing drying rate and full fluidization with a decreasing drying rate. A high drying rate could be achieved due to the fast mass and heat transfer rate in the fluidized bed. The fluidized bed dryer has a similar drying performance as a binary mixture fluidized bed dryer, however, more compact and require no separation from inert particles.

6.2. Future work

6.2.1. Integration of biomass drying and torrefaction process

To improve the energy efficiency in drying process, this research provided self-heat recuperative drying process which showed a dramatically energy-saving potential. Besides the high energy consumption associated with biomass drying operation, the regular biomass pellets also suffers the problems of low energy density, short shelf life and non-water-resistant, which limit their domestic applications as an alternate fuel for power plants (Oberberger and Thek, 2010). Torrefaction is a very promising approach to make the high quality biomass pellets, called torrefied pellets, by thermally treating the raw biomass at 250 to 300 °C to remove 20 to 30% mass as volatiles before densification. Apparent energy densities can be increased from 18 to 22 GJ t⁻¹ after torrefaction, reducing transportation volumes of biomass. Torrefaction of biomass also increases hydrophobicity, slows biological and thermal degradation, prolongs durability and improves grindability (Bergman et al., 2005; Chen and Kuo, 2011), which can improve the shelf life, storage and safe handling. Due to their high heating values and water-repelling properties, torrefied pellets have been considered as a promising renewable fuel for existing coal-fired power plants in Ontario and Alberta. As a result, interest in torrefied pellets has been growing in recent years, and efforts are being made to develop this technology.

Most previous researches on torrefaction have focussed on preparing biomass for further energy conversion processes such as gasification to lower tar formation (Arias et al., 2008; Bergman et al., 2005; Couhert et al., 2009; Deng et al., 2009; Yan et al., 2009). Little work has been reported on densification of torrefied biomass into pellets and, to our knowledge, almost no work on the optimization of an integrated torrefaction and

densification process for the production of high quality torrefied pellets (Chen and Kuo, 2011; Phanphanich and Mani, 2011; Pimchuai et al., 2010; Repellin et al., 2010; Rousset et al., 2011).

One of the major challenges in developing an integrated torrefaction process for pellet production is the selection of suitable torrefaction reactors to match the existing drying, grinding and pelleting equipments. Most torrefaction reactors under development are fixed beds, moving beds or screw types with wood chips as the feedstock, which require at least 40 to 60 minutes to torrefy the wood to the desired energy content. For a torrefied pellet plant with a typical production capacity of 100,000 metric tons per year (12 tonne/hr), the torrefaction reactor volume needs to be more than 30 m³, based on a wood chip bulk density of 250 kg/m³ and a residence time of 40 minutes. To reduce the reactor footprint, torrefaction time needs to be shortened which can be achieved by using small biomass particles like sawdust because of the improved heat and mass transfer rates. Such a torrefaction unit can be installed between the grinding unit and the pelleting machine. Although the advantage of energy savings in grinding torrefied chips is lost in such a configuration, the savings from the reduced size of reactor and the elimination of sawdust preheating before pelletization will much outweigh the loss of grindability of torrefied wood chips, because the drying and torrefaction will consume much more energy than the grinding operation based on the energy audit of existing pellet plant as discussed previously. Note that in a typical chemical plant, the reactor also accounts for the major capital investment, and a small torrefaction reactor will also potentially reduce the capital costs.

The self-heat technology can be future applied to a biomass drying and torrefaction process for more energy saving and biomass pellets production. Torrefaction of biomass

in the fluidized bed reactor takes place at a temperature of about 280 °C with a residence time of 20 minutes in order to achieve 30% weight loss (Li et al., 2011). As in biomass pyrolysis, inert gases such as nitrogen or CO₂ have been commonly used as the fluidizing gas to fluidize biomass particles as well as to provide required heat for torrefaction. On the other hand, about 30% of biomass is removed into the vapour phase during torrefaction, which contains a CO and organic compounds with a moderate heating value. Those combustible gases can be potentially used to provide required heat for the torrefaction reactor. Examining the energy flow in the biomass torrefaction process, we can see that heat is required for biomass drying at temperature (110 °C) and torrefaction in the fluidized bed reactor (280 °C), while the hot torrefied biomass needs to be cooled before fed into the pelleting machine (110 °C) to be densified into pellets. At the same time, energy-containing volatiles are produced from torrefaction, which can be potentially burned to provide required process heat. Based on the self-heat recuperation technology, an integrated torrefaction process can be proposed as shown in Fig. 6-2-1. The hot combustion flue gases above 400 °C will then pass through heat exchange tubes immersed in the fluidized bed torrefier to transfer heat to the reactor media. Then the cooled flue gases at about 300 °C will be split into two streams, one as the fluidizing gas for the torrefier and the other is used to preheat the combustion air for the incinerative combustor during the heat exchange. The hot torrefied biomass discharged from the torrefaction reactor will be cooled in a fluidized bed or moving bed heat exchanger by indirectly contact with cooling air (to avoid self-ignition) before being compressed into pellets in a pelleting machine, which is operated between 110 to 170 °C. The pellets are further cooled to below 50 °C by directly contact with fresh air before being transferred to the storage bins in a 2nd heat exchanger. The heat released

from both coolers is used to heat the biomass before the torrefier and part of the air for the incinerative combustor.

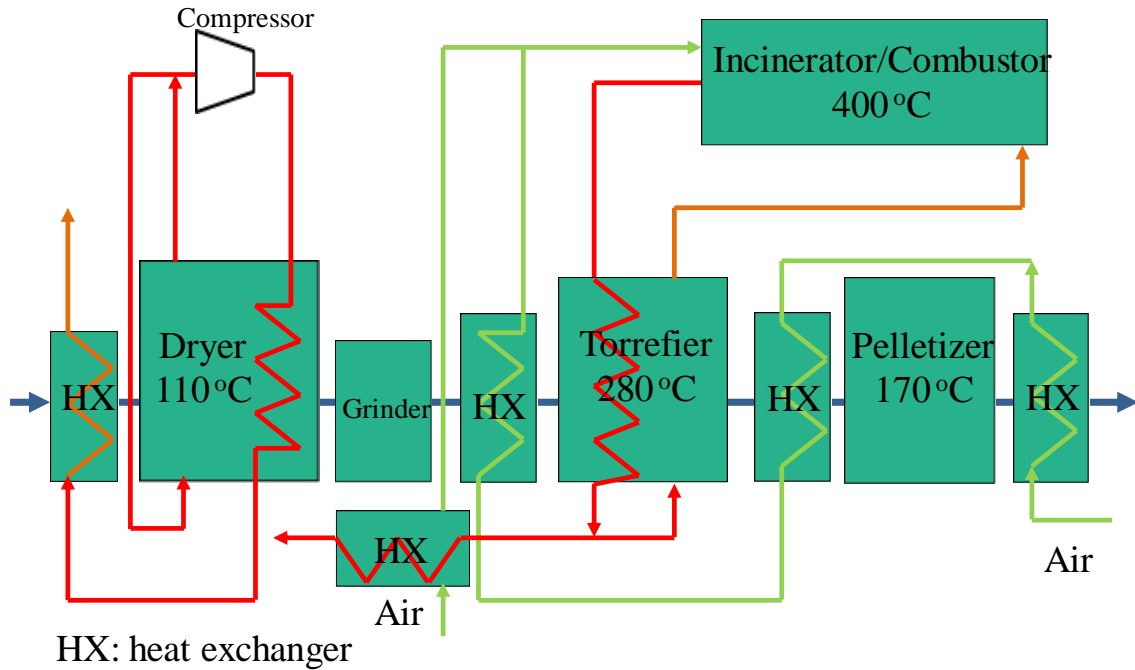


Fig. 6-2-1. An Integrated heat-recuperative fluidized bed drying and torrefaction process.

To design and scale such an integrated drying and torrefaction process, one needs to understand the heat transfer between immersed surfaces in fluidized bed torrefier/dryer or moving bed dryer/coolers for raw and torrefied biomass particles in order to determine the required total heat transfer surface areas (Fig. 6-2-2). To our knowledge, there have been little, if none, investigations on heat transfer between immersed heat transfer tubes and pure biomass particles in fluidized bed reactors because a mixture of sand and biomass particles has been commonly used in biomass combustion, gasification and pyrolysis fluidized bed reactors. The unique application of fluidized

bed for the torrefaction of biomass particles requires us to study the surface-to-bed heat transfer in pure biomass fluidized beds.

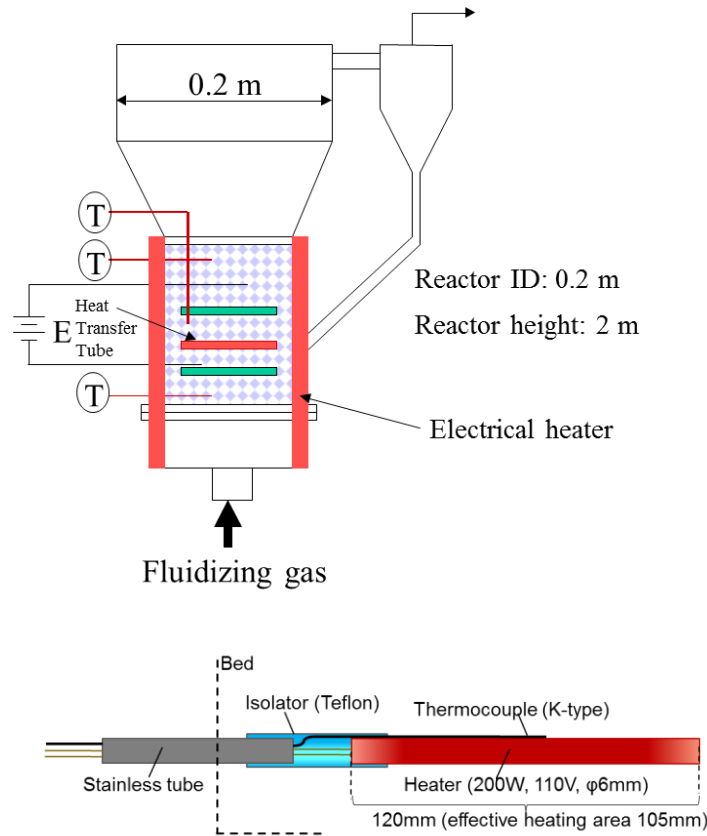


Fig. 6-2-2. Schematic diagram of the new 200 mm ID hot model bubbling fluidized beds. Column material: stainless steel without refractory lined.

The successful developments of the 2nd generation torrefied wood pellets and the reduction in energy consumption in the biomass densification process via energy integration and recuperation will enable the development of domestic and global markets for forest and agricultural biomass residues, contributing to the sustainable development of natural resources while addressing the pressing environmental and global concerns.

6.2.2 Brown coal drying

In this research, the developed drying process was used for biomass drying. We also considered to be applied the self-heat recuperation technology for low rank coal (LRC) drying. LRC including lignite, brown coal and sub-bituminous coal constitutes more than 50% of the global coal reserves and its long term future is predicated on its growing utilization as fuel and material (Karthikeyan et al., 2007). LRC has some advantages compared to other higher rank coals of lower mining cost (possibility for open-cut mining), higher reactivity, and lower sulfur content. Unfortunately, LRC also has some disadvantages on lower fuel ratio (i.e. fixed carbon to volatile matter) and high moisture content ranging from 45 to 66 wt% wb (as-mined) because the coalification is not advanced so far and the aqueous medium still exists in the pores. High moisture content results in lower calorific value, higher transportation cost, complex handling including loading and unloading, decrease of friability, etc. Using dried coals could increase its calorific value as well as efficiency of power plants, decrease the transportation cost and the greenhouse gases exhausted from power plant, simplify the loading and unloading, etc. (Allardice et al., 2004; Kudra et al., 2009; Karthikeyan et al., 2009; Pikon et al., 2009).

Moreover, in drying process, Aziz et al. (2011) have developed heat circulation based drying systems for biomass and brown coal, respectively, and found a large energy reduction in drying. Unfortunately, the existence of drying medium, which is non-condensable, in the compressed vapor inside the heat exchanger tubes reduces the performance of heat exchange inside the dryer. As the result, quite long heat exchanger tubes are required to provide an equivalent heat amount which is required for drying. This will influence the dryer size and fluidization behavior of the low rank coal particles

inside the dryer. Longer heat exchanger tubes lead to a larger size of the dryer and also higher equipment cost. In addition, longer heat exchanger tubes also decrease the fluidization performance leading to poor solid mixing and nonuniformity in drying.

To improve the heat exchange, drying performance, dryer dimension and cost, Advanced Self-heat recuperative system based Drying (ASRD) system was developed. Regarding the improvement of heat exchange during drying, the drying medium/fluidizing gas, which is non-condensable, is removed from the vapor flowing inside the heat exchanger tubes and utilized as a heat source for drying. As the largest part of heat exchange in the dryer is latent heat exchange following condensation, the existence of even small amount of drying medium/fluidizing gas leads to significant decrease in heat transfer. The existence of gas during condensation will increase the resistance of mass transfer between the bulk mixture and condensing interface (Lee et al., 1983; Kuhn et al., 1997; Wu et al., 2006). Pure steam condensation has a significantly better heat transfer performance leading to simpler and shorter heat exchanger tubes immersed inside the fluidized bed dryer. As the result decrease of capital cost can be predicted.

In separation module, the exhausted air-steam mixture is compressed with compressor CP2 to certain pressure. High exergy rate of compressed air-steam mixture is utilized to evaporate and rise the temperature of separated water and drying medium/fluidizing gas, respectively (HX3 and HX4). As the separated drying medium/fluidizing gas still has a compression energy, an expander EX is installed to recover this energy before entering the condenser CD. Evaporation heat in fluidized bed dryer (HX2) is provided by the condensation heat of the compressed pure steam. Subsequently, the sensible heat of the condensed steam is utilized for pre-heating (HX1).

The total energy consumption in ASRD system $W_{tot,ASRD}$ is expressed in eq. 6-1. W_{cp1} and W_{cp2} are compression works conducted by CP1 and CP2, respectively.

$$W_{tot,AHCD} = W_{cp1} + W_{cp2} + W_{bl} - W_{ex} \quad (6-1)$$

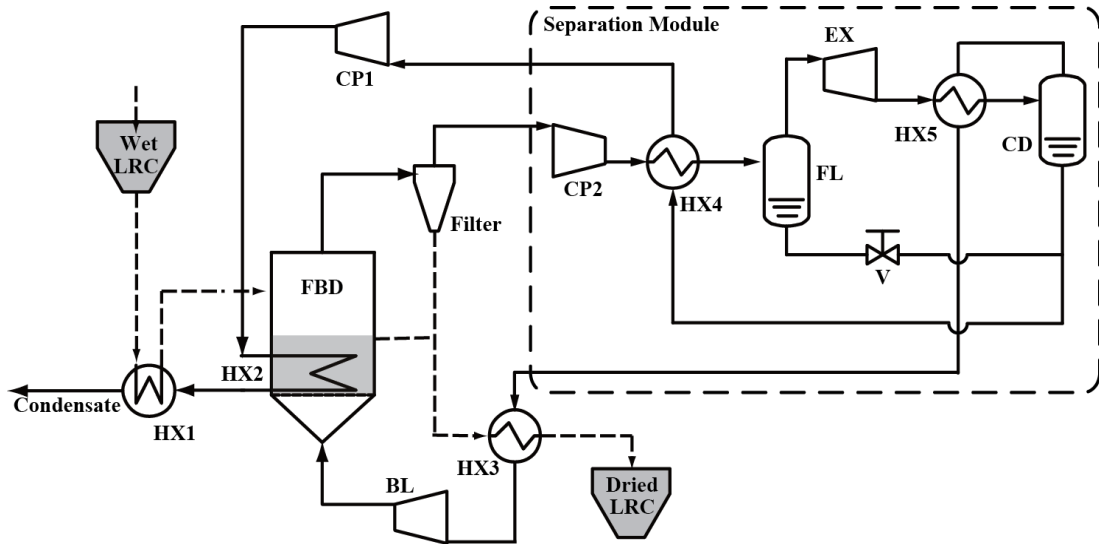


Fig. 6-2-3. Schematic drying system of the proposed ASRD system

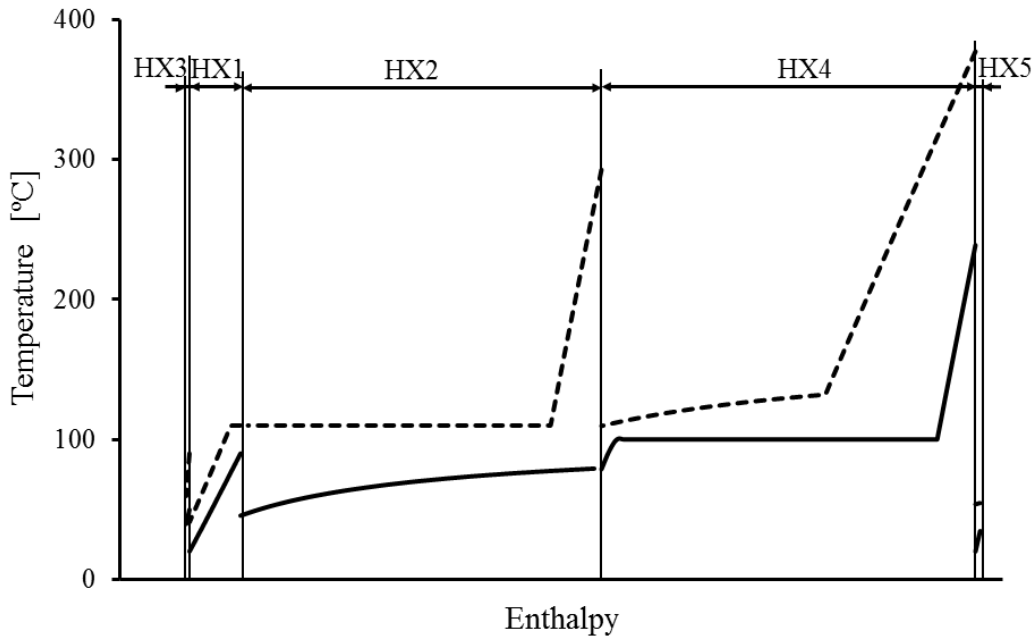


Fig. 6-2-4 shows the total energy input required for drying in each drying system.

Compared to the conventional heat recovery drying system, self-heat recuperation based drying systems can decrease the total energy input significantly. Numerically, they reduced the energy input to about 60-70% of which is required in drying with conventional heat recovery. In addition, as the fluidization velocity increases, the total energy input increases accordingly in all drying systems. The blower work W_{bl} increases following the increase of fluidization velocity due to increase of volumetric amount of drying medium/fluidizing gas (air). The temperature – enthalpy diagram of ASRD system is shown in Fig. 6-2-4. In this drying system, drying process is mainly divided into drying and separation modules. In ASRD system, the hot stream which is flowing inside the heat exchanger immersed inside the fluidized bed dryer is a compressed pure steam. Hence, the dotted line (hot stream) in HX2 is almost a straight line due to condensation of pure steam. On the other hand, a compressed air-steam mixture is flowing in HCD system and both dotted (hot stream) and solid (cold stream) lines are both curved lines due to mixing of sensible and latent heat. Furthermore, in separation module of ASRD system, the condensation heat of the air-steam mixture is exchanged with the evaporation heat of the separated water (HX4). Hence, the separated water exiting from separation module is in vapor condition before its exergy rate is elevated by the compressor in drying module. In this drying system, self-heat recuperation is performed in both drying and separation modules resulting in low total energy consumption. Although drying in ASRD system resulted in little higher energy consumption than HCD system, the design of heat exchanger inside fluidized bed dryer (HX2) becomes simpler due to a significantly better heat exchange following condensation of pure steam than air-steam mixture. As the result, it leads to a shorter and smaller heat exchanger tube, hence, the fluidization inside the fluidized bed will not

be disturbed by the existence of heat exchanger tube and the dimension size of the fluidized bed dryer could be more compact. In addition, temperature–enthalpy diagram for each drying system has been observed. It was found that intensive and optimal heat pairing for each sensible and latent heat is very important to minimize the exergy loss, hence to reduce the total energy input for drying. The decrease of total energy input also means the decrease of CO₂ emission during LRC drying. SHR technology can also be applied to brown coal steam drying process, which is more common in the brown coal drying process compared with air for the prevention of the explosion of brown coal during the drying process.

References

- Allardice DJ, Chaffee AL, Jackson WR, Marshall M (2004) Water in brown coal and its removal. In: Li CZ (ed) *Advances in the science of Victorian brown coal*. Elsevier, Oxford, pp. 85-133.
- Arias, B., Pevida, C., Feroso, J., Plaza, M.G., Rubiera F. and Pis, J.J., 2008. Influence of torrefaction on the grindability and reactivity of woody biomass. *Fuel Process. Technol.* 89, 169-175.
- Aziz M, Kansha Y, Tsutsumi A (2011) Self-heat recuperative fluidized bed drying of brown coal, *Chem. Eng. Process.* 50: 944-951.
- Bergman, P.C.A., Boersma, A.R., Kiel, J.H.A., Prins, M.J., Ptasinski, K.J. and Janssen, F.J.J.G., 2005. *Torrefaction for entrained-flow gasification of biomass*. Energy Research Centre of the Netherlands (ECN).
- Chen, W.H. and Kuo, P.C., 2011. Torrefaction and co-torrefaction characterization of hemicellulose, cellulose and lignin as well as torrefaction of some basic constituents in biomass. *Energy* 36, 803-811.
- Couhert, C., Salvador, S. and Commandre, J.M., 2009. Impact of torrefaction on syngas production from wood. *Fuel* 88, 2286-2290.
- Deng, J., Wang, G.J., Kuang, J.H., Zhang, Y.L. and Luo, Y.H., 2009. Pretreatment of agricultural residues for co-gasification via torrefaction. *J. Anal. Appl. Pyrol.* 86, 331-337.
- Karthikeyan M, Kuma JVM, Soon Hoe C, Lo Yi Ngo D (2007) Factors affecting quality of dried low-rank coals. *Drying Technol* 25:1601-1611.

- Karthikeyan M, Zhonghua W, Mujumdar AS (2009) Low-rank coal drying technologies—current status and new developments. *Drying Technol.* 27: 403-415.
- Kudra T, Mujumdar AS (2009) *Advanced drying technologies*, 2nd edn. Taylor & Francis Group, Florida.
- Kuhn SZ, Schrock VE, Peterson PF (1997) An investigation of condensation from steam-gas mixture flowing downward inside a vertical tube. *Nucl. Eng. Des.* 177:53-69.
- Lee WC and Rose JW (1983) Forced convection film condensation on a horizontal tube with and without non-condensing gas. *Int. J. Heat Mass Transfer* 27:519-528.
- Li, H., Liu, X.H., Legros, R., Bi, X.T., Lim, C.J. and Sokhansanj, S., 2011. Torrefaction of sawdust in a fluidized bed reactor, *Bioresour. Technol.*, doi:10.1016/j.biortech.2011.10.009.
- Obernberger, I. and Thek, G., 2010. *The pellet handbook: The production and thermal utilization of pellets*. Earthscan Publishing, London.
- Phanphanich, M. and Mani, S., 2011. Impact of torrefaction on the grindability and fuel characteristics of forest biomass. *Bioresour. Technol.* 2011, 1246-1253.
- Pikon J, Mujumdar AS (2009) Drying of coal. In: Mujumdar AS (ed) *Handbook of industrial drying*, 3rd edn. Taylor & Francis Group, New York, pp. 993-1018.
- Pimchuai, A., Dutta, A. and Basu, P., 2010. Torrefaction of agriculture residue to enhance combustible properties. *Energ. Fuel.* 24, 4638-4645.
- Repellin, V., Govin, A., Rolland, M. and Guyonnet, R., 2010. Modelling anhydrous weight loss of wood chips during torrefaction in a pilot kiln. *Biomass & Bioenergy* 34, 602-609.

- Rousset, P., Davrieux, F., Macedo, L. and Perre, P., 2011. Characterisation of the torrefaction of beech wood using NIRS: Combined effects of temperature and duration. *Biomass & Bioenergy* 35, 1219-1226.
- Wu T and Vierow K (2006) Local heat transfer measurements of steam/air mixture in horizontal condenser tubes. *Int. J. Heat Mass Transfer* 49:2491-2501.
- Yan, W., Acharjee, T. C., Coronella, C. J. and Vasquez, V. R., 2009. Thermal Pretreatment of Lignocellulosic Biomass. *Environ. Prog. Sustain. Energy* 28, 435-440.

Nomenclature

A	surface area, m^2
Ar	Archimedes number, dimensionless
a	heat transfer coefficient, $\text{Wm}^{-2}\text{K}^{-1}$
a_w	water content, dimensionless
C	specific heat capacity, $\text{kJ kg}^{-1} \text{K}^{-1}$
c	conversion factor, $1 \text{ kg m N}^{-1} \text{ s}^{-2}$
D	shell diameter, m
D_e	equivalent diameter, m
d	particle diameter, m
Ex	exergy, kW
f	electricity generation efficiency, dimensionless
G	mass flux, $\text{kg m}^{-2} \text{s}^{-1}$
g	gravity acceleration, m s^{-2}
H	thermal energy, kW
h	specific enthalpy, kJ mol^{-1}
h_b	bed height, m
L_e	evaporation enthalpy, kJ kg^{-1}
M	mass weight, kg
m	mass flow rate, kg h^{-1}
N	rotation speed, rpm
N_b	number of tubes, dimensionless
Nu	Nusselt number, dimensionless
Pr	Prandtl number, dimensionless

p	pressure, kPa
q	heat transfer rate, kW
R	outer diameter, m
Re	Reynolds number, dimensionless
R_{sp}	specific drying rate, g-water/g-biomass/min
R_w	drying rate, kg h ⁻¹
r	inner diameter, m
s	specific entropy, kJ mol ⁻¹
T	temperature, K
ΔT_{min}	minimum temperature difference in heat exchanger, K
t	time, h
U	overall heat transfer coefficient, Wm ⁻² K ⁻¹
U_{mf}	minimum fluidization velocity, m s ⁻¹
W	work, kW
W_{wet}	water content of biomass, wt% (wb)
W_{tot}	total rotating load (equipment plus material)
W_{mat}	load of the material, kg
w	water content of wet solid, wt%(wb)
X	water content of biomass (dry basis), dimensionless
X_{fsp}	fiber saturation point, kg/kg
x	vapor quality, dimensionless
Y	air humidity, dimensionless
Δz	short length of the dryer, m

Subscripts

0	standard condition
avi	avoidable
b	bed
bl	blower
cp	compressor
crit	critical
d	distributor
des	desorption
elect	electricity
evp	evaporation
ex	expander
f	fluidization
g	gas
ht	heater
i	state
in	incoming flow
inv	inevitable
l	liquid
mc	mechanical
mf	minimum fluidization
min	minimum
out	outgoing flow
p	particle

pre	preheating
s	solid
sorp	sorption
stm	steam
sur	surrounding
sys	system
t	heat transfer tube
tot	total
trs	transition
vap	vapor
vs	saturated vapor
w	water
wk	work
wet	wet solid

Greek letters

ε	voidage, dimensionless
λ	thermal conductivity, $\text{W m}^{-1} \text{K}^{-1}$
ν	volumetric fraction, dimensionless
μ	dynamic viscosity, Pa s
ρ	density, kg m^{-3}
η	exergy efficiency, dimensionless
Φ	sphericity, dimensionless

γ activity coefficient, dimensionless

Abbreviations

ASRD advanced self-heat recuperative system based drying

CHR conventional heat-recovery dryer

CP1 compressor for the fluidized bed dryer

CP2 compressor for the screw conveyor dryer

FBD fluidized bed dryer

HPD heat pump dryer

HR self-heat receiver

HT self-heat transmitter

HX heat exchanger

MIX mixer

MSD multistage drying process

MVR mechanical vapor recompression drying process

SCD screw conveyor dryer

SHR self-heat recuperation

SHS superheated steam

SHR dryer dryer based on the self-heat recuperation technology

SHR-FBD fluidized bed dryer based on the self-heat recuperation technology

LIST OF PUBLICATIONS

Journal Papers

- 1) Yuping Liu, Muhammad Aziz, Yasuki Kansha, Sankar Bhattacharya, Atsushi Tsutsumi, Application of the self-heat recuperation technology for energy saving in biomass drying system *Fuel Processing Technology*, Publisher: Elsevier, Ltd., 117, pp 66–74, 2014.
- 2) Yuping Liu, Muhammad Aziz, Yasuki Kansha, Atsushi Tsutsumi, A novel exergy recuperative drying module and its application for energy-saving drying with superheated steam, *Chemical Engineering Science*, Publisher: Elsevier, Ltd., Vol 100, pp 392-401, 2013.
- 3) Yuping Liu, Muhammad Aziz, Yasuki Kansha, Atsushi Tsutsumi, Drying energy saving by applying self-heat recuperation technology to biomass drying system. *Chemical Engineering Transactions*, Publisher: The Italian Association of Chemical Engineering, 29, 577–582, 2012.
- 4) Yuping Liu, Muhammad Aziz, Chihiro Fushimi, Yasuki Kansha, Kazuhiro Mochidzuki, Shozo Kaneko, Atsushi Tsutsumi, Katsuhiko Yokohama, Kazuyuki Myoyo, Koji Oura, Keisuke Matsuo, Shogo Sawa, Katsuhiko Shinoda “Exergy Analysis of Biomass Drying Based on Self-Heat Recuperation Technology and its Application to Industry—a Simulation and Experimental Study” *Industrial & Engineering Chemistry Research*, Publisher: American Chemical Society, Vol 51, pp 9997–10007, 2012.
- 5) Muhammad Aziz, Yasuki Kansha, Akira Kishimoto, Yui Kotani, Yuping Liu, Atsushi Tsutsumi. Advanced Energy Saving in Low Rank Coal Drying based on Self-heat Recuperation Technology. *Fuel Processing Technology*. Publisher:

Elsevier, Ltd., 104, 16-22, 2012.

- 6) Shinji Sakai, Yuping Liu, Rie Watanabe, Masaaki Kawabe and Koei Kawakami, An electrospun ultrafine silica fibrous catalyst incorporating an alkyl-silica coating containing lipase for reactions in organic solvents, *J Mol Catal B-Enzym*, Publisher: Elsevier, Ltd., Vol.83, 120-124, 2012.
- 7) Shinji Sakai, Yuping Liu, Tetsu Yamaguchi, Rie Watanabe, Masaaki Kawabe and Koei Kawakami “Production of butyl-biodiesel using lipase physically-adsorbed onto electrospun polyacrylonitrile fibers” *Bioresource Technology*, Publisher: Elsevier, Ltd., Vol 101, pp 7344-7349, 2010.
- 8) Shinji Sakai, Yuping Liu, Tetsu Yamaguchi, Rie Watanabe, Masaaki Kawabe and Koei Kawakami, Immobilization of *Pseudomonas Cepacia* lipase onto electrospun polyacrylonitrile fibers through physical adsorption and application to transesterification in nonaqueous solvent, *Biotechnology Letters*, Publisher: Springer, Vol 32, pp 1059-1062, 2010.
- 9) Yuping Liu, Jianghong Peng, Yasuki Kansha, Masanori Ishizuka, Atsushi Tsutsumi, Dening Jia, Xiaotao T. Bi , C. J. Lim, Shahab Sokhansanj, Novel Fluidized Bed Dryer for Biomass Drying, **Accepted by *Fuel Processing Technology***.
- 10) Yuping Liu, Yasuki Kansha, Masanori Ishizuka, Atsushi Tsutsumi, Fluidized Bed Drying of Biomass with Superheated Steam Based on Self-Heat Recuperation Technology: Theory and Experiments, **in Preparation**.

Review

- 1) Chihiro Fushimi, Yasuki Kansha, Muhammad Aziz, Yuping Liu, Kazuhiro Mochidzuki, Shozo Kaneko, Atsushi Tsutsumi, Energy-saving Biomass Drying Process based on Self-Heat Recuperation Technology, Separation Technology, Vol 41, pp 29-34, (2011). [In Japanese]

Proceeding Papers

- 1) Yuping Liu, Muhammad Aziz, Yasuki Kansha, Atsushi Tsutsumi, Self-Heat Recuperative Fluidized Bed Drying of Low rank coal, Proceedings of 29th Annual International Pittsburgh Coal Conference, pp 1-9.
- 2) Yuping Liu, Yasuki Kansha, Masanori Ishizuka, Atsushi Tsutsumi, Self-heat Recuperative Fluidized Bed Dryer for Low Rank Coal Drying with Superheated Steam, Proceedings of 2013 International Conference on Coal Science & Technology, pp 995-1001.
- 3) Masanori Ishizuka, Yuping Liu, Yasuki Kansha, Atsushi Tsutsumi, Modeling of Triple Bed Circulating Fluidized Bed Coal Gasifier Flow Behavior Based on Equivalent Circuit Model, Proceedings of 2013 International Conference on Coal Science & Technology, pp 262-268.

CONFERENCES

International Conferences

- 1) ○Qian Fu, Yuping Liu, Yasuki Kansha, Atsushi Tsutsumi, An advanced cryogenic air separation process for oxy-combustion based on self-heat recuperation technology, The 6th International Conference on Applied Energy, May 30 – June 2,

2014, Taipei, Taiwan

- 2) ○ Yuping Liu, Yasuki Kansha, Masanori Ishizuka, Atsushi Tsutsumi, Advanced energy-saving brown coal drying process with gas-steam separation module based on self-heat recuperation technology, The 12th Japan-China Symposium on Coal and C1 Chemical, Fukuoka, Japan, 28-31 October, 2013. *Oral*
- 3) ○ Yuping Liu, Yasuki Kansha, Masanori Ishizuka, Atsushi Tsutsumi, Self-heat Recuperative Fluidized Bed Dryer for Low Rank Coal Drying with Superheated Steam, International Conference on Coal Science and Technology 2013, State College, Pennsylvania, USA , 29 September-3 October, 2013. *Oral*
- 4) ○ Masanori Ishizuka, Yuping Liu, Yasuki Kansha, Atsushi Tsutsumi, Modeling of Triple Bed Circulating Fluidized Bed Coal Gasifier Flow Behavior Based on Equivalent Circuit Model, International Conference on Coal Science and Technology 2013, State College, Pennsylvania, USA, 29 September-3 October, 2013. *Oral*
- 5) ○ Masanori Ishizuka, Yuping Liu, Yasuki Kansha, Atsushi Tsutsumi, Modeling of triple bed circulating fluidized bed coal gasifier flow behavior based on equivalent circuit model, International Conference on Green Energy and Technology, Kitakyushu, Japan, 24-26, Aug. 2013. *Oral*
- 6) ○ Yuping Liu, Muhammad Aziz, Yasuki Kansha, Atsushi Tsutsumi, A Novel Exergy Recuperative Drying Module and its Application for Energy-Saving Drying with Superheated Steam, The 11th International Conference on Gas-Liquid & Gas-Liquid-Solid Reactor Engineering, Seoul, Korea, August 19-22 2013. *Oral*
- 7) ○ Yuping Liu, Jianghong Peng, Yasuki Kansha, Masanori Ishizuka, Atsushi

Tsutsumi, Dening Jia, Xiaotao T. Bi, C. J. Lim, Shahab Sokhansanj, Sawdust Fluidization and Drying in a Newly Designed Fluidized Bed Dryer, 6th International Conference on Green and Sustainable Chemistry, Nottingham, UK, August 4-7 2013. *Poster* **6th GSC Student Travel Grant Award**

- 8) ○ Yuping Liu, Yasuki Kansha, Atsushi Tsutsumi Self-Heat Recuperative Fluidized Bed Drying of Low Rank Coal, 29th Annual International Pittsburgh Coal Conference, Pittsburgh, USA. 2012.10. *Oral*
- 9) ○ Yuping Liu, Muhammad Aziz, Yasuki Kansha, and Atsushi Tsutsumi, Drying energy saving by applying self-heat recuperation technology to drying system. 15th Conference "Process integration, modeling and optimisation for energy saving and pollution reduction", Prague, Czech Republic (Aug. 25-29, 2012) *Poster*
- 10) ○ Yuping Liu, Muhammad Aziz, Yasuki Kansha, Atsushi Tsutsumi, Sankar Bhattacharya. Superheated Steam Fluidized Bed Drying of Biomass with Self-Heat Recuperation Technology, International Workshop on Clean Technologies of Coal and Biomass Utilization. Anshan, China, 2012.6. *Oral* **CTCBU Best Paper Award**
- 11) ○ Yuping Liu, Muhammad Aziz, Chihiro Fushimi, Yasuki Kansha, Kazuhiro Mochidzuki, Shozo Kaneko, Atsushi Tsutsumi, Katsuhiko Yokohama, Kazuyuki Myoyo, Koji Oura, Keisuke Matsuo, Shogo Sawa, Katsuhiko Shinoda, Exergy recuperative fluidized bed drying of rice straw. 14th Asia Pacific Confederation of Chemical Engineering, February 21-24, 2012, Singapore. *Oral* **APCChE 2012 Young Researcher Award**
- 12) ○ Yasuki Kansha, Yuping Liu, Yui Kotani, Hiroyuki Mizuno, Masanori Ishizuka,

Atsushi Tsutsumi “Self-Heat Recuperation and Its Applications in Chemical Industries” 2012 AIChE Annual Meeting, Oct. 28-Nov. 2, 2012, Pittsburgh, PA, USA. *Oral*

- 13) ○ Yuping Liu, Muhammad Aziz, Yasuki Kansha, Atsushi Tsutsumi, Exergy recuperative drying system for high water content carbonaceous materials. International Symposium on Exploring the Frontiers of Academic Collaboration between United Arab Emirates and Japan - Petroleum and Energy-related Technologies, December 5th, 2011, Tokyo. *Poster*
- 14) ○ Yuping Liu, Muhammad Aziz, Yasuki Kansha, Atsushi Tsutsumi, Energy and Exergy Analyses of Drying Process Based on Self-Heat Recuperation Technology. 4th GMSI International Symposium, March 2, 2012, Fukutake hall, Tokyo. *Poster*
- 15) ○ Yuping Liu, 2012 GMSI International Workshop on Numerical Simulations of Fluid/Thermal Systems. Development of a new energy-saving drying system based on self-heat recuperation technology March 16-20, 2012, KTH, Stockholm, Sweden and TU Delft, Delft, Netherlands. *Oral*

Domestic Conferences

- 1) ○ Yuping Liu, Yasuki Kansha, Masanori Ishizuka, Atsushi Tsutsumi, A Novel Energy-Saving Biomass Fluidized bed Dryer Based on Self-Heat Recuperation Technology, 19th Fluidization & Particle Processing Symposium, Nov. 28-29, 2013 (Gunma) *Poster*

- 2) ○ Yuping Liu, Yasuki Kansha, Masanori Ishizuka, Atsushi Tsutsumi, A Novel Fluidized Bed Dryer for Biomass Drying Based on Self-Heat Recuperation Technology, 2nd JACI/GSC Symposium (13th GSC Symposium) June 6-7, 2013 (Osaka) *Poster*
- 3) ○ Yuping Liu, Muhammad Aziz, Yasuki Kansha, Chihiro Fushimi, Atsushi Tsutsumi, Application study of Self-heat recuperation technology for drying process, 21st Annual meeting of the Japan Institute of Energy, August 6-7, 2012 (Tokyo) *Oral*

Lectures

- 1) Yuping Liu, ○Masanori Ishizuka, Self-Heat Recuperative Drying Process, 12th Coproduction Workshop, January 31st, 2013 (Tokyo) *Oral*
- 2) ○Yuping Liu, Drying Process based on Self-Heat Recuperative Technology, 11th Coproduction Workshop, February 2nd, 2012 (Tokyo) *Oral*

HONORS

- 1) Yuping Liu, 6th GSC Student Travel Grant Awards from Japan Association for Chemical Innovation, "Drying and torrefaction of biomass in fluidized beds with energy recovery and self-heat recuperation" Jun. 6, 2013.
- 2) Yuping Liu, 2012 Chinese Government Award for Outstanding Self-financed Students Abroad from China Scholarship Council, February, 2013.

- 3) Yuping Liu, Muhammad Aziz, Yasuki Kansha, Atsushi Tsutsumi, Sankar Bhattacharya, Best Paper Award (International Workshop on Clean Technologies of Coal and Biomass Utilization), "Superheated Steam Fluidized Bed Drying of Biomass with Self-heat Recuperation" June 28, 2012.
- 4) Yuping Liu, 2011 GMSI Award for Outstanding GMSI Research Assistant from the Global Center of Excellence for Mechanical Systems Innovation at University of Tokyo, April, 2012.
- 5) Yuping Liu, APCChE 2012 Young Researcher Award, (14th Asia Pacific Confederation of Chemical Engineering Congress, Singapore, "Exergy Recuperative Fluidized Bed Drying of Rice Straw" February, 21-24, 2012.
- 6) Hiroki Ashiba, Takaaki Shimura, Yuping Liu, Dong Young Kim, Hyuntaek Na, Rasul Shahid, Pham Dieu Huong, GSMI PBL Award for Most Outstanding Project Execution from the Global Center of Excellence for Mechanical Systems Innovation at University of Tokyo, January, 2012.

ACKNOWLEDGMENTS

This research was conducted in the Tsutsumi Lab, Collaborative Research Centre for Energy Engineering, Institute of Industrial Science, The University of Tokyo. I would like to first express my deep gratitude to my research supervisor Project Professor Atsushi TSUTSUMI for his guidance of this research and to provide a good study chance in his excellent group to let me learn my interesting area about energy saving in chemical process. His valuable advices are critical for me to complete my doctor research and let me know how to become a researcher. I would also like to thank Project Associate Professor Yasuki KANSHA, for his deep discussions and assistance during my whole doctor course. He gave me a lot of good suggestions during my research. My grateful thanks are also extended to Project Researcher Masanori ISHIZUKA for his technical help for the biomass drying experiment. I want to express my appreciation to Associate Professor Chihiro FUSHIMI from Department of Chemical Engineering, Tokyo University of Agriculture and Technology, and Dr. Muhammad AZIZ, Project Assistant Professor from Integrated research institute solutions research of the Tokyo Institute of Technology, for their helpful discussions and advice. I also thank to Dr. Hidetoshi YAMAMOTO, Senior Cooperator of Tsutsumi Lab, for teaching me how to use the thermal gravity analyzer, and Dr. Akira KISHIMOTO from Kobe Steel Company for his discussion about the self-heat recuperation technology.

I give my thanks to the thesis committer, Prof. Naoki SHIKAZONO, Prof. Yuji SUZUKI, Prof. Ryo SHIRAKASHI and Associate Professor Ryuji KIKUCHI for their valuable comments and helpful suggestions and comments to my doctor research. I thank Prof. X.T. Bi from Chemical and Biological Engineering, the University of British Columbia, for his advice during the development of the pure biomass fluidized bed dryer when I spent two

months in his research group. I would also like to extend my thanks to Prof. C. J. LIM, and Prof. Shahab SOKHANSANJ, from Chemical and Biological Engineering of the University of British Columbia for the advice for biomass drying. I also thank Dr. Jianghong PENG and Mr. Dening JIA from Prof. X.T. Bi's group for the assistant during the experiment and Dr. Hui LI from Hunan Academy of Forestry for his advice. Furthermore I would like to thank to Prof. Chi-Hwa Wang and Dr. Yongpan CHENG from Department of Chemical and Biomolecular Engineering, National University of Singapore for providing me a Lab visiting chance and discussion about my research. I appreciate Associate Professor Sankar BHATTACHARYA from Department of Chemical Engineering, Monash University for his direction about brown coal drying process, and Dr. MengWai WOO, Dr WeiLit CHOO and Mr. Stokie DAVID from Prof. Sankar's group for their discussion about brown coal steam drying in the fluidized bed dryer. I also give my thanks to Associate Professor Guoqing GUAN from North Japan Research Institute for Sustainable Energy, Hirosaki University for his helpful suggestions during my research. I greatly appreciate Prof. Naoki SHIKAZONO from Department of Mechanical Engineering, The University of Tokyo, to be my secondary advisor for a semester during 2012 and give me very useful suggestions on my research.

I appreciate all the members of Tsutsumi Laboratory. Ms. Seiko HONMA and Ms. Sakura HARATANI, secretary of Tsutsumi Laboratory for their great help for my study and daily life. I also thank Tsutsumi Lab members: Dr. Bokkyu CHOI, Dr. Chunfeng SONG, Dr. Qian FU, Mr. Dhruva PANTHI, Mr. Yui KOTANI, Mr. Hiroyuki MIZUNO, Mr. Yuji YOSHIE, Mr. Yonguk KWON, Mr. Mike MUSIL, Mr. Jonghee JO, Mr. Toshihiro KASEDA, Mr. Renaldo RASFULDI, Mr. Yusuke SAKAKIBARA, Mr. Sumit SRIVASTAVA, and Ms. Supachita KRERKKAIWAN for their kindness to give a good

memory in Tsutsumi Laboratory. I would like to thank Prof. Koei KAWAKAMI from Department of Material Process Engineering, Kyushu University and Associate Prof. Shinji SAKAI, Department of Materials Engineering Science of Osaka University for the their training during my master course in Kyushu University.

I appreciate the Global COE Program “Global Center of Excellence for Mechanical Systems Innovation” for financial support to complete my doctor course and my two months stay in Canada. I also thank the one year financial support from SUET Fellowship A, Doctoral Student Special Incentives Program from Graduate School of Engineering, the University of Tokyo. Finally, I want to thank all my family members for their great support during my over the five years’ stay abroad.

Yuping LIU

February 2014